March 2016

The Influence of Musculoskeletal Geometry on the Metabolic Cost of Pedaling

Lex Gidley
University of Massachusetts - Amherst

THE INFLUENCE OF MUSCULOSKELETAL GEOMETRY ON THE METABOLIC COST OF PEDALING

A Dissertation

By

ALEXIS DIANE GIDLEY

Submitted to the Graduate School of the
University of Massachusetts Amherst in partial fulfillment
of the requirements for the degree of

DOCTOR OF PHILOSOPHY

February 2016

Department of Kinesiology

THE INFLUENCE OF MUSCULOSKELETAL GEOMETRY

ON THE METABOLIC COST OF MOVEMENT

A Dissertation Presented

By

ALEXIS DIANE GIDLEY

Approved as to style and content by:

_____

Brian R. Umberger, Chair

_____

Graham E. Caldwell, Member

_____

Jane A. Kent, Member

_____

Frank Sup, Member

_____

Catrine Tudor-Locke, Department Head
Department of Kinesiology

ABSTRACT

THE INFLUENCE OF MUSCULOSKELETAL GEOMETRY
ON THE METABOLIC COST OF PEDALING

FEBRUARY 2016

ALEXIS DIANE GIDLEY

B.S. EXERCISE SCIENCE, UNIVERSITY OF UTAH

M.S. EXERCISE SCIENCE, UNIVERSITY OF UTAH

Ph.D., KINESIOLOGY, UNIVERSITY OF MASSACHUSETTS, AMHERST

Directed by: Professor Brian R. Umberger

The human musculoskeletal system consists of several muscles crossing each joint. In the human lower limb, most major muscles cross either one or two joints; labeled as uniarticular or biarticular muscles, respectively. The major biarticular muscles of the leg are the rectus femoris, hamstrings, and gastrocnemius. Several suggestions have been proposed as to how biarticular muscles may reduce the metabolic cost of human movement. Using experimental protocols, it is difficult to address the energetic effects of biarticular muscles, as individual muscle contributions to human movement cannot be measured and there is no way to determine what the effect might be on the energetics of movement if instead of a biarticular muscle there were two equivalent uniarticular muscles. Therefore, this project used a musculoskeletal modeling approach to address the question of whether biarticular muscles reduce the metabolic cost of submaximal pedaling. We used one standard model representing a simplified human musculoskeletal design with 6 uniarticular and 3 biarticular muscles and created three different models, each replacing one biarticular muscle of the standard model with two mechanically equivalent muscles. The models with the altered musculoskeletal design could not be expected to pedal in the same manner as a

human, so it was not possible to generate simulations of pedaling by tracking experimental pedaling data, a proven method for replicating submaximal pedaling computationally. Therefore, in the first study, we tested the ability of five performance-based criterion to generate predictive simulations of submaximal pedaling using the standard model. We found that minimizing muscle activations best replicated the general kinematics, kinetics and muscle excitation patterns of submaximal pedaling. In the second study, we used this performance-based criterion to generate pedaling simulations for the three new musculoskeletal models with the replaced biarticular muscles. All three new musculoskeletal designs predicted greater metabolic cost than the standard model. Analyzing the mechanisms proposed in the literature by which biarticular muscles might yield energy savings did not reveal a general cause for the increases. We conclude that the greater metabolic costs likely resulted from unique coordination patterns adopted by the altered musculoskeletal designs to meet the task demands of pedaling.

TABLE OF CONTENTS

LIST OF TABLES

LIST OF FIGURES

CHAPTER 1

INTRODUCTION

General Introduction

The design of the human musculoskeletal system consists of many muscles crossing each joint. One method of describing a muscle has been based on the number of joints it crosses. If a muscle crosses two joints it is classified as biarticular. Based on Gray's classic anatomy text, it was determined that about 50% of the muscles in the human leg cross more than one joint (Koeslag & Koeslag, 1993). Examples of the major biarticular muscles in the human lower limb are the rectus femoris, semimembranosus, and gastrocnemius. In contrast, muscles that cross one joint are commonly referred to as uniarticular muscles. The possible differences in function between biarticular and uniarticular muscles due to their different musculoskeletal design have inspired more than a century of research.

The effects of biarticular muscles on muscle coordination, joint mechanics, and mechanical energy flow have been reported in numerous studies (Cleland, 1867; Lombard, 1903; Elftman, 1939b; Andrews, 1987; Wells, 1988; van Ingen Schenau, 1989; Raasch, Zajac, Ma, & Levine, 1997; Raasch & Zajac, 1999; Hasson, Caldwell, & van Emmerik, 2008). For example, biarticular muscles are thought to play an important role in directing the application of external forces (van Ingen Schenau, 1989; van Ingen Schenau, Pratt, & Macpherson , 1994; van Ingen Schenau, et al., 1995). Biarticular muscles have also been argued to make a major contribution to the redistribution of mechanical energy throughout the limb (Bobbert, Huijing, & van Ingen Schenau, 1986; Prilutsky & Zatsiorsky, 1994). Based on these and other proposed functions, biarticular muscles have been described by some as contributing to the mechanics of human movement in a unique manner that differs fundamentally from uniarticular muscles (van Ingen Schenau, 1989). In some of this research, it has been suggested that the unique actions of biarticular muscles may reduce the metabolic cost of movement (Elftman,

1939b; Wells, 1988; Herzog & Binding, 1994). However, any effects biarticular muscles may have on the metabolic cost of movement have not been directly investigated. Therefore, this research will focus on the effects of biarticular muscles on the metabolic cost of human movement.

Biarticular Muscles and Possible Metabolic Savings

There are a few specific ways that the presence of biarticular muscles in the human musculoskeletal system might present an energetic savings. One such characteristic of biarticular muscles is that they generate a flexion torque at one joint and an extension torque at the other joint (e.g. the hamstrings generate hip extension and knee flexion torques). If task demands dictate the need for these torques to occur simultaneously, a single biarticular muscle could contribute to both of the necessary torques. For example, during the second half of the downstroke in pedaling there is a hip extension torque and a knee flexion torque (Gregor, Cavanagh, & LaFortune, 1985). If there were no biarticular hamstrings, two uniarticular muscles would have to be activated to provide the necessary torques. An active hamstring might, therefore, reduce the total volume of muscle activated, resulting in a lower metabolic cost of pedaling by activating only one muscle rather than two. As biarticular muscles simultaneously produce two joint torques, they may also act isometrically, or nearly so, if the two joints crossed are either both flexing or extending. An example of this is rising from a chair when the hip and knee are extending. Because isometric force production is less costly than faster concentric actions, biarticular muscles acting isometrically rather than concentrically could decrease metabolic cost of movement (Abbott, Bigland, & Ritchie, 1952; Beltman, van der Vliet, Sargeant, & de Haan, 2004).

A biarticular muscle acting isometrically during a dynamic task would do no work, but could potentially act to redistribute energy within the limb. A jumping simulation predicted that the gastrocnemius transfers energy from the knee to the ankle, as the knee is extending and the ankle plantar flexing (Bobbert, Huijing, & van Ingen Schenau, 1986). This energy transfer increases the

power about the ankle in jumping beyond that seen in single joint ankle movements. During submaximal activities, this proximal-to-distal energy flow could transfer energy from the larger, proximal muscles to the environment, decreasing the need for the smaller, distal muscles to produce great amounts of power. For example, taking into account the activation of both uni- and biarticular muscles the estimated mechanical work of walking decreased by 29% compared to a design assuming only uniarticular muscles (Wells, 1988). If the energy transfer results in a smaller volume of active muscle it could influence the metabolic energetics of submaximal activities.

Finally, the direction of force application on the environment is often crucial for task completion. For example, during pedaling, the crank moves in a circle, thus the force applied to the pedal must continually change directions over the pedal cycle. Biarticular muscles have been proposed to play a specific role in controlling the direction of forces applied on the environment (van Ingen Schenau, 1989; van Ingen Schenau, Pratt, & Macpherson, 1994; van Ingen Schenau, et al., 1995). In this scheme, uniarticular muscles primarily produce positive work, while biarticular muscle control the direction of force application. Thus, in the context of pedaling, biarticular muscle may play a crucial role in effectively delivering mechanical work to the crank. van Ingen Schenau, et al, (1995) also concluded that with this control pattern, energetically "wasteful" eccentric contractions were not incurred by the uniarticular muscles. Thus, under this paradigm, without biarticular muscles, uniarticular muscles would be left to produce work and direct the force on the environment, possibly leading to an increase in negative muscular work. This negative work would have to be overcome by more positive work, increasing the metabolic cost of movement.

Clinical Relevance

Understanding the possibly unique mechanical and energetic function of biarticular muscles reaches beyond that of pure scientific interest, as it may also have important clinical relevance. The biarticular rectus femoris, hamstrings, and gastrocnemius contribute considerably to movements such

as walking, running, and pedaling. These muscles also seem to be the ones most commonly affected by contractures and spasticity in cerebral palsy (Lieber, 1990; Metaxiotis & Doederlein, 2004). Surgical conversion of the major biarticular muscles of the leg to uniarticular muscles in these patients was introduced by Nils Sifversköld (1888 – 1957) and is still used to reduce the negative effects of muscular contracture. Individuals with cerebral palsy are also known to have a greater metabolic cost during locomotion than age-matched controls (e.g. Johnson, Moore, Quinn, & Smith, 2004). Some of this increased cost is due to the dramatic differences in movement patterns, but could also be due to dysfunction of biarticular muscles. A deeper understanding of how biarticular muscles contribute to the metabolic cost of movement may have important implications for the treatments and procedures for these patients.

In the amputee population, the effect of lost muscle at the affected joint(s) is obvious. What is less obvious is the loss of a biarticular muscle which has become a uniarticular muscle at the proximal joint. A more fundamental understanding of the contributions of biarticular muscles to movement may help improve the design and function of prosthetic devices (Herr & Kornbluh, 2004). In addition, understanding how musculoskeletal design affects the metabolic cost of movement may help partially explain the greater metabolic costs incurred by amputees compared with age-matched controls (Waters & Mulroy, 1999). Thus, it is important to continue to investigate the contribution of biarticular muscles to the energetics of human movement.

Using a Modeling Approach

Addressing questions of musculoskeletal design is notoriously difficult using an experimental approach, especially within a single species. A few researchers have used a modeling approach to better understand the effect of biarticular muscles on movement (Elftman, 1966; Bobbert, Huijing, & van Ingen Schenau, 1986; Jacobs, Bobbert, van Ingen Schenau, 1996; Prilutsky, Petrova, & Raitsin, 1996). A musculoskeletal model can be beneficial for examining the action of biarticular muscles, as

to date, data such as individual muscle forces or shortening velocities are inaccessible by non-invasive experimental methods. A classic analysis of muscle function in walking by Elftman (1939b) compared the mechanical efficiency of a model of the human lower limb containing only uniarticular muscles with a model containing a single tri-articular muscle. The tri-articular model was found to be more mechanically efficient at producing the necessary joint moments in walking (Elftman, 1939b). The triarticular musculoskeletal design is not actually possible in the human body, due to the need for the direction of the moment arms about the hip and knee to change throughout the gait cycle. Without the use of a computer, it was too challenging to mathematically represent a more realistic complement of biarticular and uniarticular muscles. However, Elftman suggested that the biarticular muscles would retain the positives of the triarticular muscle, such as the maintenance of force by one muscle at two joints rather than using two muscles, and the efficiency of a design with both biarticular and uniarticular muscles would fall somewhere in between the two designs investigated.

Computer technology has provided the means to study questions of how biarticular muscles may affect the mechanics of movement, of which Elftman could have only dreamt. A statically-optimized, two-segment model revealed that the inclusion of biarticular muscles was more mechanically effective than a model with only uniarticular muscles when the joint configuration allowed a biarticular muscle to satisfy the net torque requirements at both joints that it crossed (Herzog & Binding, 1994). Another study found that a model with only uniarticular muscles was capable of replicating human pedaling, but resulted in less effective pedaling coordination (Raasch, Zajac, Ma, & Levine, 1997). Prilutsky, Petrova, & Raitsin (1996) found that a design with both uni- and biarticular muscles had lower mechanical energy expenditure during walking and running than a uniarticular only design. These results imply that the presence of biarticular muscles in the human musculoskeletal system lead to a reduced metabolic cost of movement relative to a design with only uniarticular muscles. However, no study has directly evaluated the effects of biarticular muscles on the metabolic cost of submaximal movement.

Computer simulations of the human musculoskeletal system are useful tools for understanding details of movement, such as how individual muscles contribute to joint torques, powers and dynamics. Researchers have taken advantage of the opportunity models provide to change the musculoskeletal design (Herzog & Binding, 1994; Prilutsky, Petrova, & Raitain, 1996). By changing the musculoskeletal design, the results from an alternative model can provide insight into the existing system. Only a few researchers have attempted to use musculoskeletal models to predict muscular metabolic cost (Umberger, Gerritsen, & Martin, 2003; Lichtwark & Wilson, 2005). Therefore, altering the musculoskeletal design in a model that includes a metabolic cost prediction may provide unique insight as to how biarticular muscles affect the metabolic cost of movement.

Pedaling

Stationary pedaling has been used to study several aspects of non-ballistic, submaximal human movement, including efficiency (Gaesser & Brooks, 1975; Sidossis, Horowitz, & Coyle, 1992; Chavarren & Calbet, 1999), co-activation of agonist and antagonist muscles (Gregor, et al., 1985; Jorge & Hull, 1986; Andrews, 1987), directing forces on the environment (van Ingen Schenau, 1989; Hasson et al, 2008), and the possible differences in the control of uniarticular and biarticular muscles (van Ingen Schenau, Pratt, & Macpherson, 1994; van Ingen Schenau, et al., 1995). As a model movement task, stationary pedaling provides several advantages over other submaximal activities such as walking or running: (1) there is little extra effort used to maintain balance, thus the need for co-contractions of muscles to maintain upright posture is reduced, (2) there are fewer degrees of freedom to control, (3) the task can be tightly controlled and movements are highly repeatable, and (4) the joints move through a greater range of motion (Fregly & Zajac, 1996). Pedaling is an especially appropriate task for the present study as it evokes all the possible effects of biarticular muscles on the metabolic cost of movement described earlier. For example, the biarticular hamstrings may contribute to both the hip extension and knee flexion torques seen in the downstroke

of pedaling. In addition, as the hip and knee are both extending during the downstroke, the biarticular muscles may be producing force nearly isometrically. Finally, directing forces on the pedal as it rotates through 360° is crucial to pedaling. It has been proposed that biarticular muscles play a major role in controlling the direction of external forces, thus their role would be paramount to pedaling. The issue in the present study is not about cycling as a form of locomotion, but rather is about pedaling as a task that engages the entire lower limb musculature and incurs a meaningful metabolic cost. Therefore, this project will use stationary pedaling as a representative task to examine the effect of biarticular muscles on the metabolic cost of movement.

Purpose

The purpose of this project is to investigate the influence of biarticular muscles on the metabolic cost of human movement. The literature addressing this topic is sparse and unable to resolve the question of whether the purportedly unique mechanical functions of biarticular muscles result in a lower metabolic cost of movement than would otherwise be possible. Based on the proposed mechanisms through which biarticular muscles may reduce the metabolic cost of movement, it is predicted that a design including both uniarticular and biarticular muscles will result in a lower metabolic cost than a design with only uniarticular muscles. To investigate the energetic effects of biarticular muscles, different musculoskeletal designs will be created and used to simulate pedaling. One will generally represent the human musculoskeletal with both uni- and biarticular muscles, the standard model, and three alternative designs will be developed, where each of the biarticular muscles in the standard model will be individually replaced by two mechanically equivalent uniarticular muscles for each new model. Included in these models is a direct prediction of muscle energy expenditure (Umberger, et al., 2003). Muscle excitation timing and magnitudes will be used as inputs to a forward-dynamic simulation of submaximal pedaling, and will be found via an optimization process (Pandy, 2001). A sound optimization method for finding muscle activations is to

minimize the difference between experimental and simulated data (Neptune & Hull, 1998). However, since the musculoskeletal design will be altered in this project, there will be no experimental data available to track. Therefore, Study One will be conducted to identify one or more performance based cost function(s) that can be used to generate a simulation of submaximal pedaling without the need to explicitly track experimental data. This will allow musculoskeletal models, both including and excluding biarticular muscles, to simulate pedaling, and will provide the basis for pursuing the objectives of Study Two. In Study Two, the effects that biarticular muscles have on the metabolic cost of movement will be examined. In addition to identifying which musculoskeletal design has the lower cost of movement, the mechanisms by which the lower cost is achieved will be identified at the muscular level.

Operational Definitions

The following terms are used in this project and are defined here for clarification.

Forward dynamics: a mathematical process for predicting motions from forces and torques using Newtonian physics.

Inverse dynamics: a mathematical process for deriving the forces and moments from kinematics and inertial characteristics.

Dynamic optimization: a method by which the inputs (such as muscle excitations) to a forward-dynamics problem are found by minimizing (or maximizing) a cost function (e.g. minimizing fatigue).

Static optimization: a method that determines individual muscle forces from joint torques at each time step, typically determined via inverse dynamics, by minimizing (or maximizing a cost function.

Cost function: the function, or equation, to be minimized (or maximized) through optimization, usually a goal of the simulated task (also called criterion or objective function).

Performance-based criterion (or a non-tracking criterion): a mathematically defined goal of a task (e.g. minimize fatigue).

Tracking cost function: a cost function that minimizes the difference between experimental and simulated data.

Musculoskeletal model: a set of mathematical equations and parameter values that numerically represent a system of skeletal components and muscle models.

Muscle model: a series of equations that represent the behavior of the contractile (active) and elastic (passive) components of muscle.

Uniarticular muscle: a muscle that crosses a single major joint, such as the soleus which crosses just the ankle.

Biarticular muscle: a muscle that crosses two major joints, such as the gastrocnemius which crosses the knee and ankle.

Metabolic cost: the biochemical energy (e.g. ATP) used during muscular activity when performing a task, e.g. pedaling. In this study, metabolic cost is predicted from muscular work performed and a calculation of the heat released.

CHAPTER 2

LITERATURE REVIEW

Biarticular Muscles and the Cost of Movement

Muscles that cross two major joints (like the hip and knee) are often referred to as biarticular muscles. These muscles have interested many researchers for quite some time. Giovanni Alfonso Borelli (1608-1679), the man often considered the father of modern biomechanics (Pope, 1976), observed that knee joint torque is dependent on the hip angle. This concept may have been the beginning of the modern search for how biarticular muscles contribute to movement. The consideration that biarticular muscles contribute differently to movement than uniarticular muscles has blossomed into a great debate. For example, the idea that biarticular muscles affect two joint torques simultaneously has spurred years of questioning about how biarticular muscles affect human movement. Formal research on biarticular muscles has mostly focused on mechanics and control (Cleland, 1867; Lombard, 1903; Elftman, 1939; Andrews, 1987; Wells, 1988; van Ingen Schenau, 1989; Raasch, Zajac, Ma, & Levine, 1997; Raasch & Zajac, 1999; Hasson, Caldwell, & van Emmerik, 2008), but some investigators have suggested that the presence of biarticular muscles in the human musculoskeletal system may reduce the metabolic cost of movement (Wells, 1988; van Ingen Schenau, 1989; Prilutsky, Petrova & Raitsin, 1996).

One of the first modern researchers known to focus on biarticular muscle contribution to the musculoskeletal structure was Dr. John Cleland. In his work from anatomical study of humans and other animals, he believed that the major biarticular muscles of the human leg can act more like ligaments than muscles during movements, as he observed little change in muscle-tendon unit length of the biarticular muscles through a wide range of joint configurations of the leg (Cleland, 1867). Cleland stated that ligaments would not work in the place of muscles, as the long tendons do in horses, because of the joint movement limitations this presents. He added, though, that the limited

change in length of these muscles could transfer mechanical energy, decreasing the total energy production necessary to complete a task. He even speculated that this result of biarticular muscles may reduce the muscle mass of the distal leg, reducing the moment of inertia of the leg, thereby reducing the energy necessary to move the leg.

Dr. Warren P. Lombard (1903) followed Cleland's idea by proposing a tendon-like action of biarticular muscles, which could transfer energy from one joint to the other. Lombard explained that muscles on either side of a limb, like the rectus femoris and the semimembranosus in the human thigh, may act as synergists rather than as antagonists, as was often thought. If the biarticular muscles on either side of the thigh are active at the same time, they resist the opposing movements at the joints they cross. The muscles are then more tendon-like, as they shorten or lengthen minimally. Lombard explained that energy would move through the system based on muscular leverage, or moment arms. Therefore, if the biarticular muscles of the thigh are acting simultaneously and essentially isometrically, the instantaneous muscular leverage dictates energetic flow of the system which could flow either to the hip or the knee. Leverage is not easily defined, as moment arms differ for all muscles and are ever-changing during movements. Lombard remained vague on the impact of energy flow during specific activities, because he conceded that there was not yet enough information about moment arm changes during movement to "understand the true action of the muscles."

To more closely identify *the true action of muscles*, Herbert Elftman created a mathematical representation of human locomotion to explore the effect of energy transfer between adjacent joints via multiarticular muscles (Elftman, 1939b). Using inverse dynamics he determined the joint torques during walking. Then, he mathematically modeled a human leg to determine the muscular contributions to the movement (Figure 2.1). Because the human musculoskeletal system is indeterminate, the model was simplified by reducing the number of muscles crossing a given joint. The inclusion of biarticular muscles also made it such that a unique solution of a model containing biarticular muscles could not be solved by hand. Therefore, he designed two models for which a

solution could be determined: one with only uniarticular muscles crossing each side of a joint and another with only a single triarticular muscle. The triarticular muscle only model was more mechanically efficient than the design with only uniarticular muscles, since some of the muscles in the uniarticular only model absorbed the work of other muscles. However, the triarticular model would not be feasible in a humanlike system, due to the need to change the direction of the moment arms of the hip and knee (Figure 2.1). Elftman concluded that the efficiency of a system with both uni- and biarticular muscles would fall between the two models he investigated because it would incorporate both concepts of his models. Specifically this would mean that a design with both uni- and biarticular muscles (i.e., the real system) should be more efficient than the design with only uniarticular muscles.

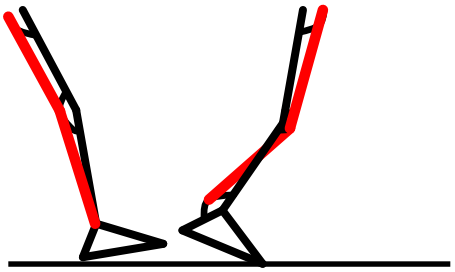

Figure 2.1: A single triarticular muscle model of the human leg during walking. The circles about the joints graphically represent the moment arms of the three-joint muscle about each joint. Note how the moment arms about the hip and knee moves from posterior to anterior. Recreated from Elftman (1939).

The study of biarticular muscle activity during movement continued with the use of pedaling as the mode of movement. Gregor, Cavanagh and LaFortune (1985) used pedaling to directly address the use of biarticular muscles. Surface electromyography was used to observe that extensor muscle activity decreased during the second half of the downstroke (90° - 180°), even though the biarticular hamstrings (hip extensors and knee flexors) were still active. This muscle coordination appears

illogical, as a knee flexor muscle was active during a knee extension motion. The reduction in knee extensor muscles as knee flexor muscles are still active in a very obvious knee flexion (negative) torque during the second half of the downstroke. An example of the knee torque during the pedal cycle from Marsh, Sanderson, & Martin (2000) is presented in Figure 2.2, where a large negative net knee flexion torque is seen as the knee is still extending between the crank angles 90° and 180°. Gregor and colleagues also observed at this point in the downstroke, the pedal reaction force vector, determined from an instrumented pedal, is directed in front of the knee, resulting in an external knee extension torque (Figure 2.3). They concluded that negative knee torque from the biarticular muscles is necessary to resist the knee extension caused by this external torque, thus making the negative knee torque necessary to complete the task. Gregor, et al. also implied that reduced co-contraction could make the movement more economical as less muscle is active.

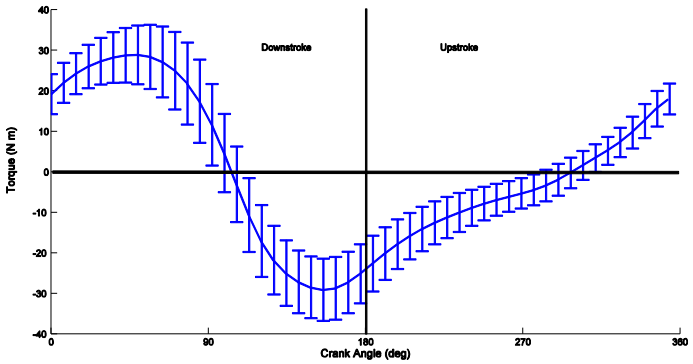

Figure 2.2: Knee torque during the crank cycle at 200 W, 80 RPM. During the second half of the downstroke (90°-180°) the net knee torque is negative. (Data from Marsh, Sanderson & Martin, 2000)

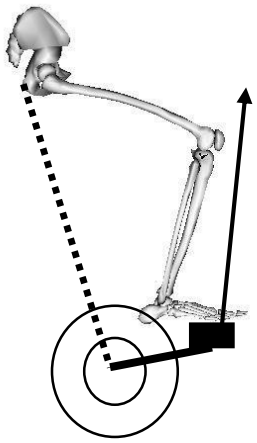

Figure 2.3: The pedal reaction force (F) directed in front of the knee during the downstroke of the pedal cycle. As explained by Gregor, et al. (1985), F will create an external extension (positive) knee torque that must be countered by an internal knee flexion torque generated by muscles.

Andrews (1987) followed up this research with a new method to determine the functional roles of muscular activity during pedaling. This method was designed to directly address the conclusion of Gregor, et al. (1985) that the biarticular hamstring was active to resist the external knee extension torque produced by the pedal reaction force. The method consisted of a mathematical model developed from experimental data assessing the motions of the system if acted upon only by the muscle of interest. The result was that the hamstrings acted *kinematically* as hip and knee extensors, while the rectus femoris acted as hip and knee flexors. In both cases, these biarticular muscles were predicted to produce an action in the opposite direction to that of the torque they generate at the knee. This counter-intuitive result at the knee is due to the coupled dynamics of the system and the constraints enforced by the closed rider-bicycle system. Andrews concluded that the active hamstring contributed to knee extension, despite producing a knee flexion torque. This method suggests a different reason for hamstring activation and an apparent need for their contribution during the downstroke.

The idea of biarticular muscles extending joints they are labeled to flex, was not new, as other researchers had already posited this theory (Duchenne, 1885; Hering, 1897, both cited in Kuo, 2001).

In fact, Lombard (1903) explained the effects of muscular leverage of biarticular muscle not only shifted energy through the system but could also cause these muscles to extend joints about which they generate flexion torques. Lombard has been credited with the description of this illogical muscular action, as it is often referred to as Lombard's paradox. In fact, Gregor and colleagues (1985) concluded that the lack of co-contraction during the downstroke "avoided" Lombard's paradox because one of Lombard's conditions for the paradoxical movement of extension was that another two joint muscle had to be active. However, it appears from Andrews (1987) that coupled dynamics and movement constraints could result in paradoxical behavior of a biarticular muscle without Lombard's necessary contribution of an opposing biarticular muscle.

Energy Transfer

The study of *energy* in human movement means different things to different researchers. For example, some researchers have attempted to define the mechanical energy, or work, of an activity, while others have focused on chemical, or metabolic, energy. Many investigations have addressed how these two different energies might relate; specifically, if the mechanical work (energy) can be determined and the metabolic work is measured, then the efficiency of the activity can be calculated. The question of how to determine mechanical energy, which is defined as the sum of potential and kinetic (translational and rotational) energy, began long ago when only kinematic measures were available for data collection (e.g. Braune & Fischer, 1889; Fenn, 1930). A simple way to study mechanical energy during locomotion, particularly the exchange between potential and kinetic energy, can be to study the sinusoidal movement of the center of mass in the sagittal plane (Cavagna & Margaria, 1966; Cavagna, Thys, and Zamboni, 1976). A major assumption with this technique is that the movement of the center of mass represents the sum of all the segment energies. While this is true, it has been shown that treating the human body as a point masses (representing the center of mass) does not adequately explain whole body mechanical energy. For example, limb segments

moving in opposite directions do not affect the movement of the center of mass, and yet there is mechanical energy associated with the movement of the limbs themselves that must be accounted for (Winter, 1979). This idea was not new in the 1960's and 70's, as Fenn (1930) had summed the mechanical energy changes of individual body segment to find the mechanical energy associated with the center of mass. However, the method by which he summated the segmental energies resulted in an inflated overall mechanical power for sprinting of nearly 2200 watts. More recent sprinting studies have resulted in lower powers of 1300 watts – 1600 watts (Ratel, Williams, Oliver & Armstrong, 2004; Morin, Samozino, Bonnefoy, Edouard, & Belli, 2010). The reason this method, and that of others (e.g. Norman, Sharratt, Pizzack & Noble, 1976), over estimates the mechanical power is that it does not take into account the possibility for exchange of potential and kinetic energy within and/or between segments (Winter, 1979; Pierrnowski, Winter, & Norman, 1980; Caldwell & Forrester, 1992).

Not accounting for the exchange between kinetic and potential energy between and within segments will lead to an overestimate of the mechanical work, thus inflating the estimation of the efficiency of the activity as more work would be performed for a given metabolic cost. However, even while accounting for the exchange of energy to determine the segmental energies a clear understanding of the mechanisms for the exchange is necessary. Energy can be transferred from segment-to-segment by the joint reaction force (Quanbury, Winter, & Reimer, 1975). In a sagittal plane inverse dynamics analysis (Elftman, 1939a), the horizontal and vertical joint reaction forces on one segment result in powers due to these forces when multiplied by the linear velocity of the segment joint center in the horizontal and vertical directions (Robertson & Winter, 1980). Calculating these joint force powers of the two segment ends forming the joint in question will illustrate the flow of energy from one segment to the other through the joint center. This energy passively transferred through the joint centers incurs no direct metabolic cost. In the same 2D inverse dynamics analysis, the powers at the ends of the two segments due to the internal joint moments can be determined. By

multiplying the internal joint moment by the angular velocity of each of the segments, the moment powers can be determined for the two segments forming the joint (Robertson & Winter, 1980). For example, if the two segments have angular velocities in the same direction and the moment acts equally in magnitude but opposite in direction on the two segments, the powers are opposite in sign and the energy is said to be transferred from one segment (with the negative power) to the other segment (with the positive power). These moment powers are attributed to the energy generated or absorbed by the muscles surrounding the joint analyzed.

The assumption when determining the moment power and attributing it to muscular action, is that there is only one uniarticular muscle crossing each joint. However, the human musculoskeletal system contains not only several uniarticular muscles crossing a single joint on either side of a joint (specifically, agonist and antagonist muscles) but also biarticular muscles. It is impossible, through the inverse dynamic technique, to determine the individual muscular contributions for a given activity. As such, the metabolic cost of co-contractions by uniarticular muscles is ignored in this type of analysis. Biarticular muscles complicate the picture further because activity in one of these muscles affects two joint moments simultaneously, and an agonist-antagonist pair, like the hamstring and rectus femoris, might also be active. Biarticular muscles are of particular interest in the study of mechanical energy because they affect the mechanical energy of two non-adjacent segments by transferring energy between them (van Ingen Schenau, 1989; Prilutsky, Herzog, & Leonard, 1996, Sasacki, Neptune, & Kautz, 2009). For example, during a jumping task if the gastrocnemius were isometric when the knee is extending during push-off, the ankle would plantar flex purely because the gastrocnemius is attached to the thigh and the calcaneous of the foot.

Pertinent to this project is this transfer of energy via biarticular muscles. If the moment powers of neighboring joints are of opposite sign, this could indicate energy transferred between the non-adjacent segments via a biarticular muscle (Wells, 1988; Prilutsky & Zatskiorsky, 1994). Mathematical methods have been developed to try to account for the energy transfer, or

intercompensation, via biarticular muscles. Intercompensation appears as energy absorbed at one joint and utilized at another. Using a mathematical model of walking, Wells (1988) estimated that the presence of biarticular muscles would reduce the mechanical work over a model that does not allow for intercompensation. Using intercompensation when calculating mechanical energy during walking resulted in a predicted saving of 7 to 29% in mechanical energy cost compared with not including biarticular musculature. Broker and Gregor (1994) confirmed that using intercompensation reduced the estimate of mechanical energy expenditure in sub-maximal pedaling by 20%. Wells postulated that this reduction in mechanical work would reduce the metabolic cost of movement (1) by only activating one muscle rather than two and (2) if the muscle acted isometrically or nearly so. However, he concluded that the effect of intercompensation on metabolic cost could not be described by this type of research because mechanical work and metabolic cost are not equivalent.

Another research group focused on energy transfer by biarticular muscles using musculoskeletal models during different activities, such as jumping and sprinting (Bobbert, Huijing, & van Ingen Schenau, 1986; Bobbert & van Ingen Schenau, 1988; Jacobs, Bobbert, & van Ingen Schenau, 1996). Specifically, 25% of the work done about the ankle during maximal-effort vertical jumping was estimated to be due to a proximal-to-distal flow of energy from the knee to the ankle via the gastrocnemius (Bobbert, et al., 1986). Jacobs et al. (1996) followed with research addressing the transfer of energy between the hip and the knee by the rectus femoris and the hamstrings using the same technique. They concluded that these biarticular muscles transferred work done by larger, proximal uniarticular muscles to distal joints (Figure 2.4). This transfer ensures a necessary high power output at a joint like the ankle without the need for a large distal muscle mass. While this idea does not directly address the metabolic cost effect of transferring energy, it does support the idea that if biarticular muscles transfer energy, there can be a decreased distal muscle mass. This decreased distal muscle mass would decrease the moment of inertia of the limb, making it less costly to move about the hip joint.

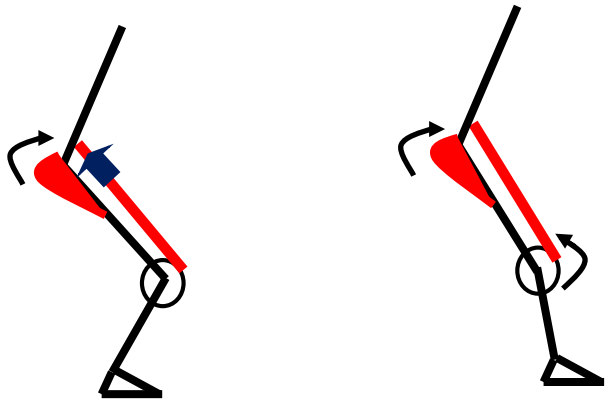

Figure 2.4: Energy transfer between the hip and knee via biarticular muscles. (a) The gluteus maximus (GMAX) generates force while shortening (work), resulting in hip extension. This effectively lengthens (blue arrow) the biarticular rectus femoris (RF) at the hip. (b) If the RF generates enough force to resist lengthening, and remains isometric (no work), the knee will extend. Knee extension is then due to the work performed by the GMAX and not work done by the RF.

Energy transfer during ballistic activities does not, however, directly relate to metabolic consequences. However, this same group built on the concept of energy transfer via biarticular muscles from joint-to-joint using the submaximal activity of pedaling (van Ingen Schenau, 1989; van Ingen Schenau, et al., 1995). The timing of muscle excitation during pedaling appears to support the idea that biarticular muscles distribute the energy from the proximal uniarticular muscles as they control the direction of the external force. The larger, proximal muscles (e.g. vasti, gluteals, and rectus femoris) are active earlier in the pedal cycle than the distal muscles (e.g. soleus and gastroc) (van Ingen Schenau, et al., 1992; van Ingen Schenau, et al., 1995). They believe that not only are these excitation patterns necessary for effective task completion, but also limit "wasteful" eccentric force production to the biarticular muscles. Thus, under this paradigm, uniarticular muscles are work generators and biarticular muscles redistribute that work to properly direct the external force. This conclusion is also contrary to the idea that agonist-antagonist co-contractions are uneconomical, as was claimed by earlier researchers who had observed these same excitation patterns during pedaling (Gregor et al.,1985).

However, there is no evidence of the metabolic effects of these muscular excitation patterns and how they may differ from a musculoskeletal design without biarticular muscles. Only if individual muscular contributions to the metabolic cost of movement are quantified can the contribution of biarticular muscles to metabolic cost be concluded. In addition, the idea of biarticular muscles acting uniquely to direct external force application has recently been challenged. Hasson, et al. (2009) showed evidence in a single-legged pedaling learning task that the uniarticular muscle excitation patterns changed as much as the biarticular muscles as the subjects became more proficient at directing the external force on the crank. Not all subjects followed the same pattern of change and it was concluded that may be due to different learning strategies. Therefore, it appears that the mechanical roles of uni- and biarticular muscles in controlling movements are not yet fully understood, and any assertions that biarticular muscles make movement more economical are still subject to verification (Kuo, 2001).

Energy transfer between two non-adjacent segments has been proposed as a unique mechanism of biarticular muscles. Elftman (1940) stated that energy transfer "is, of course, not unique to two-joint muscles; in one-joint muscles its utility is restricted, however, by the fact that the connect only adjacent parts of the body." This energy transfer differs from the joint-to-joint transfer mentioned previously, in that Elftman is referring to energy transferred from segment-to-segment. Using a musculoskeletal model of pedaling, Kautz and Neptune (2002) demonstrated that both uni- and biarticular muscles can redistribute energy by accelerating and decelerating limb segments. For example, the gastrocnemius and soleus act as shank decelerators during the downstroke. Because of the constraints of the rider-bicycle system knee extension would cause ankle dorsiflexion. If energy from knee extension were used to dorsiflex the ankle, less energy would be available to rotate the crank. Therefore, the gastrocnemius and the soleus are recruited to generate a resistive plantar flexion torque to decelerate the lower leg. This synergism also slows knee extension, which culminates in less energy going into moving the segments and more energy transferred to the crank for external

work. Thus, it appears an evaluation of segment-to-segment energy transfer demonstrates that all muscles may contribute to distributing energy from the muscles to the environment. It is important to recognize that this type of energy transfer is different from the joint-to-joint transfer and does not necessarily negate the possible uniqueness of the energy transferred to distal joints by biarticular muscles.

The effects of this segmental redistribution of energy by the muscles to the environment were not connected to any sort of metabolic consequences by Kautz and Neptune (2002). But it might be speculated from these results that a design with only uniarticular muscles might be able to redistribute energy effectively, bypassing the need for biarticular muscles to transfer energy from one joint to another. Thus, the energetic question would have to be answered by understanding the cost of transferring energy by a given muscle. As was proposed early in the research, biarticular muscles would be more energetically advantageous if they transferred energy or generated necessary torques for the task isometrically or nearly isometrically. Were only uniarticular muscles performing the same actions two muscles would have to be activated rather than one and they would be shortening at higher velocities causing an increased cost. At this time, this question cannot be answered experimentally, as it is not possible to measure individual muscular forces and the associated metabolic cost. Previous researchers have desired to shed light on this question using musculoskeletal models. But as will be discussed, they have not yet answered the long time speculation about the energetic consequences of a musculoskeletal design containing biarticular muscles.

Metabolic Cost

A significant part of this project deals with the metabolic energy used to generate movement via muscular force production, or the metabolic cost of movement. The cost to produce force comes from the energy from biochemical processes, namely the release, use and production of adenosine triphosphate (ATP). Specifically, energy from ATP hydrolyzation by myosin is used during the

cross-bridge cycle (Huxley, 1957) and by sarcoplasmic reticular (SR) calcium pumps to take calcium up from the cytosol back into the SR (MacLennan & Holland, 1975). In the context of this project, this energy usage is important because it is essential to produce movement. Of particular interest is the effect of muscular work on the metabolic cost of movement.

Muscular work is a result of a change in length in conjunction with force production. Nearly a century ago, Wallace O. Fenn (1923) conducted experiments on frog muscle to investigate the relationship of muscular work and metabolic cost. He found that the total energy, heat released plus the muscular work performed, increases as work becomes greater. In fact, this relationship became known as the Fenn effect, which is that the total cost of performing muscular work increases "roughly proportional[ly]" with the amount of work done (Fenn, 1924). Additionally, Hill (1938) showed that the metabolic energy used increased roughly proportionally to the speed of shortening, and not just the work being performed.

These concepts have been supported by others using isolated muscle experiments (Fischer, 1931; Katz, 1939; Hill, 1949; Beltman, et al., 2004); however, using *in vivo* experiments this relationship is difficult to establish. Measuring heat liberated and work produced from individual muscles during activity is much too invasive at this point to perform during human activity. However, using expired gas measurements, metabolic cost of an activity can be estimated. Abbot, Bigland and Ritchie (1952) compared the metabolic cost of forward and backward pedaling at different pedaling rates. First they found that metabolic cost increased with pedaling rate, analogous to the increase seen with shortening of isolated muscle. Additionally, they found that metabolic cost of forward pedaling (analogous to shortening or concentric force production) was greater than backward pedaling (analogous to lengthening or eccentric force production). While isometric activity was not measured, it could be assumed that it would fall somewhere between the two. Bigland-Ritchie & Woods (1976) followed up on this research by relating the cost of forward and backward pedaling to the volume of active muscle estimated from integrated EMG. They found that the oxygen uptake per unit of muscle

activity for forward pedaling was about three times greater than during backward pedaling. However, it is unclear from both studies how, or if, each muscle generated work, as a muscle may have been isometric, and what the metabolic cost incurred by each muscle was.

It appears that the results from whole body activities, such as pedaling, can provide some insight into how muscles as a whole use metabolic energy during an activity; however, it is impossible to determine how each muscle generates work during an activity and how much metabolic energy each muscle uses. Within the context of this project, understanding how individual muscles use energy to produce movement is important, as biarticular muscles may act in a manner that is closer to isometric than uniarticular muscles, and this has been described as being less metabolically costly than concentric force production. Since, this data cannot be collected using experimental data, using a modeling approach may provide the first clear evidence as to how biarticular muscles affect the metabolic cost of movement.

A Modeling Approach

Elftman (1940) had set out to determine the energetic consequences of biarticular muscles during running. Using data from Fenn (1930), he concluded that biarticular muscles decreased the amount of duplicate work performed compared to having only uniarticular muscles generate the calculated joint torques. This means that the uniarticular only model would perform more eccentric muscular action, which would have to be overcome with more concentric activity to generate the necessary joint torques. The muscular energy consumption was estimated by using the relationship that eccentric force production cost 40% of concentric, as no muscle metabolic data were available (Fenn, 1930). This amazing paper-and-pencil solution provides evidence that biarticular muscles decrease the cost of movement. Of special interest is the insight that the biarticular muscles would produce work at slower shortening velocities which would cost less than the faster velocities of the uniarticular muscles. Elftman acknowledged, however, that the additional cost of antagonist activity

or isometric muscular contributions were missing from his calculations. Additionally, this form of analysis did not allow the uniarticular only model a different dynamical solution. The joint torques and angular velocities used to calculate the joint or muscular works were from human experimental data, and this constrained the uniarticular only model to solve those torques. While this paper does provide evidence for energetic savings of biarticular muscles, the question of how much savings still remained and if the movement were unconstrained to experimental data would these results hold.

More recently a simple computational model compared the cost effectiveness of two designs, one with both uni- and biarticular muscles and one with only energetically equivalent uniarticular muscles (Herzog & Binding, 1994). Cost effectiveness was Herzog and Binding's way of quantifying the mechanical energy expenditure, as they could not discuss efficiency because there was no account of metabolic cost in their model. The model contained two rigid segments, with a fixed end, and simple muscles crossing the two joints (Figure 2.5). The joint moments necessary to generate a given force at the free end were determined by a static, non-linear optimization minimizing muscle stress for all joint configurations using each model. The assumption was that if the moments were generated with a minimal amount of muscle force, the metabolic cost would also be minimal. This system predicted that in joint configurations where a biarticular muscle contributed to both joint torques, the model with both uni- and biarticular muscles was more cost effective.

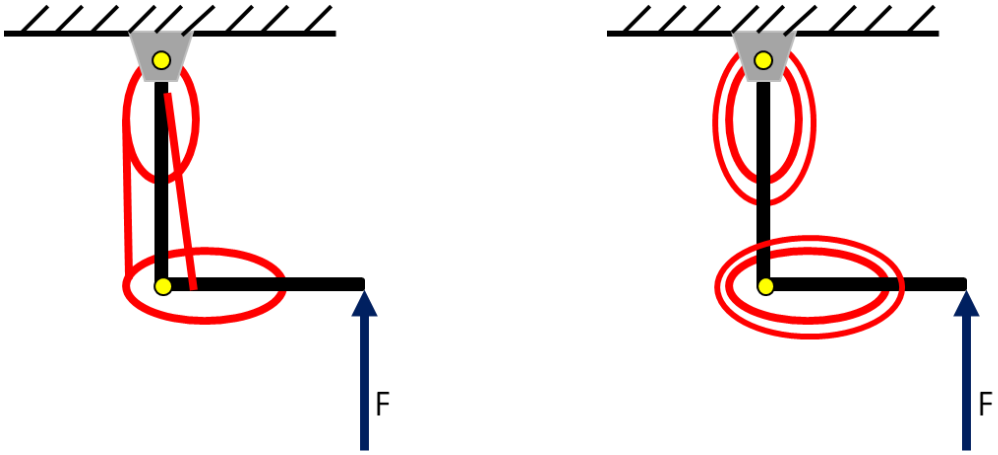

Figure 2.5: Simple two segment, muscle models. The force at the free end (F) is resisted by the muscles while the system was placed in the complete range of joint configurations. (Recreated from Herzog & Binding, 1994)

An example of this situation would be if the hip were extending and the knee were flexing for the biarticular hamstrings. Otherwise, the uniarticular only model was more effective, possibly because it never produced a result involving agonist-antagonist co-contraction. However, the authors point out that as a biarticular muscle contributes to the torque at two joints acting in the same direction (e.g. hip extending, knee flexing) during dynamic movements, the muscle would be acting at a high shortening velocity. Based on the force-velocity curve, the high velocity would limit the amount of force produced by the muscle. This type of muscle contraction would also have a high metabolic cost. The dynamics of muscle activity are not part of a static optimization, to which the authors concede that this type of analysis may not be the best approach for determining the contributions of biarticular muscles to movements. While this research has provided insight into the effect biarticular muscles could have in the human musculoskeletal design, the static analysis and the lack of metabolic representation leaves the question about the impact of biarticular muscles on the metabolic cost of movement unanswered.

A similar comparison of models with and without biarticular muscles was used to investigate the mechanical energy expenditure (MEE) of human walking and running (Prilutsky, Petrova & Raitsin, 1996). The MEE of a given model was determined as the sum of the absolute values of each muscular power from a model, integrated over the time of the gait cycle. Joint moments and powers from experimental data and muscle excitation timings were used to determine muscular activity during the two modes of movement. The model with both uni- and biarticular muscles was determined to have a lower MEE than the uniarticular only model in both walking and running. However, there were some assumptions made in order to calculate the mechanical energy distribution among the modeled muscles. For example, the muscles were modeled as straight lines and no muscle characteristics were included in either of the models (e.g. contractile or series elastic element parameters); thus, there was no detail on muscle dynamics included in the evaluation. The next major assumption was that these authors did not calculate the mechanical energy for the two models during phases of the gait cycles when biarticular antagonistic muscles produced force, or co-contracted. For example, when the rectus femoris and hamstrings or the rectus femoris and the gastrocnemius are simultaneously active no evaluation was performed. Thus, their conclusions were made with a portion of the gait cycle excluded from the analysis. Additionally, no energy transfer or energy released from a previous absorption phase was included in the analysis. Therefore, while Prilutsky, et al. (1996) expanded on the work of Herzog & Binding, (1994) by using a more realistic musculoskeletal model and an actual human movement sequence, the ability to draw direct conclusions regarding the effects of biarticular muscles on the metabolic cost of movement was still limited.

For over a century, the effect of biarticular muscles on human movement has interested many researchers. Some have speculated that biarticular muscles not only contribute to human movement differently than uniarticular muscles, but may also confer an energetic savings. Experimentally, this idea is impossible to confirm, as individual muscle dynamics and energetic costs cannot be determined. Few mathematical models have been used to examine aspects of this question by

replacing biarticular with uniarticular muscles, but they have been constrained to experimental results or have been over-simplified. In addition, other physiological details have not been modeled, such as how the dynamics of movement affect the biarticular muscle's force production or the use of an integrated metabolic cost equation. Therefore, utilizing the techniques of previous researchers by comparing different musculoskeletal designs using a forward dynamic approach, while incorporating a muscle energetics model, could provide evidence of whether or not biarticular muscles minimize the metabolic cost of movement.

Optimization Criteria

Forward dynamics is a method used in biomechanical simulations that can take muscle excitations (on and off timing, and magnitudes) as inputs to predict muscle forces (Pandy, 2001). These forces are then applied to the musculoskeletal system to determine joint torques. The joint torques lead to joint accelerations, which are integrated twice to find musculoskeletal positions (Figure 2.6). This process occurs for each time step simulated from an initial configuration to a final time, representing a full cycle of motion (Pandy, 2001). A comparison of task kinematics and kinetics to exemplar data is often used to evaluate whether the simulation is realistic. The muscle excitations can be found using an optimization process based on a defined goal of the task (Figure 2.7). Finding the excitation inputs for maximal efforts, like maximal height jumping or maximal power pedaling, is straightforward because the goal of the activity is easy to define mathematically. However, determining excitations for submaximal simulations is not an easy process. The goal of the activity is used as a framework, but for submaximal activities, like pedaling, the goal is difficult to define. Minimizing the difference between simulated and experimental data, called a tracking problem, has been used to find muscle excitations of submaximal activities, like pedaling (Neptune & Hull, 1998). But if there are no experimental data available because, for example, a novel movement is simulated or the musculoskeletal design is altered, tracking is not possible. Thus, finding non-tracking criteria that define a submaximal activity is essential for such a study.

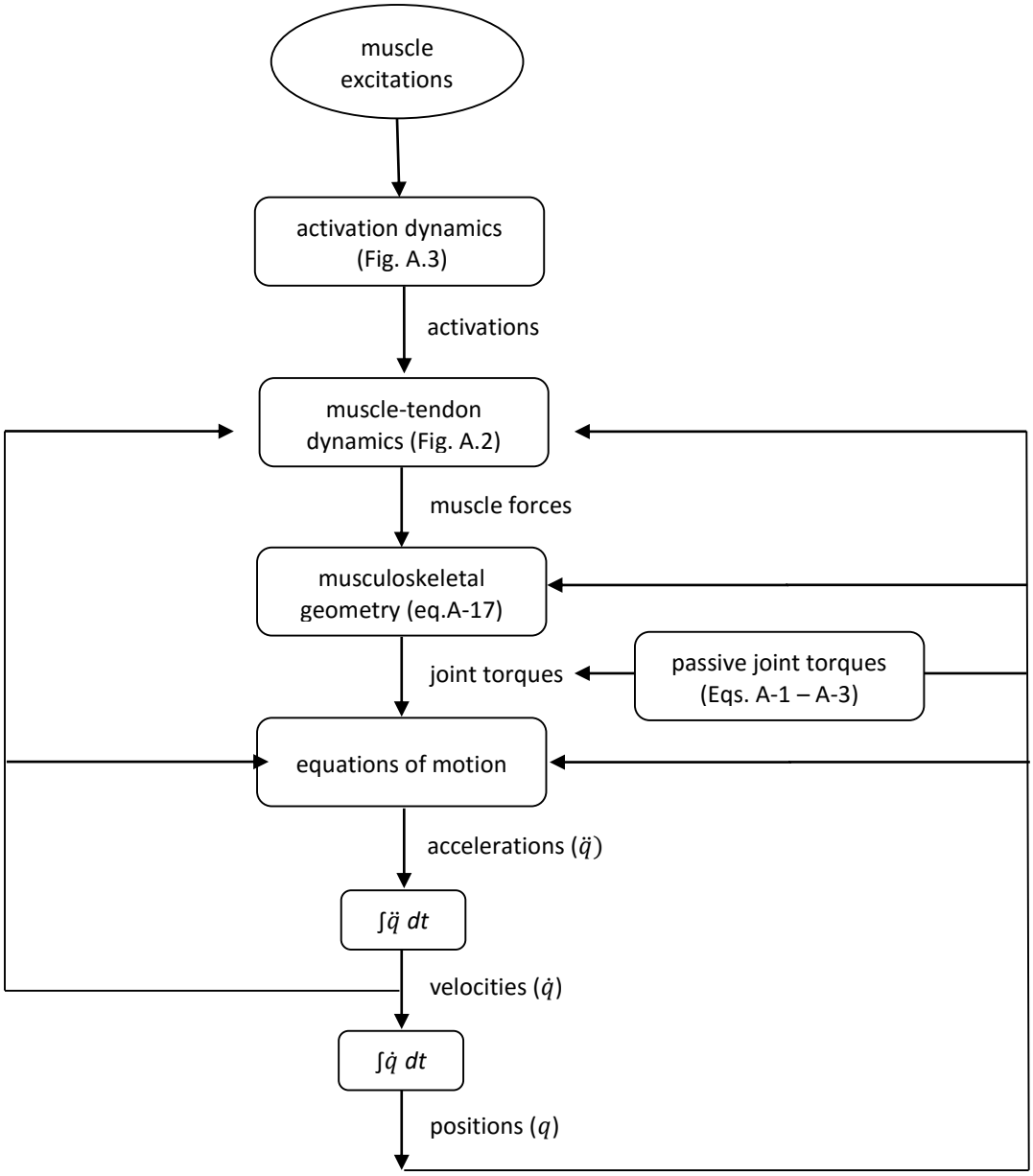

Figure 2.6: Forward dynamic simulation flow-chart. The inputs to forward dynamic simulations are muscle excitation patterns and the outputs are the motions and positions of body segments. Figures and equations listed are found in Appendix A.

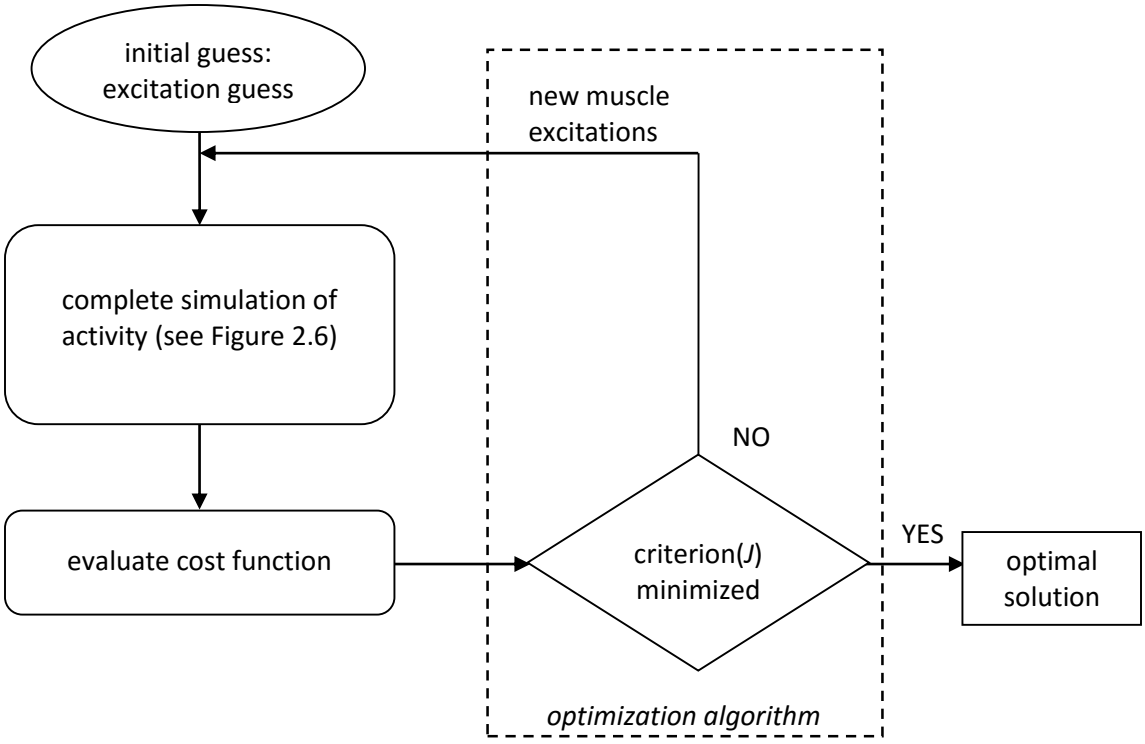

Figure 2.7: A flow chart of the integration of the pedaling simulation into the optimization algorithm. Initial muscle excitations (on, off and magnitude) are used to run a simulation of the activity. Using data from the simulation, a specific cost function is evaluated. New muscle excitations are used to run simulations until a minimum cost function solution is determined. The muscle excitations that resulted in the minimum cost function solution are called the optimal solution, which will be used in single simulation (Figure 2.6) for further analysis of the activity.

The solution for the muscle excitations is found by minimizing (or maximizing) the cost function. Cost functions are mathematical representations of a goal of the task. The results of the muscle excitations are highly sensitive to the cost functions, or performance criteria. Such mathematical representations of submaximal activity have been used to find the excitations for several tasks such as human walking, running and even cat walking. The goal of these optimizations is to distribute the muscular load among the muscles in the model such that it represents human muscle coordination patterns (Seireg & Arvikar, 1974). Of special concern for many researchers has been the inability of such cost functions to replicate co-contractions observed experimentally (Herzog & Leonard, 1991). However, no comprehensive comparison of different non-tracking cost functions

using a forward dynamic simulation of pedaling has been performed. Several cost functions will be discussed and their physiological relevance (or submaximal goal) explained for this review.

Muscle coordination is dictated by the nervous system, but how it does this for submaximal activities is unclear. One suggestion is to minimize whole body metabolic energy. This criterion comes from the idea that humans choose movement patterns so as to minimize the metabolic cost (Ralston, H.J., 1976; Sparrow & Newell, 1998). Anderson and Pandy (2001) minimized the cost of transport to optimize the muscle excitations of 54 muscles in a simulation of human walking. There were some obvious differences between the model and experimental data. The authors presented many reason for these differences, for example, the limitation of pelvic movement and the model of the foot-floor reaction. However, it is encouraging that many similarities between the model and experimental data existed. In contrast, Raasch and Zajac (1999) found that just minimizing a metabolic energy term did not result in a sufficient pedaling simulation. Combining their energy term with a task oriented term, "smooth pedaling", resulted in a simulation that looked like human pedaling. Umberger, Gerritsen, and Martin (2006) used a minimization of energy criterion along with a few tracking variables, and found that the simulation quantitatively resembled experimental data well. Minimizing metabolic cost alone may not result in an adequate simulation of pedaling, but combining it with other performance based criteria may be worth investigating.

A different non-tracking criterion researchers have mathematically represented is fatigue. An early attempt was to minimize muscle stress (Crowninshield & Brand, 1981). This criterion is a gross approximation of the amount of active muscle volume. It has been used by many researchers to solve the force sharing problem, especially in static optimizations. Another fatigue-oriented cost function favors muscles with more slow twitch fibers for low intensity activities (Dul, Johnson, Shiavi, & Townsend, 1984). This criterion was originally used to solve the force sharing problem in cats, and predicted co-contraction of antagonist muscles similar to experimental results. Herzog & Leonard (1991) reported that these two fatigue-based cost functions do not predict co-contractions in a cat

ankle simulation. However, their optimization was constrained to matching the resultant joint moments and the two-joint action of the gastrocnemius and plantaris was not taken into account. A more recent fatigue-based criterion that minimizes the excitation of a muscle generated a realistic simulation of walking, and does not depend on the size or strength of the muscle (Ackermann & van den Bogert, 2010). The idea is that any one muscle will not be used to exhaustion. This cost function found excitations for a running simulation as well (Miller, 2011). However, none of these fatigue-based criteria have been tested in a forward dynamic simulation of pedaling.

Smoothness of movement has been used as a non-tracking criterion as well. The minimization of jerk, the third derivative of position, was an early method used to define smoothness of movement (Flash & Hogan, 1982). Building off this idea, Pandy, Garner and Anderson (1995) developed a criterion that represented smooth muscular force production.. The criterion is defined as the minimization of the derivative of muscular force integrated over time. This is equivalent to minimizing the rate of change of acceleration, or jerk. This cost function was used to optimize the muscle excitations for a sit-to-stand activity. But they found that it only simulated the stand portion, and needed a minimization of stress term to simulate the whole activity. Since the downstroke in pedaling is similar to the standing motion in that the hip and knee are extending simultaneously, it would be appropriate to test this function in a submaximal pedaling optimization. At a more global, task level, the smooth pedaling criterion, mentioned earlier, minimized the difference between the simulated and desired crank angular velocity (Raasch & Zajac, 1999). The authors claimed that the simulation was a reasonable representation of pedaling. However, no kinematic or kinetic comparisons were presented, and the evaluation was based on a visual assessment of the simulated motion. Taking a look at the difference in kinematics and kinetics between the simulation and experimental data would be helpful to evaluate the strength of this cost function.

Conclusion

Biarticular muscles have fascinated researchers for a long time. However, it is still unclear if their function is somehow unique compared with uniarticular muscles. What is even less clear is if they influence the metabolic cost of movement in any meaningful way. Using a musculoskeletal model to simulate submaximal pedaling, a comparison between a design with both uni- and biarticular muscles and a uniarticular-only design could provide evidence as to whether the presence of biarticular muscles in the human musculoskeletal system influences the metabolic cost of movement. A model will also allow for individual muscle mechanics to be evaluated, thus helping to explain the source of any differences in the overall energetic cost. Because the uniarticular-only design does not exist, the solution should be free to choose a different coordination pattern than the unaltered design. Therefore, finding a non-tracking cost function that results in muscle excitations simulating human pedaling is an important step so as to not constrain the novel design to experimental data.

CHAPTER 3 – STUDY ONE PROPOSAL

Optimization Criteria for Submaximal Pedaling

Introduction

The inputs for many forward dynamics simulations of human movement are muscle excitation patterns, which are usually determined by using numerical optimization (Davy & Audu, 1987; Pandy, 2001). The optimization process solves the indeterminate force sharing problem of the redundant human musculoskeletal system. Solving the optimization problem requires one to mathematically define the goal, or optimization criterion, for the movement being studied. Goals such as maximum height jumping (Bobbert, Huijing, & van Ingen Schenau, 1986) or maximal-speed pedaling (Raasch, Zajac, Ma, & Levine, 1997) are relatively easy to define and quantify. However, the goals for submaximal activities are difficult to identify. Thus, optimizing muscle excitation patterns for submaximal activities have proven to be complicated, and often multiple performance criteria, including tracking experimental data, have been incorporated into the cost function (Pandy, Garner, & Anderson,1995; Neptune & Hull, 1998; Umberger, Gerritsen, & Martin, 2003, Umberger, Gerritsen, & Martin, 2006; Vanreterghen, Bobbert, Casius, & Clercq, 2008).

One approach for simulating submaximal activities is to solve a so-called tracking problem, in which the differences between model and experimental data are minimized (Neptune & Hull, 1998). This approach eliminates the need to define the goal of the movement task, but requires one to have a set of experimental data for the movement being studied. Neptune and Hull investigated the viability of using a tracking approach for submaximal pedaling, using seven combinations of performance criteria to determine which cost function resulted in predictions most resembling experimental pedaling data. Two similar cost functions found muscle excitations that matched human pedaling data most completely. One function minimized the difference between crank torque, joint moments, and pedal angle, and the other also constrained the onset and offset timing of the muscles

from electromyography. These two functions tracked the most experimental data, thus it makes sense they would match the experimental data well. However, a cost function that only tracked the crank torque and the pedal angle, also provided a result deemed by the authors as satisfactory (Neptune & Hull, 1998). Neptune, Kautz, and Zajac (2000) used a similar simple cost function, tracking only the radial and tangential pedal forces and the pedal angle, to successfully replicate forward and backward pedaling. Umberger, et al. (2006) minimized the difference between crank torque and pedal angle simulation and experimental data and a minimizing energy consumption term to simulate pedaling. Therefore, tracking relatively few experimental variables has provided reasonable simulations of pedaling.

The method of tracking experimental data is a proven way to simulate submaximal activities, including pedaling, with an unclear goal when there are experimental data. However, this method constrains the researcher to investigating questions for which experimental data are available. If novel movements or musculoskeletal designs are involved in answering a question, experimental data may not be available to track, and a performance based cost function is needed to solve for muscle excitations. Some non-tracking cost functions that have been used to simulate submaximal human movements are based on minimizing fatigue (Crowninshield & Brand, 1981; Dul, Johnson, Shiavi, & Townsend, 1984; Ackermann & van den Bogert, 2010), creating smooth movements (Pandy, Garner, & Anderson, 1995; Raasch & Zajac, 1999), or minimizing metabolic energy cost (Anderson & Pandy, 2001; Umberger, 2010). Some researchers have also combined minimizing metabolic energy with other non-tracking and tracking criteria, to produce simulations of human movement (Raasch & Zajac, 1999; Umberger, et al., 2003). In particular, Raasch and Zajac (1999) reported generating good simulations of submaximal pedaling based on a combined energy and smoothness criterion; however, they did not provide quantitative details on the quality of the simulations. Thus, there is a need to further evaluate the possible approaches that may be used to generate forward dynamics simulations of submaximal pedaling without reliance on tracking experimental data. The goal of this project is to

identify one or more cost functions that may be used to predict muscle excitation patterns for simulating human pedaling without tracking experimental data. The ability of several existing cost functions to optimize muscle excitation onset and offset timings, and magnitudes for submaximal pedaling will be evaluated. The strength of each cost function will be determined by how closely it matches experimental pedaling data.

Methods

Bicycle-Rider Model

A planar, two-legged bicycle-rider model will be used to evaluate the submaximal cost functions. The model is summarized here, with more detail provided in Appendix A. Each leg is represented by three rigid segments: the thigh, shank, and foot. Nine joints are represented: two hips, knees, and ankles, the connection between the pedal and the crank, and the crank center. The hip and crank centers are fixed in space, with the foot fixed to the pedal. The musculoskeletal model contains 18 two component, Hill-type muscle actuators, 9 for each leg. A muscle energetics model is also incorporated (Umberger, et al., 2003), thus individual muscle contributions to the metabolic cost of movement can be predicted (for further explanation of the energetics model, see Appendix A and Umberger, et al., 2003, 2006a, 2006b; Umberger, 2010).

Optimization

Numerical optimization will be used to determine muscle excitation patterns for simulating pedaling at 80 rpm and 200 W. The excitation onset and offset timings and magnitudes will be optimized by minimizing a cost function, J. The general form of J is given by:

$$J = OC_i + pen1 + pen2 \tag{3.1}$$

where OC_i is one of the specific optimization criteria, and $pen1$ and $pen2$ are penalty terms ensuring that the optimization results in simulated pedaling at 80 rpm and 200 watts, respectively. For example, the predicted power output for a simulation run is compared to the desired (200 ± 1% watts). The absolute value of the difference between the two is added to the OC_i term, increasing J.

Crank, pedal and joint angle, horizontal and vertical pedal force, and crank and joint torque data from previously published data will be used for tracking and evaluation of each cost function (Marsh, Martin, and Sanderson, 2000). The muscle onset, offset and magnitudes for the 18 muscles will be optimized using a simulated annealing algorithm (Goffe, Ferrier, & Rogers, 1994; Neptune &

Hull, 1998). Simulated annealing is a robust optimization algorithm that has been used frequently to optimize muscle excitation patterns for obtaining simulations of human movement. A diagram of the integration of the forward dynamic simulation, cost function and the optimization algorithm is presented in Figure 3.1.

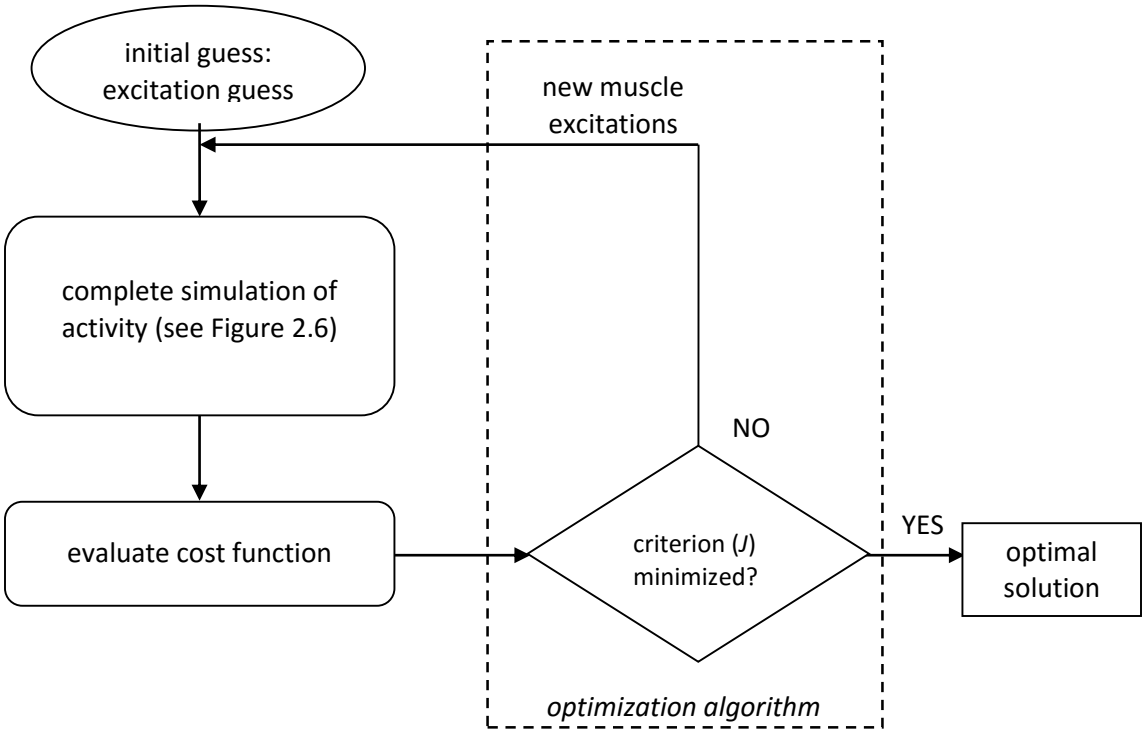

Figure 3.1: Integration of the pedaling simulation and the optimization algorithm.

Cost Functions

The cost functions in this project have been used to find muscle excitation onset and offset timings and magnitudes replicating submaximal movement, but not all have been used with pedaling. Each will be evaluated separately, but further investigation may occur by combining criteria, as others have done (Pandy, et al., 1995; Raasch & Zajac, 1999; Umberger, et al., 2003).

Initially, a cost function tracking several experimental variables will be used to determine the ability of the model to reproduce human pedaling. Neptune and Hull (1998) found tracking data resulted in a simulation resembling experimental kinematic, kinetic and muscle timing and magnitude

for submaximal pedaling (90 rpm and 225 W) usually within ± 1SD of experimental data. The cost function minimizes the difference between the model prediction and experimental data for the pedal forces in the horizontal and vertical directions, the joint moments from the ankle, knee and hip, the crank torque and pedal angle.

$$OC_1 = \sum \frac{\left(F_x - \hat{F}_x\right)}{SD_{F_x}^2} + \sum \frac{\left(F_y - \hat{F}_y\right)}{SD_{F_y}^2} + \sum \frac{\left(M_A - \hat{M}_A\right)}{SD_{M_A}^2} + \sum \frac{\left(M_K - \hat{M}_K\right)}{SD_{M_K}^2} + \tag{3.2}$$

$$\sum \frac{\left(M_H - \hat{M}_H\right)}{SD_{M_H}^2} + \sum \frac{\left(T_{crank} - \hat{T}_{crank}\right)}{SD_{T_{crank}}^2} + \sum \frac{\left(q_{pedal} - \hat{q}_{pedal}\right)}{SD_{q_{pedal}}^2}$$

where the simulated data are represented by

F_x, F_y = right horizontal and vertical pedal forces

M_A, M_K, M_H = right ankle, knee and hip joint moments

T_{crank} = crank torque

q_{pedal} = right pedal angle

and the experimental data are represented by variables with carats. The solution to this problem will represent the minimum tracking error that is possible with the pedaling model. The minimum tracking error will establish a reference against which each of the performance-based optimization criteria will be evaluated.

Minimizing the metabolic cost of movement has resulted in appropriate simulations of human walking (Anderson & Pandy, 2001; Umberger 2010). The musculoskeletal model in the current project incorporates a metabolic energy equation for each muscle (Umberger, et al., 2003), from which the sum of the muscular energetic cost over the pedal cycle can be minimized, and will be termed “MinEnergy”:

$$OC_2 = \sum_{1}^{m} \int_{0}^{t} E_{CE} \tag{3.3}$$

where E_{CE} is contractile element metabolic energy. For all cost function integrals or summations: m is the number of muscles and t is pedal cycle time. Because of the experimental finding that humans self-select gait patterns that minimize energy consumption (Ralston, 1976; Taylor & Heglund, 1982; Cavanagh & Kram, 1985; Sparrow & Newell, 1998) it is possible that this criterion could be added to others to form successful cost functions. For example, Umberger et al. (2006b) combined this term and a few tracking variables (crank torque and pedal angle) to replicate submaximal pedaling.

Raasch & Zajac (1999) combined a task specific criterion with a metabolic cost term to simulate submaximal pedaling. They defined the task specific term as pedaling smoothness term, which minimized the difference between simulated and desired crank angular velocity plus a MinEnergy term. This criterion will be termed "SmoothPedal":

$$OC_3 = \int_0^t \left|\dot{\omega}_{crank} - \dot{\omega}_{average}\right| + \sum_1^m \int_0^t E_{CE} \tag{3.4}$$

where $\dot{\omega}_{crank}$ is the simulated angular velocity of the crank and $\dot{\omega}_{average}$ is the desired crank angular velocity (80 rpm = 8.38 radians per second).

Because coordinated human movements are smooth the criterion of smooth pedaling is task appropriate (Neptune & Kautz, 2001; Rohrer, et al., 2002). Pandy et al. (1995) defined this smoothness by minimizing the time derivative of muscular force for a sit-to-stand simulation. This characterization ultimately represents the smoothness of acceleration, thus minimizing jerk at the muscular level. This criterion will be termed "MinJerk":

$$OC_4 = \int_0^t \sum_1^m (\dot{F}_i^{MT}/F_i^{MAX})^2 dt \tag{3.5}$$

where $\dot{F}_i^{MT}$ is the time derivative of force produced by the muscle i and F_i^{MAX} is its maximal isometric force capability. The sit-to-stand simulation resulted from minimizing this smoothing criterion with a variation of the oft-used static optimization criterion for force sharing problems: minimization of stress (Crowninshield & Brand, 1981). This criterion will be termed "MinStress":

$$OC_5 = \int_0^t \sum_1^m (F_i^{MT}/F_i^{MAX})^2 dt \quad (3.6)$$

where (F_i^{MT}/F_i^{MAX}) is the normalized force.

Muscle excitations were found for a walking simulation by developing a cost function that would not exhaust any single muscle, and avoid quick burst muscle excitations (Ackermann & van den Bogert, 2010). This criterion will be termed "MinACT":

$$OC_6 = -\frac{1}{t_f} \sum_{i=1}^{m} (\int_0^{t_f} A_i^2 \, dt) \quad (3.7)$$

where A is time-varying muscle activation, t_f is the pedal cycle, and m is the number of muscles. Ackerman and van den Bogert (2010) investigated several combinations of the criterion variables, but found equation 3.7 represented walking the best. Recently, this cost function was shown by Miller (2011) to be effective for predicting excitation patterns for a running simulation.

Evaluation

A tracking solution using equation 3.2 will be obtained to determine the ability of the model to replicate human pedaling data. The root mean squared deviation (RMSD) between experimental and simulated data of the crank angle, pedal angle, and ankle, knee and hip joint moments will be calculated. Based on results in the literature, it is expected that the tracking approach will yield RMSD values for these variables that fall within 1 SD of experimental data (Neptune & Hull, 1998). The RMSD values from the tracking solution will be used as a standard by which to judge the performance-based optimization criteria. The RMSD values for these variables will then be calculated for each of the optimization results, and the performance based criteria will be evaluated by how similar the RMSD values are to the tracking RMSD values. The performance based criterion (or potentially criteria) that yield the RMSD value closest to the tracking solution with be regarded as the "best" criterion. It is assumed that the non-tracking criteria will not yield RMSD values as low as

with the tracking solution. Thus, in order for a performance based criterion to be considered acceptable, it must yield an average RMSD value within 2 SD of experimental data. While this threshold is somewhat arbitrary, a level of 2 SD would correspond to simulations that qualitatively resemble human pedaling, and a solution that deviates from the mean by no more than an amount capturing 95% of the population. Additionally, the metabolic cost from a simulation must fall within 2 SD of the experimental data in order to be deemed acceptable.

There is a sound basis for assuming that a performance based function can be used to find excitations to simulate submaximal pedaling. For example, Raasch & Zajac (1999) reported that their cost function (equation 3.4) resulted in muscle excitations that adequately simulated pedaling based on visual evaluation. Moreover, there has been success simulating several other submaximal tasks, such as walking or rising from a chair, using performance based criteria (Pandy et al., 1995; Anderson & Pandy, 2001; Umberger 2010; Ackermann & van den Bogert, 2010). However, if none of the performance based cost functions result in excitations that simulate human submaximal pedaling within 2 SD of experimental data, an alternative approach of tracking only a small number of variables could be used to pursue the goals of Study Two. For example, Umberger et al., (2006) tracked only crank torque and pedal angle data to find excitations which effectively simulated pedaling. The two models of Study Two, one with uni- and biarticular muscles and one with only uniarticular muscles, will have the same joint torque-angle generating capabilities, and it is reasonable to believe that the two models could pedal with similar kinematics and kinetics. A tracking function combining only a few variables dictates some degree of conformance to existent patterns of human movement (e.g. crank torque over the pedal cycle); however, a range of freedom would still remain within theses boundaries to evaluate any apparent coordination, mechanical or energetic uniqueness used by a model with only uniarticular muscles. Sensitivity analyses could also be used to evaluate the impact of loosely constraining the movement patterns.

CHAPTER 4 – STUDY TWO PROPOSAL

Biarticular Muscles and Energetics of Pedaling

Introduction

Some muscles in the human musculoskeletal system cross more than one major joint (i.e., hip, knee, or ankle). These muscles are commonly labeled biarticular, while muscles crossing just one joint are designated as uniarticular. The rectus femoris, semimembranosus and gastrocnemius are some of the major biarticular muscles of the human lower limb. The biomechanical and motor control contributions of biarticular muscles to human movement have inspired over a century of research (Cleland, 1867; Lombard, 1903; Elftman, 1939; Andrews, 1987; Wells, 1988; van Ingen Schenau, 1990; Raasch, Zajac, Ma, & Levine, 1997; Raasch & Zajac, 1999; Hasson, Caldwell, & van Emmerik, 2008). Based on some of the findings, researchers have suggested that biarticular muscles may decrease the metabolic cost of movement relative to an alternative musculoskeletal design consisting only of uniarticular muscles. However, these suggestions have not been investigated directly. Biarticular muscles could potentially decrease the cost of movement if they: (1) contribute to two simultaneous joint torques that are both necessary for task completion, (2) operate at slower velocities than would a comparable pair of uniarticular muscles, (3) transfer energy between joints in a manner that aids task completion and (4) acted as prime contributors directing the external forces on the environment, which might reduce the need for uniarticular muscles to generate negative work. These concepts are difficult to address using an experimental approach which is likely why they have not been tested directly. However, these questions can be addressed using a musculoskeletal modeling technique. This project will use a human musculoskeletal model simulating pedaling to investigate the effect of biarticular muscles on the energetics of movement.

The contributions of individual muscles to joint torques are not discernable from experimental data due to the redundancy of the musculoskeletal system (Elftman, 1939, 1940;

Crowninshield & Brand, 1981). Biarticular muscles further confound our understanding of the muscular contributions to joint torques because they influence two joint torques simultaneously. For example, the force produced by the hamstrings will contribute hip extension and knee flexion torques. If this torque combination is necessary for a task, activating a biarticular muscle may be more cost effective than using two uniarticular muscles. Herzog and Binding (1994) showed that in some joint configurations, having both biarticular and uniarticular muscles could be mechanically effective at producing the necessary joint torques for completing a static task. They compared the results of two models, one with both biarticular and uniarticular muscles and one in which the biarticular muscles were replaced with two uniarticular muscles. The model contained two rigid segments, simplified muscles with no detailed physiological parameters (e.g. series elastic element elasticity or maximum isometric force), and no means for predicting metabolic energy consumption. Extending this approach by using a more detailed musculoskeletal model to study a real-life task such as pedaling could provide more insight as to the effects biarticular muscles have on the metabolic cost of movement.

A detailed musculoskeletal model would also be helpful to evaluate the effects of joint kinematics on the individual muscle velocities during pedaling (Gregoire, Veeger, Huijing, & van Ingen Schenau, 1984). The effect of joint kinematics on uniarticular muscles may be relatively straightforward. For example, the uniarticular vasti muscles lengthen when the knee flexes. Because biarticular muscles cross two joints, their velocities during force production are not as straight forward as uniarticular muscles. For example, if the two joints are acting in the same direction (e.g. extension), a biarticular muscle will lengthen at one joint and shorten at the other (Cleland, 1867; Duchene, 1879). Thus, the biarticular muscle could be producing force isometrically, or nearly isometrically, even in the presence of high joint velocities. Isometric force production is less metabolically costly than with faster muscle shortening velocities (Abbott, Bigland, & Ritchie, 1952; Beltman, van der Vliet, Sargeant, & de Haan, 2004). However, whole muscle-tendon-unit (MTU) velocity does not fully explain the metabolic cost of muscle force production. A muscle-tendon-unit

can be modeled as two elements: contractile (CE) and series elastic (SEE) (Hill, 1938). The CE activity dictates the metabolic cost of a given muscle. Therefore, investigating the changes in the CE velocities is also important to understand the costs incurred by these muscles.

While biarticular muscles may produce force economically by acting isometrically or nearly so, they also serve to transfer energy between the two joints they cross (Cleland, 1867; Elftman, 1966; Bobbert, Huijing, & van Ingen Schenau, 1986; Jacobs, Bobbert, van Ingen Schenau, 1996). Such a transfer of energy can be demonstrated by the activity of the gastrocnemius during jumping (Bobbert, et al., 1986). During the push-off phase, the extensor knee joint power from the quadriceps is resisted by a knee flexor power generated by the gastrocnemius. Because the gastrocnemius also crosses the ankle, the muscular activity about the knee results in an increased plantar flexion power rather than further knee extension. In an activity like pedaling, this proximal-to-distal flow of muscular energy could deliver the muscular power from the larger, proximal muscles to the pedal, decreasing the need for the smaller, distal muscles to produce large amounts of muscular power (Gregorie, et al., 1984). This mechanism could potentially reduce the total volume of active muscle necessary to complete the task, thereby decreasing the metabolic cost of pedaling. Other researchers have used a different, segment-based power analysis to show that both biarticular and uniarticular muscles cause energy to be transferred between segments (e.g. Zajac, Neptune, & Kautz, 2002; Kautz & Neptune, 2002). This segment-to-segment analysis is important to understand how all muscles distribute muscular energy throughout the body. However, it is not as relevant to the current investigation, as this method does not allow the potentially unique function of biarticular muscles to be as clearly identified.

Another unique characteristic of biarticular muscles proposed in the literature is that they play a major role in controlling the direction of forces exerted on the environment (van Ingen Schenau, 1989; van Ingen Schenau, Pratt, & Macpherson , 1994; van Ingen Schenau, et al., 1995). Directing forces on the environment is essential for task completion. For example, during pedaling the crank is always rotating, thus to maintain a desired power output the direction of force that the foot transmits

to the crank must be constantly changing. If biarticular muscles are the main contributors to directing external forces, the uniarticular muscles can be left to contribute positive work to the task (van Ingen Schenau, et al., 1995). It has also been proposed that in order for uniarticular muscles to generate the proper joint torques to direct forces on the environment, they would have to produce more negative work. However, uniarticular muscles have been shown to work in concert with biarticular muscle to direct forces on the environment (Hasson, Caldwell, & van Emmerik, 2008). This study did not elucidate on whether the uniarticular muscles produced negative work while contributing to the direction of external forces. Therefore, there may be a cooperative interaction of uni- and biarticular muscles directing forces on the environment, but how this may affect the metabolic cost of movement has never been directly investigated. However, it could be supposed that a design with both uni- and biarticular muscles would employ minimal positive work as there may be less negative work to overcome. Thus, it might be believed that a design with only uniarticular muscles would produce excessive amounts of negative work to accomplish the task of directing force on the environment. This negative work must be overcome with more positive work to produce the necessary amount of external work, thereby increasing the metabolic cost of completing the task.

The purpose of this project is to formally test whether the mechanical function of biarticular muscles may affect the metabolic cost of movement. Based on the proposed mechanisms through which biarticular muscles may influence the metabolic cost of movement, it is predicted that a design including both uniarticular and biarticular muscles will result in a lower metabolic cost than a design with only uniarticular muscles. The predicted metabolic cost from pedaling simulations using a model with both uniarticular and biarticular muscles will be compared to that of the predicted metabolic cost using a uniarticular-only model. The differences in cost of pedaling (or lack thereof) will be investigated in terms of the contributions that individual muscles make to each of the necessary joint torques, the CE velocities, the energy transfer between joints, and how effectively the pedal force is directed. In addition to replacing all of the major biarticular muscles together, each biarticular muscle

will be replaced individually, to isolate the contribution of each biarticular muscle to any differences that are found in the metabolic cost of pedaling.

Methods

Musculoskeletal Models

A two-legged, sagittal plane bicycle-rider model (see Appendix A) will be used in this project. Each leg is represented by three rigid segments: the thigh, shank, and foot. Four frictionless joints per leg represent the hip, knee, ankle, and the connection between the pedal and the crank. The hip and crank centers are fixed in space, with the foot fixed to the pedal. The synergistic uniarticular muscles (e.g., vastus lateralis, intermedius, and medialis) are combined into a single muscle group, by combining the maximal isometric force values of the muscles included, finding a weighted average of the length of the contractile elements, and optimizing the length of the series elastic element (Winters & Stark, 1985). Thus, the standard musculoskeletal model contains nine Hill-type muscle actuators for each leg, 6 uniarticular and 3 biarticular muscles. The three biarticular muscles are the rectus femoris, biarticular hamstrings, and gastrocnemius, and the six uniarticular muscles are the iliopsoas, gluteus maximus, vastus, biceps femoris short head, soleus and tibialis anterior. A muscle energetics model is also incorporated (Umberger, Gerritsen, & Martin, 2003). Thus individual muscle contributions to the metabolic cost of movement can be determined (for further explanation of the energetics model, see Appendix A and Umberger, et al., 2003; Umberger, 2010). To assess the effect of biarticular muscles on the metabolic cost of movement, the standard model will be modified to include only uniarticular muscles.

Defining the Uniarticular Only Model

The three biarticular muscles represented in the standard model (biceps femoris, rectus femoris, and gastrocnemius) will each be replaced by two uniarticular muscles, creating a novel design containing only uniarticular muscles. There are few examples in the literature where biarticular muscles have been replaced with two “equivalent” uniarticular muscles in musculoskeletal models. Herzog and Binding (1994) divided biarticular muscles into two identical uniarticular

muscles in a simplistic mechanical model. Later this technique of dividing biarticular muscles in half was used to study the mechanical energy in walking and running (Prilutsky, Petrova, & Raitsin, 1996). Both of these studies divided the length of the biarticular muscles in half, while maintaining the same maximal force production and moment arm lengths. However, muscle characteristics, such as contractile element lengths and volumes, or series elastic element lengths and elasticity were not represented in either model, which greatly simplified the process of splitting a biarticular muscle in two. In the proposed study, this general approach is extending to address the partitioning of the internal muscular structure between the two uniarticular muscles that replace a biarticular muscle.

The musculoskeletal geometry of the new uniarticular muscles are defined by the muscle paths of the biarticular muscles of the standard model (Appendix A, Table A-4). Each biarticular muscle pathway is represented by an equation defining the muscle-tendon unit length and the moment arms. A simplified symbolic notion is:

$$L_{MTU} = A_0 + B_1\theta_P + B_2\theta_P^2 + C_1\theta_D + C_2\theta_D^2 \quad (4.1)$$

where A_0 represents the muscle tendon unit length when all $\theta = 0$, B and C are polynomial coefficients representing the muscle pathway at the proximal and distal joints respectively, and θ_P and θ_D are the instantaneous proximal and distal joint angles, respectively. Therefore, within the polynomials for the biarticular muscles, the pathways about each joint they cross are specifically defined. For the new uniarticular muscles, A_0will be divided by two and the corresponding coefficient for a given joint will be used to define the muscular path about that joint. This process will result in two uniarticular muscles that are each half the length and have the same moment arms of the original biarticular muscle:

$$L_{MTU} = {}^{A_0}/_2 + B_1\theta_P + B_2\theta_P^2 \quad (4.2)$$

$$L_{MTU} = {}^{A_0}/_2 + C_1\theta_D + C_2\theta_D^2 \quad (4.3)$$

Muscle parameters, such as maximum isometric force production (F_{MAX}), optimal length of the contractile element (L_{CEOPT}), and the slack length of the series elastic element (L_{SLACK}), are specific for each muscle and will need to be determined for the new uniarticular muscles from the divided biarticular muscles of the standard model. Pennation angle, fiber type and the width of the parabola defining the force length curve are assumed to be the same for all muscles in the model, and will not differ for the new uniarticular muscles. To maintain the force producing capabilities of the biarticular muscle about each joint, F_{MAX} of both uniarticular muscles will be equal to that of the biarticular muscle they replace. Next, L_{CEOPT}, will be divided in two. These two parameters together will ensure that the two uniarticular muscles are exactly half the volume of the biarticular muscles they replace. Finally, since musculoskeletal model torque production is most sensitive to L_{SLACK}, (Lehman & Stark, 1982; Out, Vrijkotje, van Soest, & Bobbert, 1996; Scovil & Ronsky, 2005) an optimization process minimizing the difference between the standard model and the uniarticular-only model isometric joint torques at different joint angles will be used to determine the L_{SLACK} values for the new uniarticular muscles (Gerritsen & van den Bogert, 1995; Umberger, 2003).

The method described will produce a novel musculoskeletal design with 12 uniarticular muscles, with all but one joint crossed by more than one muscle. Synergistic, uniarticular muscles, such as these, were combined in the standard model by combining the maximal isometric force values of the muscles included, finding a weighted average of the length of the contractile elements, and optimizing the length of the series elastic element (Winters & Stark, 1985). For example, three vasti muscles (medialis, lateralis and intermedius) were combined in this way and are represented by one vasti muscle in the standard model. Therefore, a model combining the new uniarticular muscles with the uniarticular muscles from the original model will be developed, resulting in a model with 6 muscles. The pedaling kinematics, kinetics and metabolic cost of this simpler model will be compared to the uniarticular only model with 12 muscles. If the kinematics, kinetics and metabolic cost of the two models are similar, the simpler model with 6 muscles will be used for the analysis explained in

detail later. However, if these two models produce different simulations of pedaling, the two models will be used separately for the analysis, leading to further explanation of the importance of musculoskeletal design on the metabolic cost of movement.

Optimization

The muscle excitation onset, offset, and magnitude patterns for the two model designs will be optimized using a simulated annealing algorithm (Goffe, Ferrier, & Rogers, 1994; Neptune & Hull, 1998). The muscular patterns will simulate submaximal pedaling at 80 rpm and 200W. Therefore, a non-tracking cost function will be used to find the muscle excitations for each model. The cost function used will be based on the results of Study One.

Analysis

The influence of biarticular muscles on the metabolic cost of submaximal pedaling will be assessed by evaluating the contributions of biarticular muscles to pedaling joint torques, muscle-tendon unit and CE velocities as it relates to work, and the joint-to-joint energy transfer of biarticular muscles.

The prediction that the metabolic cost of the uniarticular-only model will be less than the standard model will be tested by simply comparing the predicted costs of the two models. Given the dramatic differences in musculoskeletal geometry between the two models, it would be just as interesting if there were no difference in cost of pedaling. However, there is no statistical method available to subjectively compare the metabolic cost results of these different musculoskeletal designs. Experimental pedaling data shows that across a variety of pedaling rate-power output combinations, 1 SD represents ~10% change in metabolic cost within a subject group (e.g. Chavarren & Calbet, 1999; Belli & Hintzy, 2002; McDaniel, et al, 2002). Thus, 10% difference in the energetic cost of pedaling would represent falling outside the 95% confidence interval within a given group.

For this project, a difference in the energetic costs of the standard and uniarticular only models greater than 10% will be regarded as noteworthy.

The total metabolic cost will provide only a global view of the influence of biarticular muscles on the energetics. Each biarticular muscle may play a specific role for completing the pedaling task, which may lead to a different contribution to the overall metabolic cost of pedaling. To investigate the individual influence of each biarticular muscle to the cost of pedaling, each biarticular muscle will be reinserted one at a time into the uniarticular-only model. This will result in three new models, each with only one biarticular muscle, being used to simulate submaximal pedaling. The assumption will be that the difference in the predicted metabolic cost of each of these designs from the standard model will reflect the influence of the replaced biarticular muscle on the cost of movement. This analysis will provide information on the contributions of biarticular muscles in general to the cost of movement, as well as the relative influence of the three major biarticular muscles in the lower limb.

Net joint torques provide incomplete information as to which muscles are generating the torques. In addition, the effect of antagonist muscles working in opposition to the net joint torques is indiscernible. Musculoskeletal models predict individual muscle activity. This predicted muscular activity will be used to determine if a biarticular muscle in the standard model is simultaneously contributing to two necessary joint torques. For example, during the second half of the downstroke, a hip extension and a knee flexion torque are present. If the biarticular hamstring is active, it would contribute to the two joints torques. To establish whether a biarticular muscle is aiding or opposing the two net joint torques, first the timing of biarticular muscle activity in the standard model during the pedal cycle will be determined. Then, the percentage of that active time the muscles are contributing to the net torques at both joints will be calculated.

At this time, only by using a musculoskeletal model is it possible to estimate the energy transferred by a biarticular muscle (e.g. Bobbert, et al., 1986; Prilutzky & Zatsiorsky, 1994). Bobbert

and colleagues determined the power transferred by a biarticular muscle using the product of the torque produced by the muscle (muscle force × moment arm) and the angular velocity of the joint. For example, if the knee is extending, an active gastrocnemius biarticular muscle will produce a negative power at the knee, illustrating the power transferred from the knee to the ankle via this muscle. In addition, the whole muscle power, CE and SEE powers can also be determined from the model. The integration of each of these power curves yields the total work for the whole pedal cycle. Thus, the CE, SEE, and whole muscle work and the energy transferred by the biarticular muscles can be determined to help explain any energy transfer.

Muscle-tendon unit shortening velocity is dictated by the joint kinematics. For biarticular muscles this can be complicated. For example, if the hip and knee are extending, the biarticular hamstring will be shortening at the hip and lengthening at the knee. These kinematics could lead to force production in the MTU that is nearly isometric, resulting in very little MTU work being done. However, the CE could be shortening while the MTU is producing very little work. In addition, MTU work does not dictate the energetics of the muscle, rather the CE work does. The MTU and CE work about each joint will be compared between the standard and uniarticular-only model to help explain the distribution of work and the source of the metabolic cost. The net muscle power output will be the same between the two models (i.e., equal to the average power output per pedal cycle of 200 W), thus this analysis will provide information on the distribution of work among the muscles.

The ability of each design to direct force on the pedal will be studied by comparing pedal reaction forces from the simulations. The net pedal reaction force of the right pedal will be decomposed into tangential (or rotational) and radial forces with respect to the crank. The rotational component directly relates to the amount of crank torque produced. Since the average power and average pedaling rate are the same for all models, the average torque will have to be the same. However, the way in which each model produces the crank torque through the pedal cycle will help

explain the effectiveness of the application of force. An index of force effectiveness (IE) will be determined as a percentage over the whole crank cycle by:

$$IE = \frac{\int_0^{2\pi} F_{Tan}(\theta) \times d\theta}{\int_0^{2\pi} F_{Tot}(\theta) \times d\theta} \times 100 \quad (4.4)$$

where, $F_{Tan}(\theta)$ is the tangential force and $F_{Tot}(\theta)$ is the resultant force, as a function of crank angle (Coyle, et al., 1991). If a difference in metabolic cost exists between the two designs, any change in the percent tangential pedal force between the two designs may help explain the results.

CHAPTER 5

MODIFICATIONS SUBSEQUENT TO THE PROPOSAL

To test the hypothesis that biarticular muscles reduce the metabolic cost of pedaling, the proposed research proposed in STUDY TWO called for using a standard model that possessed all three of the major biarticular muscles (hamstrings, rectus femoris and gastrocnemius), three models where only a single biarticular muscle was replaced by two uniarticular muscles, and two variants of a model where all of the three major biarticular muscles were simultaneously replaced by uniarticular muscles (one version with six muscles and another version with 12 muscles). To make the comparisons fair among the models, constraints were established such that the various non-standard models were required to generate the same isometric joint torque-angle relations and have the same total muscle volume as the standard model. It was possible to simultaneously satisfy these constraints for the three models where only a single biarticular muscle was replaced; however, it was not possible to simultaneously satisfy both constraints for either variant of the model where all of the biarticular muscles were replaced. Nearly 100 optimizations were run over the course of more than one year in an effort to find values for several different combinations of musculoskeletal parameter values that could satisfy both constraints, but to no avail. The difficulty arose primarily from having to simultaneously match a set of target hip extension, knee flexion and ankle plantar flexion joint torques over a wide range of joint angles without the biarticular hamstrings or biarticular gastrocnemius. Matching the target joint torques with the uniarticular hamstrings and gastrocnemius muscles was only possible with a considerably greater total muscle volume, which would have confounded comparisons of metabolic energy consumption with the standard model. Due to the greater muscle volume needed to match the isometric joint torques in the standard model, the predicted metabolic cost of pedaling for both variants of the model without biarticular muscles would

certainly have been considerably greater than in the standard model, and preliminary pedaling simulations that were conducted suggest that was indeed the case. Such a result is consistent with the findings presented in Study 2, though without the scientific controls deemed necessary to have adequate confidence in the results. Therefore, Study 2 was conducted using the standard model and the three models where only a single biarticular muscle was replaced at a time.

CHAPTER 6

OPTIMIZATION CRITERIA FOR SUBMAXIMAL PEDALING

Introduction

The inputs for many forward dynamics simulations of human movement are muscle excitation patterns, which are usually determined using numerical optimization (Davy & Audu, 1987; Pandy, 2001). The optimization process solves the indeterminate force sharing problem of the redundant human musculoskeletal system. Solving the optimization problem requires one to mathematically define the goal, or optimization criterion, for the movement being studied. Goals such as maximum height jumping (Bobbert, Huijing, & van Ingen Schenau, 1986) or maximal-speed pedaling (Raasch, Zajac, Ma, & Levine, 1997) are relatively easy to define and quantify. However, the goals for submaximal activities are more difficult to identify. Thus, optimizing muscle excitation patterns for submaximal activities has proven to be complicated, and often multiple performance criteria, including tracking experimental data, have been incorporated into the cost function (Pandy, Garner, & Anderson, 1995; Neptune & Hull, 1998; Umberger, Gerritsen, & Martin, 2003, Umberger, Gerritsen, & Martin, 2006; Vanreterghen, Bobbert, Casius, & Clercq, 2008).

One approach for simulating submaximal activities is to solve a so-called tracking problem, in which the differences between model and experimental data are minimized (Neptune & Hull, 1998). This approach eliminates the need to define the goal of the movement task, but requires one to have a set of experimental data for the movement being studied. Neptune and Hull investigated the viability of using a tracking approach for submaximal pedaling, using seven different combinations of tracking variables to determine which cost function resulted in predictions most resembling experimental pedaling data. Two similar cost functions resulted in muscle excitations that matched human pedaling data most completely. One function minimized the differences between crank torque,

joint moments, and pedal angle, and the other also constrained the onset and offset timing of the muscles based on experimental electromyography data. These two functions tracked the most experimental data variables, thus it makes sense they would match the experimental data well. However, a cost function that only tracked the crank torque and the pedal angle also provided a result deemed by the authors as satisfactory (Neptune & Hull, 1998). Neptune, Kautz, and Zajac (2000) used a similar simple cost function, tracking only the radial and tangential pedal forces and the pedal angle, to successfully replicate forward and backward pedaling. Umberger, et al. (2006) minimized the difference between simulated and experimental crank torque and pedal angle data and minimized metabolic energy consumption to simulate submaximal pedaling. Therefore, tracking relatively few experimental variables can provide reasonable simulations of pedaling.

The method of tracking experimental data is a proven way to simulate submaximal activities, including pedaling, where the goal of the task is unclear and experimental data are available. However, this method constrains the researcher to investigating questions for which experimental data are available. If novel movements or musculoskeletal designs are involved in answering a question, then a performance-based cost function is needed to solve for muscle excitations. Some non-tracking cost functions that have been used to simulate submaximal human movements are based on minimizing fatigue (Crowninshield & Brand, 1981; Dul, Johnson, Shiavi, & Townsend, 1984; Ackermann & van den Bogert, 2010), creating smooth movements (Pandy, Garner, & Anderson, 1995; Raasch & Zajac, 1999), or minimizing metabolic energy cost (Anderson & Pandy, 2001; Umberger, 2010). Some researchers have also combined minimizing metabolic energy with other non-tracking and tracking criteria, to produce simulations of human movement, in particular, pedaling (Raasch & Zajac, 1999; Umberger, et al., 2006). Raasch and Zajac (1999) reported generating good simulations of submaximal pedaling based on a combined energy and smoothness criterion; however, they did not provide quantitative details on the quality of the simulations. Thus, there is a need to further evaluate the possible approaches that may be used to generate forward dynamics simulations

of submaximal pedaling without reliance on tracking experimental data. The goal of this project is to identify one or more cost functions from the literature that may be used to predict muscle excitation patterns for simulating human pedaling without tracking experimental data.

Methods

Bicycle-Rider Model

A planar, two-legged bicycle-rider model was used to evaluate the submaximal cost functions. The model is summarized here, with more detail provided in Appendix A. Each leg was represented by three rigid segments: the thigh, shank, and foot. Nine joints were represented: two hips, knees, and ankles; the connection between each pedal and the crank; and the crank center. The hip and crank centers were fixed in space, with the foot fixed to the pedal. The musculoskeletal model contained 18 two component, Hill-type muscle actuators, 9 for each leg: gluteals (GMAX), iliospsoas (PSOA), hamstrings (HAMS), rectus femoris (RECT), biceps femoris short head (BFSH), vastii (VAST), gastrocnemius (GAST), soleus (SOLE) and tibialis anterior (TIBA). A muscle energetics model was also incorporated (Umberger, et al., 2003), thus individual muscle contributions to the metabolic cost of movement were predicted (for further explanation of the energetics model, see Appendix A and Umberger, et al., 2003, 2006a, 2006b; Umberger, 2010).

Optimization

Numerical optimization was used to determine muscle excitation patterns for simulating pedaling at 80 rpm and 200 W. The excitation onset and offset timings and magnitudes were optimized by minimizing a cost function, J. The general form of J is given by:

$$J = \gamma_1 OC_i + \gamma_2 pen1 + \gamma_3 pen2 + \gamma_4 pen3 + \gamma_5 pen4 \quad (6.1)$$

where OC_i is one of the specific optimization criteria (optimization criterion), and $pen1$, $pen2$, and $pen3$ are penalty terms which ensured that the optimal solution pedaled at 80 rpm, 200 watts and completed four full pedal revolutions, (deviations from top dead center for the final crank angle were

penalized), respectively. For the non-tracking cost functions, a penalty on passive joint moments, *pen*4, was also included to prevent extreme joint postures (Miller, Umberger, Hamill & Caldwell 2012). Weights (γ) were determined for each term for a given cost function combination (Table 6.1). Cost function weights were assigned such that all terms were of the same order of magnitude, and penalty weights were heuristically set as low as possible while still achieving the desired effect (e.g., matching the target cadence).

Table 6.1: Weight values of each term for a given cost function. SMOOTH ENERGY, not listed and explained further below, had the same weighing scheme as ENERGY plus the SMOOTH term which was multiplied by 100.

	Cost function	**Pedaling Rate (pen1)**	**Crank Power (pen2)**	**Crank Angle (pen3)**	**Passive Moments (pen4)**
TRACKING	1	10	10	25	-
STRESS	0.0000001	10	10	0.001	0.01
ACT	100	10	10	0.0001	0.01
ENERGY	0.01	10	10	0.1	0.01
FDOT	1	10	10	0.01	0.01

Previously published crank and pedal angles, pedal forces, and crank and joint torques were used for tracking and evaluation of each cost function (Marsh, Martin, & Sanderson, 2000). The experimental pedaling data were from 24 males (25.8 ± 4.7 yrs, 74.5 ± 7.8 kg, 176.9 ± 7.0 cm) with varying pedaling experiences: cyclists, runners and less trained non-cyclists. The muscle onset, offset and magnitudes for the 18 muscles were optimized using a parallel simulated annealing algorithm (Higginson, Neptune, & Anderson, 2005) that was run on a small computer cluster with 8 nodes.

Simulated annealing is a robust optimization algorithm that has been used frequently to optimize muscle excitation patterns for obtaining simulations of human movement. For each cost function, four different initial guesses for activation onset and offset timings and magnitudes were each used twice to find an optimal solution. From these 8 solutions, the lowest cost function solution was then used twice more to find a better cost function solution. The lower solution of these two is reported as the optimal solution.

Cost Functions

The cost functions in this project have been previously used to generate simulations of submaximal human movements, but not all have been used with pedaling. Initially, a cost function tracking several experimental variables was used to determine the ability of the model to reproduce human pedaling. Neptune and Hull (1998) found that tracking data resulted in a simulation resembling experimental kinematic, kinetic and muscle timing and magnitude for submaximal pedaling (90 rpm and 225 W) usually within ± 1SD of experimental data. The cost function minimizes (equation 6.2) the difference between the model prediction and experimental data for the pedal forces in the horizontal and vertical directions, the joint moments from the ankle, knee and hip, the crank torque and pedal angle. This cost function is referred to as "TRACKING." The solution to this problem represents the minimum tracking error that is possible with the pedaling simulation.

$$TRACKING = \sum \frac{\left(F_x - \hat{F}_x\right)}{SD_{F_x}^2} + \sum \frac{\left(F_y - \hat{F}_y\right)}{SD_{F_y}^2} + \sum \frac{\left(M_A - \hat{M}_A\right)}{SD_{M_A}^2} + \sum \frac{\left(M_K - \hat{M}_K\right)}{SD_{M_K}^2} + \tag{6.2}$$

$$\sum \frac{\left(M_H - \hat{M}_H\right)}{SD_{M_H}^2} + \sum \frac{\left(T_{crank} - \hat{T}_{crank}\right)}{SD_{T_{crank}}^2} + \sum \frac{\left(q_{pedal} - \hat{q}_{pedal}\right)}{SD_{q_{pedal}}^2}$$

where the simulated data are represented by

F_x, F_y = right horizontal and vertical pedal forces

M_A, M_K, M_H = right ankle, knee and hip joint moments

T_{crank} = crank torque

q_{pedal} = right pedal angle

and the experimental data are represented by variables with carats.

The first of the performance-based cost functions (equation 6.3) is minimization of metabolic cost. Minimizing the metabolic cost of movement has resulted in appropriate simulations of human walking (Anderson & Pandy, 2001; Umberger 2010). The musculoskeletal model in the current project incorporated a metabolic energy equation for each muscle (Umberger, et al., 2003), from which the sum of the muscular energetic cost over the pedal cycle is minimized, and is termed "ENERGY":

$$ENERGY = \sum_{1}^{m} \int_{0}^{t} \dot{E}_{CE} \tag{6.3}$$

where $\dot{E}_{CE}$ is the rate of metabolic energy consumption of the contractile element. For this and all cost function integrals or summations: m is the number of muscles and t is pedal cycle time.

Raasch & Zajac (1999) combined a task-specific criterion with a metabolic cost term to simulate submaximal pedaling. They defined the task specific term as a pedaling smoothness term, which minimized the difference between simulated and desired crank angular velocity plus an ENERGY term (equation 6.4). This criterion is termed "SMOOTH ENERGY":

$$SMOOTH\ ENERGY = \int_{0}^{t} \left| \dot{\omega}_{crank} - \dot{\omega}_{average} \right| + \sum_{1}^{m} \int_{0}^{t} \dot{E}_{CE} \tag{6.4}$$

where $\dot{\omega}_{crank}$ is the simulated angular velocity of the crank and $\dot{\omega}_{average}$ is the desired crank angular velocity (80 rpm = 8.38 radians per second).

Because coordinated human movements are smooth the criterion of smooth pedaling is task appropriate (Neptune & Kautz, 2001; Rohrer, et al., 2002). Pandy et al. (1995) defined this smoothness by minimizing the time derivative of muscular force for a sit-to-stand simulation (equation 6.5). This characterization ultimately represents the smoothness of acceleration at the muscular level. This criterion is termed "FDOT":

$$FDOT = \int_0^t \sum_1^m (\dot{F}_i^{MT}/F_i^{MAX})^2 dt \tag{6.5}$$

where $\dot{F}_i^{MT}$ is the time derivative of the force produced by muscle i and F_i^{MAX} is its maximal isometric force capability. The sit-to-stand simulation resulted from minimizing this smoothing criterion with a variation of the oft-used static optimization criterion for force sharing problems: minimization of stress (Crowninshield & Brand, 1981) (equation 6.6). This criterion is termed "STRESS":

$$STRESS = \int_0^t \sum_1^m (F_i^{MT}/F_i^{MAX})^{exp} dt \tag{6.6}$$

where (F_i^{MT}/F_i^{MAX}) is the normalized force. The positive integer of *exp* will be explained further in the next section.

Muscle excitations were found for a walking simulation by developing a cost function that would not exhaust any single muscle, and avoid brief, large muscle excitation bursts (Ackermann & van den Bogert, 2010) (equation 6.7). This criterion is termed "ACT":

$$ACT = -\frac{1}{t_f}\sum_{i=1}^{m}\left(\int_0^{t_f} A_i^{exp}\, dt\right) \tag{6.7}$$

where A is time-varying muscle activation, t_f is the pedal cycle, and m is the number of muscles. The positive integer of *exp* will be explained further in the next section.

Exponents for STRESS and ACT cost functions

Crowninshield and Brand (1981) and Ackerman and van den Bogert (2010) initially investigated several possible exponents for their respective cost functions. Both concluded that exponents greater than 1 replicated walking relatively well. Greater exponents disproportionately penalize larger muscle stresses or activations, decreasing the possibility of only a few muscles contributing to meeting the task demands, which can happen with lower exponents (Ackermann & van den Bogert, 2010; Rasmussen, Damsgaard, and Voigt, 2001) . For this project, exponents of 2, 3 and 10 were investigated for both STRESS and ACT. Briefly, the exponent 10 was most successful at replicating human pedaling for both STRESS and ACT, so these results will be presented. The use of a large exponent is supported by the min/max concept evaluated by Rasmussen, et al. (2001), in that a few muscles should not be overloaded.

Evaluation

A tracking solution using equation 3.2 was obtained to determine the ability of the model to replicate human pedaling data. The root mean squared deviation (RMSD) between experimental and simulated data of the crank angle, pedal angle, and ankle, knee and hip joint moments was calculated. RMSD was expressed in multiples of the between-subject standard deviation for each variable. Based on results in the literature, it was expected that the tracking approach would yield RMSD values for these variables that fell within 1 SD of experimental data (Neptune & Hull, 1998). Simulations were also generated for each of the performance-based cost fucntions. The RMSD values for the tracking

variables were calculated for each of the performance-based cost function results. It was assumed that the non-tracking criteria would not yield RMSD values as low as the tracking solution. Thus, in order for a performance-based criterion to have been considered acceptable, it was to yield an average RMSD value within 2 SD of experimental data. While this threshold is somewhat arbitrary, a level of 2 SD would correspond to simulations that qualitatively resemble human pedaling, and a solution that deviates from the mean by no more than an amount capturing 95% of the population.

Additionally, for a solution to be considered acceptable the metabolic cost and muscle activations need to be physiologically appropriate. Metabolic power is compared to a range of literature values for pedaling at 200 W, 80 RPM (Abrantes, Sampaio, Reis, Sousa, & Duarte, 2011; Foss & Hallen, 2004; Belli & Hintzy, 2002; Marsh, Martin & Foley, 2000; Böning, Gönen & Maassen, 1984; Coast & Welch, 1985; Takaishi, Yamamoto, Ono, Ito, & Moritani, 1998). Whole body energy rate was determined by summing the energy rate of 18 muscles during the final pedal revolution, plus the energetic contribution of the rest of the body (3.2 W/kg). The energy rate of the rest of the body (187.72 W) was taken from Umberger, Gerritsen and Martin (2006). This rate represents pedaling at 80 RPM against no load. Muscle activation on- and offset timings were compared to EMG data drawn from the literature (Umberger et al., 2006). No EMG data for the biceps femoris short head muscle were collected.

Results

Tracking

The data-tracking simulation replicated the gross kinematics and kinetics of pedaling at 200 W, 80 RPM within 1 SD (Figure 6.1). Crank torque was replicated most closely (0.43 SD) and the knee moment was least closely (0.79 SD) (Table 6.2). The predicted metabolic energy consumption was within the range of value from the literature, but was near the upper end of the range at 1063.30 W (3.34 L·min^{-1}) (Figure 6.1). Visually, the muscle activation timing (on- and off-sets) were replicated well via the tracking solution (Figure 6.2).

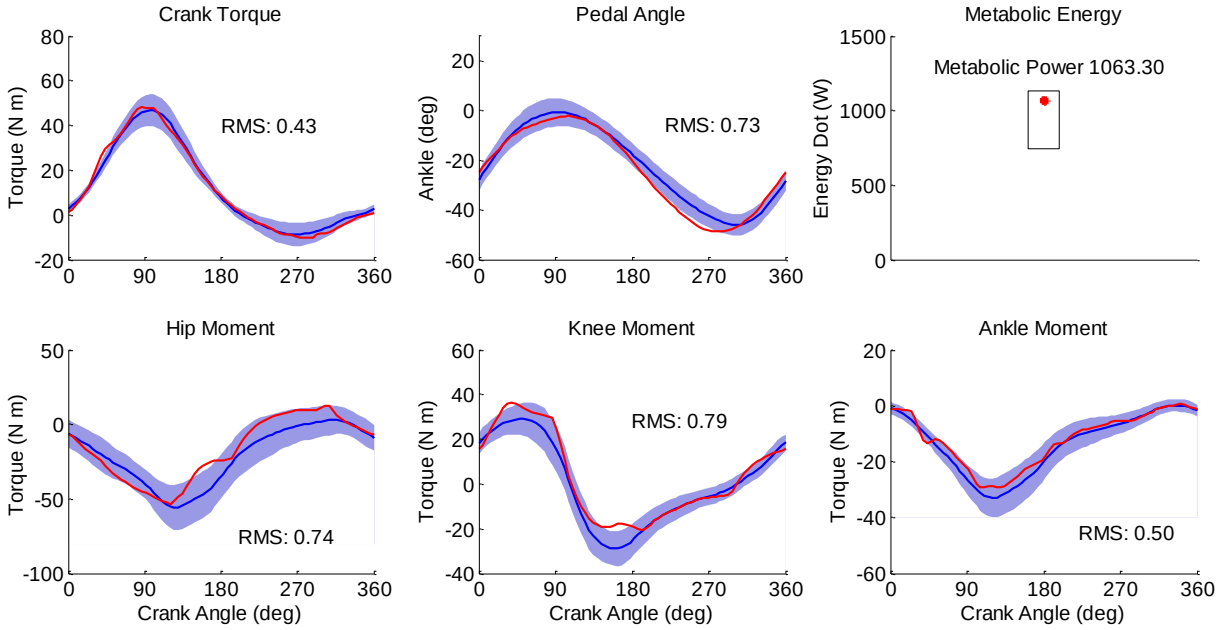

Figure 6.1: Kinematic (pedal angle), kinetic (crank torque and joint moments) and energetic variables of submaximal pedaling at 200W and 80 RPM as predicted by data-tracking compared with experimental data. The blue line represents experimental means, with blue shaded area as 1 SD (Marsh, Martin, & Sanderson, 2000). The red line is the predicted values by TRACKING. In the Metabolic Energy figure, the red dot represents the simulated metabolic power and the box represents the range of experimental data from the literature (Abrantes, Sampaio, Reis, Sousa, & Duarte, 2011; Foss & Hallen, 2004; Belli & Hintzy, 2002; Marsh, Martin & Foley, 2000; Böning, Gönen & Maassen, 1984; Coast & Welch, 1985; Takaishi, Yamamoto, Ono, Ito, & Moritani, 1998). Other kinematic and kinetic data is reported in Appendix A.

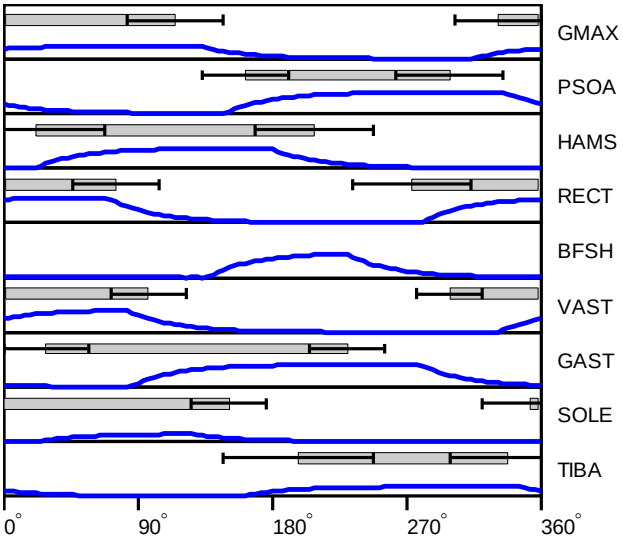

Figure 6.2: Muscle activations for the nine muscles, labeled on the right axis, from TRACKING (BLUE line) compared to experimental data (GREY bars with standard deviations) for a complete pedal cycle, x-axis (0° – 360°). The height of the blue line represents the activation magnitude, between 0% and 100%. No activation magnitude is represented for the experimental data.

Performance-based Cost Functions

All five performance-based cost functions predicted the gross kinematics and kinetics of pedaling at 200 W, 80 RPM relatively well (Figure 6.3). The average RMSD for STRESS (1.27 SD) and ACT (1.55 SD) fell well within the 2 SD limit that we established; SMOOTH ENERGY (1.97 SD) and ENERGY (2.05 SD) were near 2 SD, and FDOT (2.16 SD) had the highest average RMSD (Table 6.2).

The results for the individual variables for each cost function are shown in Table 6.2 and Figures 6.3 and 6.4. All five performance-based cost functions replicated the hip moment and crank torque within 2 SD. Whereas, the knee moment was the worst replicated variable; only ACT (1.80 SD) replicated the knee moment within 2 SD. In addition, only STRESS (1.65 SD) was able to predict a pedal angle within 2 SD. All metabolic energy values fell within the range of literature

values, with ENERGY predicting the lowest energy (824.5W) and ACT the highest energy (1018.6W).

Table 6.2: Results of individual kinematic, kinetic and energetic variables predicted from all cost functions. The values for all but the Metabolic Energy are reported as RMSD compared to experimental data. The Metabolic Energy is reported in watts.

COST FUNCTION	Crank torque	Pedal angle	Hip torque	Knee torque	Ankle torque	Average RMS	Metabolic Energy
TRACKING	0.37	0.74	0.71	0.84	0.52	0.64	1063.3
STRESS	1.01	1.65	0.55	2.26	0.87	1.27	1015.2
ACT	0.85	2.49	0.84	1.80	1.78	1.55	1018.6
SMOOTH ENERGY	1.40	2.59	0.93	3.11	1.84	1.97	897.9
ENERGY	1.69	2.56	1.33	2.76	1.95	2.06	824.5
FDOT	1.54	2.88	0.60	3.69	2.07	2.16	1006.1

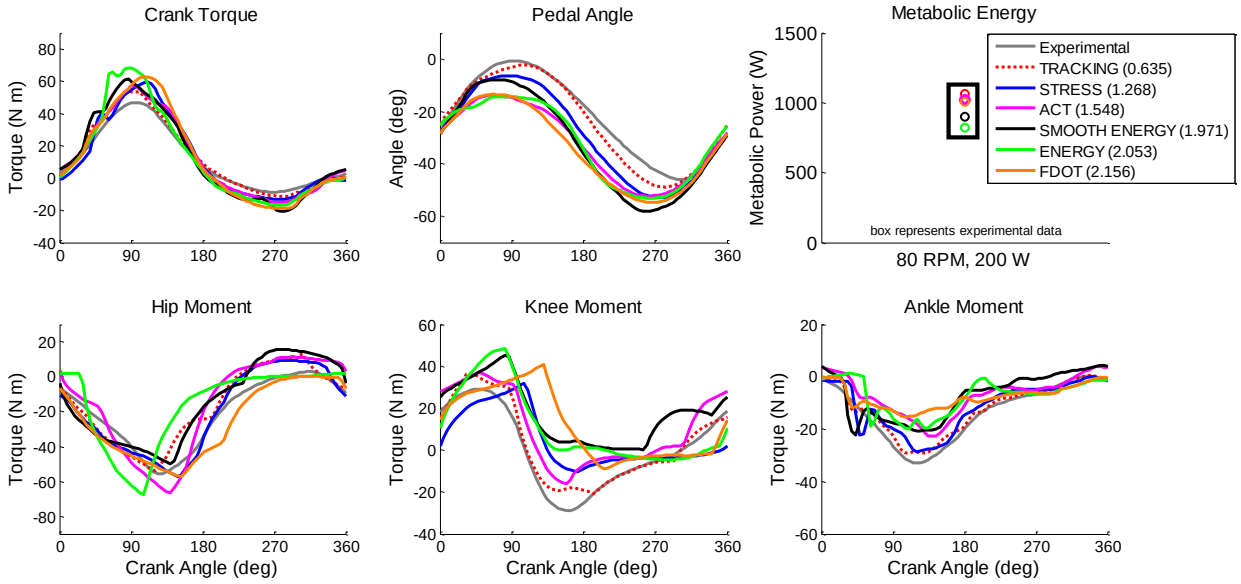

Figure 6.3: Predicted kinematic, kinetic and energetic values of all cost functions. For clarity, standard deviations for the experimental data is not represented, but it is the same as in Figure 6.1.

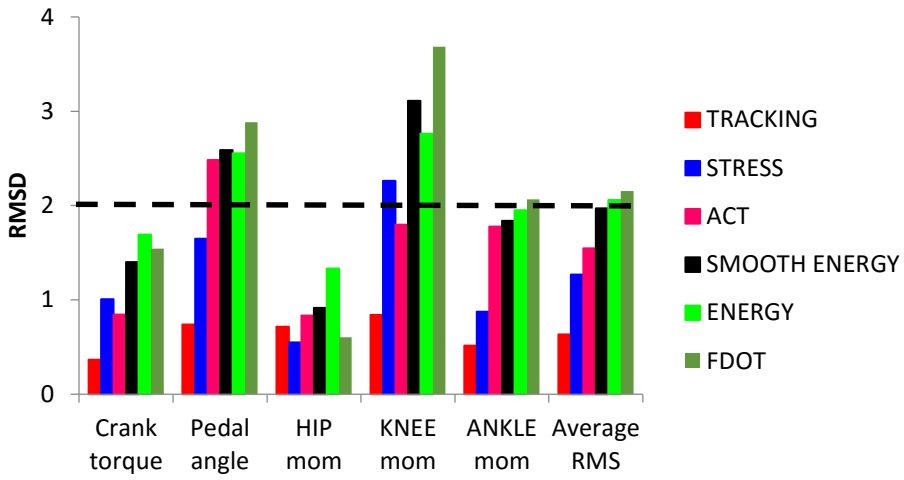

Figure 6.4: A summary of individual predicted RMSD values of the kinematic and kinetic variables for each performance-based cost function. The dashed line indicates the 2 SD cut off.

In general, for all five performance-based cost functions, when a muscle was active, its on- and off-set timing was similar to the TRACKING results (Figure 6.5) which was already shown to be physiologically appropriate compared to the experimental data (Figure 6.2). However, SMOOTH ENERGY and ENERGY did not activate all muscles (Figure 6.5), and FDOT predicted five of the nine muscle activations under 15% of maximal, including BFSH with an activation level of 2% (Figure 6.6). SMOOTH ENERGY and ENERGY compensated for the inactive muscles with near maximal activations in RECT and GMAX, respectively. Visually, STRESS and ACT each replicate the timings relatively well (Figure 6.5), and have reasonable magnitudes (Figure 6.6). It should be noted, however, that for STRESS, the tibialis anterior (TIBA) is active during most of the pedal cycle (Figure 6.5).

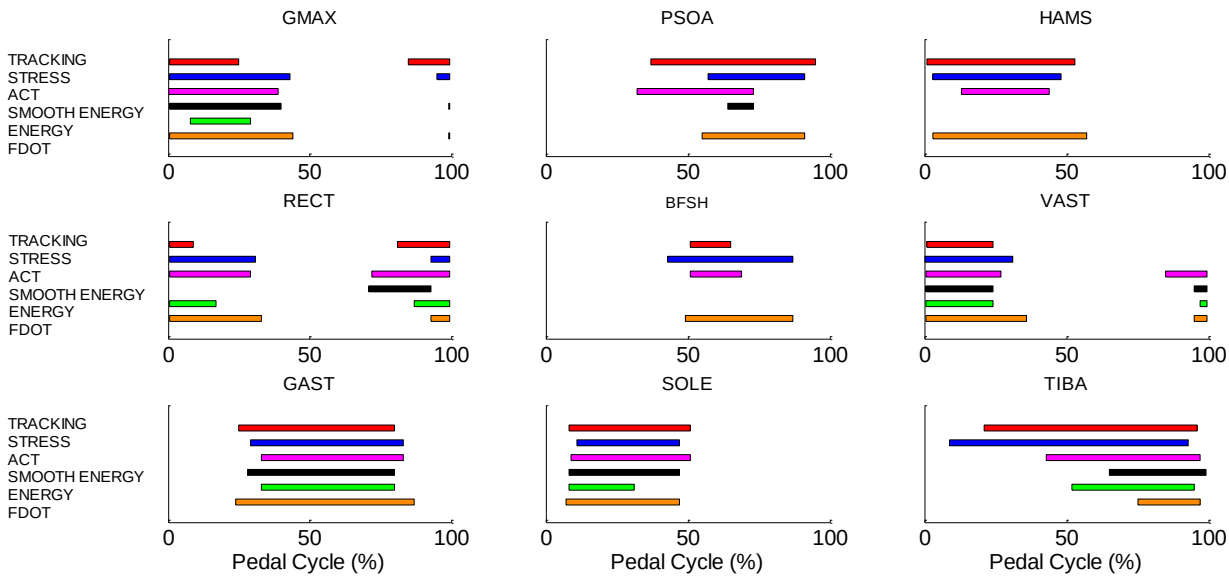

Figure 6.5: Excitation on- and off-set timings of the nine muscles of the standard model for each cost function, including TRACKING. X-axis is percent pedal cycle (0% – 100%). While some performance-based cost functions did not activate all muscles, the timing of all muscles were relatively similar to TRACKING.

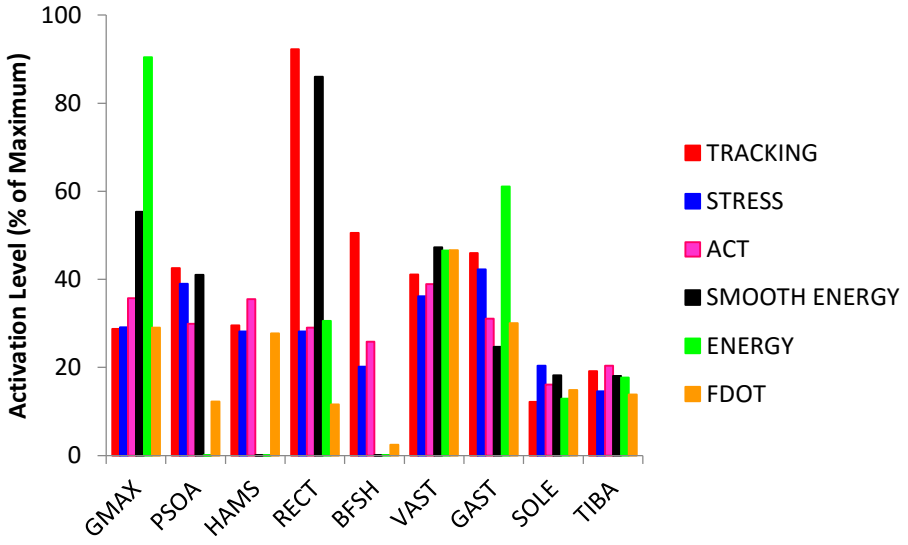

Figure 6.6: Predicted excitation magnitudes for each cost function, including TRACKING. The values are reported as a percent of maximum. Most muscles were activated less than 50% of maximal activation.

Discussion

Previously, simulations of submaximal pedaling have been generated by tracking experimental data, alone or in combination with a performance-based criterion (Neptune & Hull, 1998; Umberger et al., 2006). Using a data tracking approach, the musculoskeletal model in this study successfully replicated submaximal pedaling, with all individual variable RMSD values < 1.0 SD (Figure 6.1). The goal of this project was to use this model to generate simulations of submaximal pedaling using a performance-based cost function. Five cost functions that have been proposed in the literature were evaluated. All five cost functions were able to reproduce the gross kinematics and kinetics of pedaling reasonably well, although the muscle activation patterns for some cost functions were not in good agreement with experimental EMG data. Of the cost functions evaluated, minimizing muscle stress (STRESS) and muscle activation (ACT) yielded the lowest RMSD and the most reasonable muscle excitation timings.

STRESS was the most successful at reproducing the gross kinematics and kinetics of submaximal pedaling (Figure 6.3, Table 6.2), with an average RMSD of 1.27 SD. Knee moment for STRESS was the least successful replication (RMSD = 2.26). While the main characteristics of the knee moment are captured, knee extension during the down stroke occurs later than experimental or tracking data. This late knee extension moment is due to the late VAST and RECT and early HAMS activation (Figure 6.5). The knee extension moment magnitude is also lower than the TRACKING and experimental data (Figure 6.3). Another muscle activation issue of STRESS is that TIBA is excited for most of the pedal cycle (Figure 6.5). While this does not replicate experimental timing well, it did result in a pedal angle trajectory that better matched experimental data than any other performance-based cost function (Figure 6.3). The ankle moment of STRESS was replicated better than all other performance-based cost functions (RMSD = 0.87, Table 6.2). However, there is a noticeable deviation of the ankle moment during the first portion of the down stroke. This moment

abnormality is driven by late SOLE activation (Figure 6.5). However, this striking muscle activation alone would not have caused the abnormality in the ankle moment. Since, TIBA turned on slightly after SOLE, countering the contributions of SOLE, this sharply decreased the ankle plantar flexion moment, contributing to the abnormality. Despite STRESS simulating pedaling with the lowest average RMSD, we conclude that it was not the best performance-based cost function for simulating submaximal because of the poor knee moment replication and the elongated TIBA activity throughout most of the pedal cycle.

ACT was the next most successful performance-based cost function after STRESS at reproducing the gross kinematics and kinetics of submaximal pedaling (Figure 6.3, Table 6.2), with an average RMSD of 1.55 SD. Knee moment was the least successful kinetic replication (RMSD = 1.80), however, ACT was the only performance-based cost function to replicate the knee moment under 2 SD. The magnitude of the knee flexion moment around bottom dead center is lower in ACT than TRACKING and the experimental data (Figure 6.3). This is due to a lower GAST activation magnitude, despite good timing. There is also an earlier knee extension moment as compared to all other cost functions just before top dead center (Figure 6.3) which is due to an earlier activation of VAST and RECT. Ankle moment predicted a similar error to the knee moment (RMSD = 1.78). The ankle moment predicted less plantar flexion than the tracking and experimental data. The lower plantar flexion ankle moment is due to the relatively greater amplitude and slightly later activation of the TIBA and the slightly earlier SOLE activation, resulting in an increased overlapping of muscle activations by muscles spanning either side of the ankle. This muscular activity about the ankle also resulted in a smaller ankle moment abnormality than was predicted by STRESS just after top dead center (Figure 6.3). Another advantage of ACT over STRESS is that no excitation times or activation levels are extraordinarily long or high relative to the tracking results. A similar finding that ACT minimalized levels of muscle activations compared to STRESS resulted in a better running simulation (Miller, Umberger, Hamill, & Caldwell, 2012). Thus, since ACT simulated pedaling with the second

best replication of the kinematic and kinetic variables (avg. RMSD = 1.55 SD), and the activation timing of the simulation was in better agreement with the TRACKING and experimental EMG data than STRESS, we conclude that the ACT performance-based cost function replicated pedaling best of those tested in this project.

The other three performance-based cost functions, SMOOTH ENERGY, ENERGY and FDOT, each replicated pedaling with an average RMSD near 2 SD (Table 6.2); however, each has specific problems with individual muscle activations. SMOOTH ENERGY and ENERGY did not activate all muscles. This deletion led to compensation by other muscles. Interestingly, the compensation was in activation amplitude (SMOOTH ENERGY: GMAX and RECT; ENERGY: GMAX and GAST), not in duration (Figures 6.5, 6.6). Thus, the solution to minimizing ENERGY is to not activate some muscles. Since the muscles not activated by SMOOTH ENERGY and ENERGY are major contributors to submaximal pedaling, per experimental data, these performance-based cost functions were not deemed acceptable for replicating submaximal pedaling despite the reasonable output variables. FDOT did activate all muscles, however, PSOA, RECT, BFSH, SOLE and TIBA were all activated under 15% of maximum, with BFSH at 2% maximum. These low activation magnitudes plus the long activations of the knee extensors and flexors contribute to the poor timing of the knee moment (Figures 6.3, 6.5) and the poorest prediction of knee moment (RMSD = 3.69 SD) of all performance-based cost functions. The low muscle activations also produced the worst ankle moment of all performance-based cost functions (RMSD = 2.16 SD). These three performance-based cost functions also produced an ankle moment abnormality early in the down stroke similar to that induced by STRESS (Figure 6.3). Despite the proximity of these performance-based cost function results to the 2 SD qualifier, muscle activation timing and individual kinetic variables argue against using these performance-based cost functions to generate simulations of submaximal pedaling.

STRESS and ACT were the most successful cost functions, but did not yield exactly the same results. The differences depend on how the instantaneous muscle dynamics affect the optimization of

the input variables: muscle on- and off-set timing and amplitude. A muscle can produce a given force with several combinations of contractile element length, shortening or lengthening velocity and activation amplitude. For example, if two identical muscles were to produce force, but each were on a different part of the force-length curve, the one farther from its optimal contractile element length would require more activation to achieve the desired force. Similarly, if these two muscles were shortening or lengthening at different rates, the activations would also be different to produce a particular force. STRESS manipulates muscle excitations to minimize muscle forces (scaled by muscle physiological cross sectional area) without any consideration for the instantaneous muscle dynamics (i.e., contractile element length and velocity). However, as ACT minimizes the integrated muscle activation, it must take into account the contractile state of the muscle. What is remarkable is that these two cost functions were so similar in their solutions. The subtle differences between them were due primarily to the influence of instantaneous muscle dynamics.

It should be noted, that while STRESS and ACT were successful at replicating submaximal pedaling, neither was as good as tracking. This difference is due to the fact that the central nervous system (CNS) likely takes into account more than one criterion when developing muscle activations as this project has done only using one minimization criterion. This statement is not original as it is a similar supposition has been discussed by other researchers in studies designed to determine whether a performance-based cost function can replicate human movement (e.g. Kautz, Neptune, & Zajac, 2000; Miller, Umberger, Hamill, & Caldwell, 2012). STRESS and ACT replicated pedaling relatively well in the current project, thus the individual underlying physiological processes represented by these cost functions may be of some relevance to the CNS in selecting a movement pattern. The CNS would have some information of activation, including recruitment and rate coding. While it is unlikely that the CNS would have information about muscle stress *per se*, it does receive feedback about muscle tension from Golgi tendon units. It is possible that the CNS utilizes information from the muscles activations and the Golgi tendon units to develop muscle activation patterns, thus

minimizing muscle tension and activation. However, there are other feedback mechanisms that may contribute to the development of motor patterns. For example, muscle spindles could relay strain information back to the CNS, which could utilize this information to minimize muscle strain. Therefore, it is important to recognize that this project demonstrates that simulations of submaximal pedaling can be generated by minimizing muscle stress or activation, but these results do not imply that the CNS operates in the same manner in coordinating actual human pedaling.

Another interesting result from this project is that no single performance-based cost function could replicate the pedal angle of the experimental data or TRACKING simulation (Figure 6.3). All five performance-based cost functions predicted a more toe-down pedal angle, which represents a more plantar flexed ankle. STRESS replicated the pedal angle with the least toe-down angle (Figure 6.3). With a fixed hip, as simulated in this project, a more plantar flexed ankle alters the ranges through which all muscles of the leg may act, as the hip and knee joints would be more flexed with a more plantar flexed ankle (Neptune & Herzog, 2000). The increased flexion of the knee and hip would alter, the location of the muscles of the knee and hip on their force-length curves, thus altering the excitation patterns of the muscles based on their need to produce a given force to achieve a certain joint moment. While the toe-down pedal angle and subsequent kinematic joint changes do not completely explain the differences among the performance-based cost functions results simulating sub-maximal pedaling, this outcome does contribute to the previously stated idea that there are other elements of the submaximal pedaling task that the CNS may incorporate to optimize human pedaling.

In conclusion, STRESS and ACT were the most successful at replicating submaximal pedaling. STRESS was the most successful at reproducing the kinematic and kinetic variables of pedaling; however, some of the muscle activation patterns were not in as good agreement with experimental EMG data as the ACT cost function. ACT did not reproduce the target kinematic and kinetic variables quite as well as STRESS, but it did so with acceptable accuracy and had activation patterns that agreed better with experimental data. Therefore, while both cost functions replicated

submaximal pedaling within the 2 SD threshold, we conclude that ACT is preferred as it predicted muscle activations that better represent submaximal pedaling. Because the CNS presumably uses more than one optimality criterion, further work is necessary to more fully understand how the CNS develops muscle activation patterns or if a combination of performance-based cost functions would replicate pedaling even more successfully.

CHAPTER 7

BIARTICULAR MUSCLES AND ENERGETICS OF PEDALING

Introduction

Some muscles in the human musculoskeletal system cross more than one major joint (e.g., hip, knee, or ankle). These muscles are commonly labeled biarticular, while muscles crossing just one joint are designated as uniarticular. The rectus femoris, semimembranosus and gastrocnemius are some of the major biarticular muscles of the human lower limb. The potential biomechanical and motor control contributions of biarticular muscles to human movement have inspired over a century of research (Cleland, 1867; Lombard, 1903; Elftman, 1939; Andrews, 1987; Wells, 1988; van Ingen Schenau, 1990; Raasch, Zajac, Ma, & Levine, 1997; Raasch & Zajac, 1999; Hasson, Caldwell, & van Emmerik, 2008). Based on their results, researchers have suggested that biarticular muscles may decrease the metabolic cost of movement relative to an alternative musculoskeletal design consisting only of uniarticular muscles. However, these suggestions have not been investigated directly. Biarticular muscles could potentially decrease the cost of movement if they: (1) contribute to two simultaneous joint torques that are both necessary for task completion, (2) operate at slower velocities and thus produce less positive work, than would a comparable pair of uniarticular muscles, (3) transfer energy between joints in a manner that aids task completion, and (4) act as prime contributors directing the external forces on the environment, which might reduce the need for uniarticular muscles to generate negative work. These concepts are difficult to address using an experimental approach, which is likely why they have not been tested directly. However, these questions can be addressed using a musculoskeletal modeling technique. This project will use a human musculoskeletal model simulating pedaling to investigate the effect of biarticular muscles on the energetics of movement.

The contributions of individual muscles to joint torques are not discernable from experimental data due to the redundancy of the musculoskeletal system (Elftman, 1939, 1940; Crowninshield & Brand, 1981). Biarticular muscles further confound our understanding of the muscular contributions to joint torques because they influence two joint torques simultaneously. For example, the force produced by the hamstrings will contribute hip extension and knee flexion torques. If this torque combination is necessary for a task, activating a biarticular muscle may be more cost effective than using two uniarticular muscles. Herzog and Binding (1994) showed that in some joint configurations, having both biarticular and uniarticular muscles could be mechanically effective at producing the necessary joint torques for completing a static task. They compared the results of two models, one with both biarticular and uniarticular muscles and one in which the biarticular muscles were replaced with two uniarticular muscles. The model contained two rigid segments, simplified muscles with no detailed physiological parameters (e.g., series elastic element elasticity or maximum isometric force), and no means for predicting metabolic energy consumption. Extending this approach by using a more detailed musculoskeletal model to study a real-life task such as pedaling could provide more insight as to the effects of biarticular muscles on the metabolic cost of movement.

A detailed musculoskeletal model would also be helpful to evaluate the effects of joint kinematics on the individual muscle velocities and work during pedaling (Gregoire, Veeger, Huijing, & van Ingen Schenau, 1984). The effect of joint kinematics on uniarticular muscles may be relatively straightforward. For example, the uniarticular vasti muscles lengthen when the knee flexes. Because biarticular muscles cross two joints, their velocities during force production are not as straight forward as uniarticular muscles. For example, if the two joints are acting in the same direction (e.g. extension), a biarticular muscle will lengthen at one joint and shorten at the other (Cleland, 1867; Duchene, 1879). Thus, the biarticular muscle could be producing force isometrically, or nearly isometrically, even in the presence of high joint velocities. These kinematics would also mean that these muscles would be producing less positive work as they produce force nearly isometrically.

Isometric force production is less metabolically costly than force produced with faster muscle shortening velocities (Abbott, Bigland, & Ritchie, 1952; Beltman, van der Vliet, Sargeant, & de Haan, 2004). However, muscle-tendon-unit (MTU) velocity does not fully explain the metabolic cost of muscle force production. A muscle-tendon-unit can be modeled as two elements: contractile (CE) and series elastic (SEE) (Hill, 1938). The CE activity dictates the metabolic cost of a given muscle. The joint kinematics and CE and SEE interactions would determine the CE velocity and thus CE work performed. Therefore, investigating the changes in the CE work is also important to understand the costs incurred by these muscles.

While biarticular muscles may produce force economically by acting isometrically or nearly so, they also serve to transfer energy between the two joints they cross (Cleland, 1867; Elftman, 1966; Bobbert, Huijing, & van Ingen Schenau, 1986; Jacobs, Bobbert, van Ingen Schenau, 1996). Such a transfer of energy can be demonstrated by the activity of the gastrocnemius during jumping (Bobbert, et al., 1986). During the push-off phase, the extensor knee joint power from the quadriceps is resisted by a knee flexor power generated by the gastrocnemius. Because the gastrocnemius also crosses the ankle, the muscular activity about the knee results in an increased plantar flexion power rather than further knee extension. In an activity like pedaling, this proximal-to-distal flow of muscular energy could deliver the muscular power from the larger, proximal muscles to the pedal, decreasing the need for the smaller, distal muscles to produce large amounts of muscular power (Gregorie, et al., 1984). This mechanism could potentially reduce the total volume of active muscle necessary to complete the task, thereby decreasing the metabolic cost of pedaling. Other researchers have used a different, segment-based power analysis to show that both biarticular and uniarticular muscles cause energy to be transferred between segments (e.g. Zajac, Neptune, & Kautz, 2002; Kautz & Neptune, 2002). This segment-to-segment analysis is important to understand how all muscles distribute muscular energy throughout the body. However, it is not as relevant to the current investigation, as this method does not allow the potentially unique function of biarticular muscles to be identified.

Another unique characteristic of biarticular muscles proposed in the literature is that they play a major role in controlling the direction of forces exerted on the environment (van Ingen Schenau, 1989; van Ingen Schenau, Pratt, & Macpherson , 1994; van Ingen Schenau, et al., 1995). Directing forces on the environment is essential for task completion. For example, during pedaling the crank is always rotating, thus to maintain a desired power output the direction of force that the foot transmits to the crank must be constantly changing. If biarticular muscles are the main contributors to directing external forces, the uniarticular muscles can be left to contribute positive work to the task (van Ingen Schenau, et al., 1995). It has also been proposed that in order for uniarticular muscles to generate the proper joint torques to direct forces on the environment they would have to produce more negative work. However, uniarticular muscles have been shown to work in concert with biarticular muscles to direct forces on the environment (Hasson, Caldwell, & van Emmerik, 2008). This study did not elucidate whether the uniarticular muscles produced negative work while contributing to the direction of external forces. Therefore, there may be a cooperative interaction of uni- and biarticular muscles directing forces on the environment, but how this may affect the metabolic cost of movement has never been directly investigated. However, it could be supposed that a design with both uni- and biarticular muscles would employ minimal positive work as there may be less negative work to overcome. Thus, it might be that a design with only uniarticular muscles would produce excessive amounts of negative work to accomplish the task of directing force on the environment. This negative work must be overcome with more positive work to produce the necessary amount of external work, thereby increasing the metabolic cost of completing the task.

The purpose of this project is to formally test whether the mechanical function of biarticular muscles may affect the metabolic cost of movement. Based on the proposed mechanisms through which biarticular muscles may influence the metabolic cost of movement, it is predicted that a standard design including all representative uniarticular and biarticular muscles will result in a lower metabolic cost than designs where one of the biarticular muscles is replaced with two uniarticular

muscles. Three such models were used, one for each of the major biarticular muscles in the human lower limb. The predicted metabolic cost from pedaling simulations using a standard model will be compared to that of the predicted metabolic cost of each of the three models with a biarticular muscle replaced with two uniarticular muscles. The differences in cost of pedaling (or lack thereof) will be investigated in terms of the contributions that individual muscles make to each of the necessary joint torques, CE work, energy transfer between joints, and how effectively the pedal force is directed.

Methods

Musculoskeletal Models

A two-legged, sagittal plane bicycle-rider model (see Appendix A) was used in this project. Each leg is represented by three rigid segments: the thigh, shank, and foot. Four frictionless joints per leg represented the hip, knee, ankle, and the connection between the pedal and the crank. The hip and crank centers were fixed in space, with the foot fixed to the pedal. The synergistic uniarticular muscles (e.g., vastus lateralis, intermedius, and medialis) were combined into a single muscle group by combining the maximal isometric force values of the muscles included, finding a weighted average of the length of the contractile elements, and optimizing the length of the series elastic element (Winters & Stark, 1985). Thus, the standard musculoskeletal model contained nine Hill-type muscle actuators for each leg: 6 uniarticular and 3 biarticular muscles. The three biarticular muscles were the rectus femoris, biarticular hamstrings, and gastrocnemius, and the six uniarticular muscles were the iliopsoas, gluteus maximus, vastus, biceps femoris short head, soleus and tibialis anterior. A muscle energetics model was also incorporated (Umberger, Gerritsen, & Martin, 2003). Thus, individual muscle contributions to the metabolic cost of movement were determined. (For further explanation of the energetics model, see Appendix A and Umberger, et al., 2003; Umberger, 2010). To assess the effect of biarticular muscles on the metabolic cost of movement, the standard model was modified by replacing each biarticular muscle with two independent uniarticular muscles, creating three new models with 10 muscles (10 MUS) on each leg.

Defining the New 10 Muscle Models

Three models were created by replacing each biarticular muscle individually (RECT – 10 MUS, HAMS – 10 MUS, GAST – 10 MUS) to address the effect of biarticular muscles on the metabolic cost of movement. There are few examples in the literature where biarticular muscles have

been replaced with two "equivalent" uniarticular muscles in musculoskeletal models. Herzog and Binding (1994) divided biarticular muscles into two identical uniarticular muscles in a simplistic mechanical model. Later this technique of dividing biarticular muscles in half was used to study the mechanical energy in walking and running (Prilutsky, Petrova, & Raitsin, 1996). Both of these studies divided the length of the biarticular muscles in half, while maintaining the same maximal force production and moment arm lengths. However, muscle characteristics, such as contractile element lengths and volumes, or series elastic element lengths and elasticity were not represented in either model, which greatly simplified the process of splitting a biarticular muscle in two. In the current study these muscle properties are represented so as to clarify the mechanics and energetics during pedaling. Therefore, in this study the biarticular muscle-tendon units were divided in two equal lengths similar to previous studies. In addition, the contractile element and series elastic element lengths and maximal force production muscle properties were optimized so the new models would match the joint angle torque relationships of the standard model while maintaining total muscle volume.

The musculoskeletal geometry of the new uniarticular muscles is defined by the muscle paths of the biarticular muscles of the standard model (Appendix A, Table A-4). Each biarticular muscle pathway is represented by an equation defining the muscle-tendon unit length and the moment arms. A simplified symbolic notion is:

$$L_{MTU} = A_0 + B_1\theta_P + B_2\theta_P^2 + C_1\theta_D + C_2\theta_D^2 \quad (7.1)$$

where A_0 represents the muscle tendon unit length when all $\theta = 0$, B and C are polynomial coefficients representing the muscle pathway at the proximal and distal joints respectively, and θ_P and θ_D are the instantaneous proximal and distal joint angles, respectively. Therefore, within the polynomials for the biarticular muscles, the pathways about each joint they cross are specifically

defined. For the new uniarticular muscles, A_0 was optimized while the coefficients for a given joint remained the same. This process resulted in two uniarticular muscles with muscle-tendon lengths that were half that of the original biarticular muscle, but with the same moment arms as the original biarticular muscle:

$$L_{MTU} = {}^{A_0}/_{2} + B_1\theta_P + B_2\theta_P^2 \quad (7.2)$$

$$L_{MTU} = {}^{A_0}/_{2} + C_1\theta_D + C_2\theta_D^2 \quad (7.3)$$

Muscle parameters, such as maximum isometric force production (F_{MAX}), optimal length of the contractile element (L_{CEOPT}), and the slack length of the series elastic element (L_{SLACK}), are specific for each muscle and were optimized to determine the new uniarticular muscles characteristics. These values were also optimized for the old uniarticular muscles about the same joints (Appendix B, Tables B-1, B-2, B-3). Pennation angle, fiber type and the width of the parabola defining the force length curve are assumed to be the same for all muscles in the model.

The method described of dividing the biarticular muscles in two produced three novel musculoskeletal designs with ten muscles: two remaining biarticular muscles and eight uniarticular muscles. There were two specific constraints employed while designing these new models: (1) they needed to match the standard model isometric torque-angle relations as closely as possible and (2) they needed to have the same muscle volume as the standard model (Appendix B). These two constraints were important so that the three new musculoskeletal designs were as similar as possible to the standard model, so as to assure that differences in mechanics and energetics during submaximal pedaling were due to the new musculoskeletal design and not to strength or muscle volume differences. To test the dynamic performance characteristics of the new models, pedaling simulations

were generated where the models tracked experimental data (see STUDY ONE for methods) to evaluate whether the new models could pedal in a manner similar to the standard model.

Optimization

Muscle excitation onset, offset, and magnitude patterns for the three new musculoskeletal designs were optimized using a simulated annealing algorithm (Goffe, Ferrier, & Rogers, 1994; Neptune & Hull, 1998). The muscular patterns simulated submaximal pedaling at 80 rpm and 200W. Because there are no experimental data to track for these models, a non-tracking, performance-based cost function was used. Muscle excitations for this same pedaling simulation, 80 rpm and 200 W, were found using a criterion called minimization of activation (ACT) (Ackermann & van den Bogert, 2010):

$$ACT = -\frac{1}{t_f}\sum_{i=1}^{m}\left(\int_0^{t_f} A_i^{exp}\ dt\right) \tag{7.4}$$

where A is time-varying muscle activation, t_f is the pedal cycle, m is the number of muscles and *exp* was 10. (STUDY ONE, Chapter 6)

Analysis

The influence of biarticular muscles on the metabolic cost of submaximal pedaling was assessed by evaluating the contributions of biarticular muscles to pedaling joint torques, CE velocities as they relate to work, and the joint-to-joint energy transfer of biarticular muscles. The first step in the analyses was to compare the predicted metabolic costs of the three 10 MUS models with that of the standard model. The metabolic cost is reported as work and was determined by integrating the metabolic power with respect to time as calculated in the model (See Appendix A). There is no standard statistical method to objectively compare the metabolic cost results of these different

musculoskeletal designs. Experimental pedaling data show that across a variety of pedaling rate-power output combinations, one standard deviation represents an approximately 10% difference in metabolic cost within a subject group (e.g. Chavarren & Calbet, 1999; Belli & Hintzy, 2002; McDaniel, et al, 2002). Thus a 10% difference in the energetic cost of pedaling could be taken to represent a meaningfully large difference between model conditions. For this project we operationally defined a difference in the predicted metabolic cost of a uniarticular model and the standard model of less than 5% as a small difference, 5-10% as a moderate difference, and greater than 10% as a large difference. Additionally, individual muscle contributions to the overall metabolic cost were analyzed for comparison. The metabolic energy of each muscle was determined, the way in which how each muscle contributes to the overall metabolic differences of the different models was examined. Specifically, the effect of the new uniarticular muscles on the metabolic cost was compared to the original biarticular muscle metabolic cost from the standard model simulation.

The net joint torques, crank torque and pedal angle of the standard model were compared to experimental data from STUDY ONE (Marsh, Martin, & Sanderson, 2000) via root-mean-squared values, expressed as multiples of the between-subject standard deviations of the experimental data. The results of the three 10 MUS models were then compared to the standard model. Net joint torques provide incomplete information as to which muscles are generating the torques. In addition, the effect of antagonist muscles working in opposition to the net joint torques is indiscernible. Musculoskeletal models predict individual muscle activity. This predicted muscular activity was used to determine where in the pedal cycle a biarticular muscle in the standard model was simultaneously generating torques in the same directions as the net joint torques. For example, around bottom dead center of the pedal cycle, a net hip extension and a net knee flexion torque are present. If the biarticular hamstring was active in this part of the pedal cycle, it would generate torques that simultaneously match the directions of both net joint torques. To establish whether a biarticular muscle was aiding or opposing the two net joint torques, first the timing of biarticular muscle activity in the standard model during

the pedal cycle was determined. Then, the percentage of time the muscles are actively contributing to the net torques at both joints was calculated.

At this time, only by using a musculoskeletal model is it possible to estimate the energy transferred by a biarticular muscle (e.g. Bobbert, et al., 1986; Prilutzky & Zatsiorsky, 1994). Total energy transferred to or from a joint can be determined by comparing the total joint power to the summed muscle tendon unit power produced by the muscles about that joint. If there is greater net joint power than summed muscle tendon power, then power has been transferred to the joint. Bobbert and colleagues also determined the power transferred to or from a joint by an individual biarticular muscle using the product of the torque produced by the muscle (muscle force × moment arm) at that joint and the angular velocity of the joint. For example, as the knee is extending the torque produced by the gastrocnemius at the knee is transferred to the ankle. This transfer away from the joint is due to the joint angular velocity which is opposite to the direction of torque production by that muscle at the knee thus lengthening the muscle at the knee. Interestingly, based on the results of this technique the amount of energy transferred to one joint may not equal the amount transferred away from the other joint. While the force produced by the muscle is the same at both joints, the effect of that force at each joint is different because of the different moment arms of that muscle at each joint and the angular velocities of the two joints. Thus, the power transferred by a singular biarticular muscle to and away from each joint must be calculated separately.

Muscle-tendon unit shortening velocity is dictated by the joint kinematics. For biarticular muscles this can be complicated. For example, if the hip and knee are extending, the biarticular hamstring will be shortening at the hip and lengthening at the knee. These kinematics could lead to force production in the MTU that is nearly isometric, resulting in very little MTU work being done. However, the CE could be shortening while the MTU is producing very little work. In addition, MTU work does not dictate the energetics of the muscle, rather the CE work does. The CE work of each muscle was compared between the standard and 10 MUS models to help explain the distribution of

work and the source of the metabolic cost. The net muscle power output was the same for all models (i.e., equal to the average power output per pedal cycle of 200 W), thus this analysis provided information on the distribution of work among the muscles and the amounts of positive and negative work.

The ability of each musculoskeletal design to direct force on the pedal was studied by comparing pedal reaction forces from the 10 MUS simulations with the standard model. The net pedal reaction force of the right pedal was decomposed into tangential (or rotational) and radial forces with respect to the crank. The rotational component directly relates to the amount of crank torque produced. Since the average power and average pedaling rate are the same for all models, the average torque will have to be the same. However, the way in which each model produces the crank torque through the pedal cycle will be used to explain the effectiveness of the application of force. An index of force effectiveness (IE) was calculated as a percentage over the whole crank cycle by:

$$IE = \frac{\int_0^{2\pi} F_{Tan}(\theta) \times d\theta}{\int_0^{2\pi} F_{Tot}(\theta) \times d\theta} \times 100 \quad (7.5)$$

where, $F_{Tan}(\theta)$ is the tangential force and $F_{Tot}(\theta)$ is the resultant force, as a function of crank angle (Coyle, et al., 1991).

Results

Model Evaluation

The analyses in this study were based on simulations where pedaling was generated by minimizing the sum of muscle activations (STUDY ONE, Chapter 6), subject to target time (80 RPM) and power (200 W) constraints. For the standard model, this performance-based cost function resulted in simulated pedaling (Figure 7.1) that was within two standard deviations of the experimental means for every variable except pedal angle (RMSE is reported in standard deviations of the mean: crank torque = 0.85, hip torque = 0.84, knee torque = 1.80, ankle torque = 1.78, pedal angle = 2.49). Using the performance-based cost function with the 10 MUS models resulted in simulated pedaling that was similar to the standard model in some aspects but differed in others. All three 10 MUS models generated crank torques that were similar to the standard model but did so with a more toes-down pedal angle for most of the pedal cycle (Figure 7.1), with RECT - 10 MUS predicting the most extreme toe down pattern. Each of the three 10 MUS models also generated a unique joint torque pattern that differed from the standard model (Figure 7.1). Specifically, RECT – 10 MUS used similar hip and knee torques, but very a different ankle torque pattern, while HAMS – 10 MUS used less hip torque and more knee torque. HAMS – 10 MUS and GAST – 10 MUS produced maximal ankle plantar flexion torque close to top dead center of the pedal cycle rather than approaching bottom dead center, as with the standard model. Kinematically the hip and knee angles are the most similar among all four models (Figure 7.2). The ankle angle is the most dissimilar from the standard model, with the RECT – 10MUS simulating the most different ankle pattern.

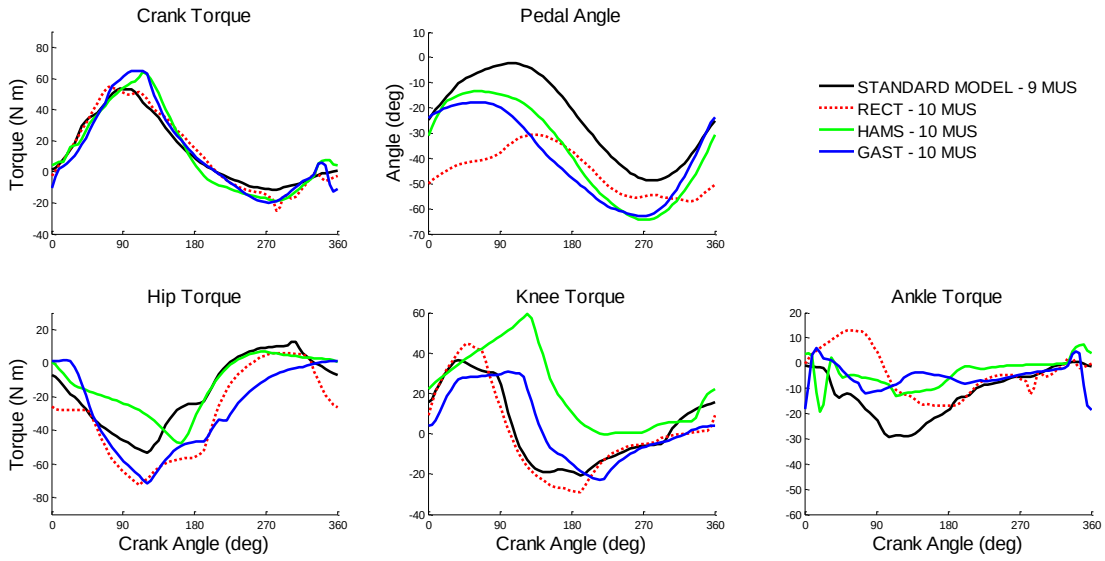

Figure 7.1: Performance-based cost function simulation results for the standard model (9 muscles) and the three altered musculoskeletal models (10 muscles) each with a replaced biarticular muscle. Top dead center is at a crank ankle of 0° or 360°, whereas bottom dead center is considered 180°. All models portrayed relatively similar torque and pedal angle patterns, except for RECT – 10 MUS which had very different pedal angle and ankle torque patterns.

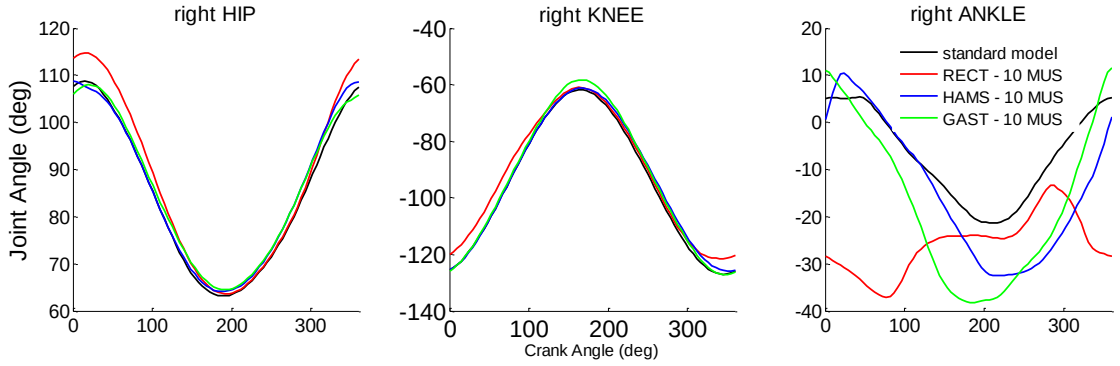

Figure 7.2: Joint angles of the right hip, knee and ankle joints for the standard model (black) and the three altered musculoskeletal models (10 muscles) each with a replaced biarticular muscle. Top dead center is at a crank angle of 0° or 360°, whereas bottom dead center is considered 180°. The hip and knee joint angles are relatively similar for all four models, while the ankle angle differs the most. Larger hip angles represent flexion. Larger knee angles represent knee flexion. Positive angle angles are dorsiflexion, while negative values are plantar flexion.

Metabolic Cost

All three 10 MUS models predicted greater metabolic energy consumption than the standard model (Table 7.1): RECT – 10 MUS was 7.0% greater (moderate difference), HAMS – 10 MUS 3.8% greater (small difference) and GAST 10 – MUS 5.6% greater (moderate difference). No 10 MUS model fell outside of the range of experimental values in the literature for pedaling at 200 W and 80 rpm (740.1 – 1131.8 W) (Abrantes, Sampaio, Reis, Sousa, & Duarte, 2011; Foss & Hallen, 2004; Belli & Hintzy, 2002; Marsh, Martin & Foley, 2000; Böning, Gönen & Maassen, 1984; Coast & Welch, 1985; Takaishi, Yamamoto, Ono, Ito, & Moritani, 1998). The greater metabolic cost of each of the 10 MUS models over the standard model can be explained by examining the individual muscle differences between each mono-articular model and the standard model (Figure 7.3).

Table 7.1: Metabolic power values for the performance-based cost function simulations for pedaling at 200 W and 80 rpm for all the models used: the standard model and the three altered models.

	Metabolic Power (W)	**Percent difference from Standard Model**
Standard Model	1018.6	-
RECT – 10 MUS	1079.0	5.9
HAMS – 10 MUS	1057.3	3.8
GAST – 10 MUS	1070.9	5.6

RECT – 10 MUS

The two new uniarticular muscles (RECT – hip and RECT – knee) combined to consume 13.1 J more than the original RECT in the standard model. These two new uniarticular RECT muscles consumed the most metabolic energy of all the new uniarticular pairs (Figure 7.3). VAST metabolic energy consumption was lower by 17.8 J from the standard model, while the biarticular HAMS predicted greater energy consumption, by 26.9 J. The only other major difference in metabolic cost

was in the PSOA which was 23.1 J less in this model from the standard model. This model also had the greatest difference in hip torque and ankle torque relative to the standard model (Figure 7.1).

HAMS – 10 MUS

The two new HAMS muscles together used only 1 J more energy than the original HAMS muscle from the standard model (Figure 7.3). However, there were considerable differences for other muscles. Lower costs were predicted for three muscles (differences: GMAX: -21.3 J, PSOA: -10.6 J, and GAST: -11.5 J) while substantially greater costs were predicted for two muscles (differences: VAST: 19.6 J and SOLE: 23.1 J). Despite these considerable individual-muscle differences, as a whole this model predicted the smallest overall metabolic cost difference relative to the standard model. (Table 7.1).

GAST – 10 MUS

This model resulted in the fewest individual muscle metabolic cost differences between the uniarticular and the standard model (Figure 7.3). The combined effect of the two new GAST muscles predicted the use of 4.8 J more energy than the original single GAST from the standard model. The largest differences were greater costs in HAMS (22.0 J) and SOLE (25.2 J) and lower cost in PSOA (-20.5 J). Thus, the net effect was a moderately greater metabolic cost used by this model than the standard model.

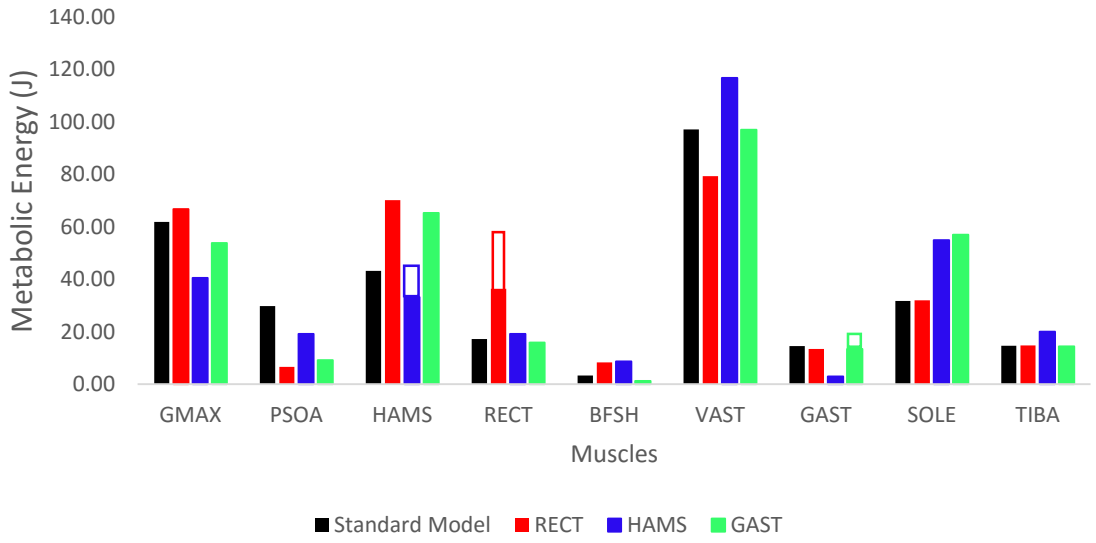

Figure 7.3: Metabolic energy (J) consumed by each muscle for each of the four simulations. The open portions of the HAMS, RECT and GAST bars represent the new distal muscle in the pair of uniarticular muscles that replace a biarticular muscle (e.g., uniarticular GAST at the ankle) while the solid represents the proximal muscle. Thus the total bar represents the whole metabolic cost of the two new uniarticular muscles which replaced the biarticular muscle of the same name in the standard model.

Energy Transfer by Biarticular Muscles

The biarticular muscles in the standard model transfer energy between joints throughout the pedal cycle, and the greatest amount of energy is transferred during the downstroke (Figures 7.4a-c). The primary direction of energy transfer is from the knee to the hip (positive dashed line in Figure 3a and negative dashed line in Figure 7.4b) during hip extension in the downstroke. The greatest amount of energy was transferred via the HAMS from the knee to the hip (solid blue lines in Figures 7.4d & e). Thus, the biarticular HAMS transfers some mechanical energy that was generated by the knee extensors to aid with extending the hip. Also during the downstroke, RECT transfers a small amount of energy generated by the hip extensors to the knee joint (solid red lines in Figures 7.4d & e).

Finally, GAST transfers the least amount of energy, transferring energy generated by the ankle dorsiflexors to aid with knee flexion in the upstroke (solid green lines in Figures 7.4e & f).

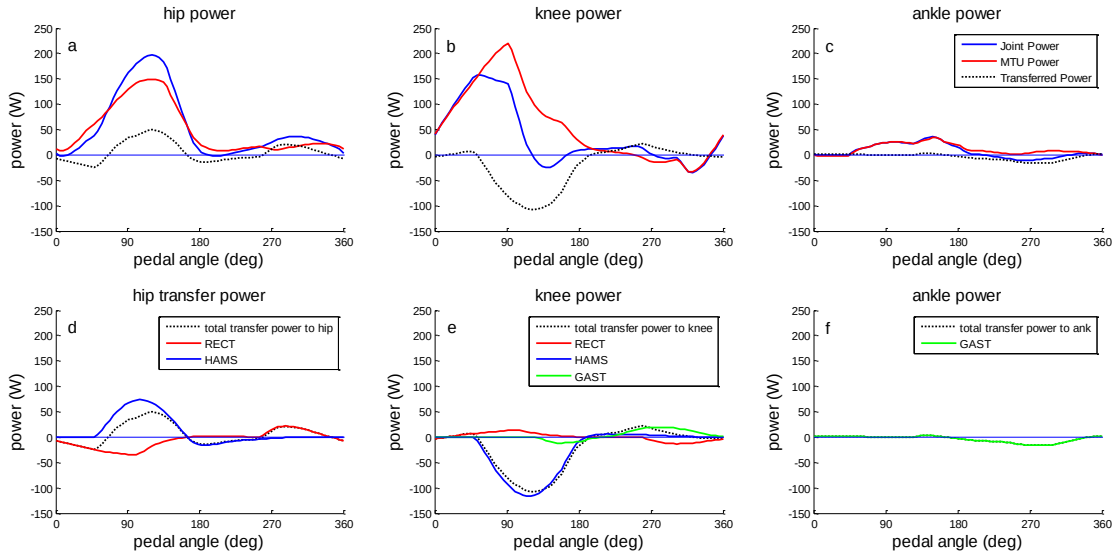

Figure 7.4: Energy transfer by individual biarticular muscles from one joint they cross to the other from the prediction of the standard model. (a-c) Joint power, muscle-tendon power, and power transfer by biarticular muscles at the hip, knee and ankle, respectively. (d-f) Biarticular muscle contributions to power transfer at the hip, knee and ankle, respectively. HAMS predicted the greatest amount of energy transferred during the downstroke while RECT predicted the greatest amount during the upstroke (panels d and e).

Biarticular Muscle Activation Timing

Biarticular muscles contribute to two joint torques while producing force. For example, the RECT produces hip flexor and knee extension torques. However, the two torques produced by each muscle are not always in the same direction as the two net joint torques during the pedal cycle. In this section, we first identify where during the pedal cycle the net joint torques are both in the same direction as the torques produced by each biarticular muscle. Then, we quantify the overlap between these regions and the actual activation timing of the biarticular muscles. For each biarticular muscle,

the two corresponding net joint torques were in the same direction as the torque produced by the biarticular muscle for no more than 10% of the pedal cycle (BLUE bars in Figure 7.5). In contrast, each biarticular muscle was active over a substantial portion of the pedal cycle (RED/ORANGE bars in Figure 7.5). The RED portion represents the period of excitation of each muscle, while the ORANGE represents the decay of activation following the cessation of excitation. As muscle activation decays, force production, and thus torque production, would decrease but still exist to some degree. Each biarticular muscle is active during the portion of the pedal cycle when the two net joint torques matched the torques produced by each biarticular muscle. However, HAMS (Figure 7.5b) is contributing to net hip extension and knee flexion torques as the activation level is falling. For all biarticular muscles, the two net joint torques generated by a biarticular muscle only occur during a small portion of the time the muscles are active (Figure 7.5). The two net joint torques generated by RECT occur during only 8.3% of the time when the muscle is active. The two net joint torques for HAMS occur during only 9.1% of the time when the muscle is active. The two net joint torques for GAST occur during only 14.4% of the time when the muscle is active. Thus, the major biarticular muscles in the lower limb are active when they act in the same direction as the net joint torques at both joints that they cross. However, they are not only, or even primarily active when the torques they produce match the directions of the net joint torques.

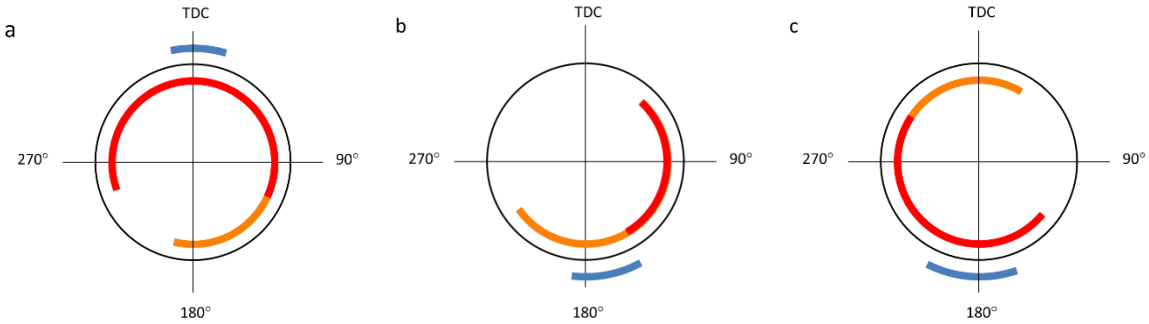

Figure 7.5: Individual biarticular muscle activity in the standard model during one pedal cycle. (a) RECT, (b) HAMS, and (c) GAST excitation (RED) and activation (ORANGE) timings during the pedal cycle. The BLUE line represents when during the pedal cycle the net joint torques are in the same direction as the torques produced by each biarticular muscle. For example, RECT is a hip flexor and knee extensor. The BLUE line in 5a represents the period during the pedal cycle when the net joint torques are simultaneously hip flexion and knee extension. Top dead center (TDC) is at 0° of the pedal cycle.

Muscle Excitations

The muscle excitations of the muscles in the 10 - MUS models were similar to the standard model in both timing and magnitude, with a few exceptions (Figures 7.6, 7.7).

RECT – 10 MUS

The RECT – 10 MUS simulation predicted a longer TIBA excitation and was the most dissimilar excitation from the standard model of any muscle (Figure 7.6). RECT – hip activation was active during the downstroke of the pedal cycle, during which the hip is extending and it was active much earlier than the PSOA, a similarly functional muscle. Most muscles had higher excitation amplitudes in the RECT – 10 MUS simulation over the standard model, except for PSOA (Figure 7.7). RECT – knee excitation timing was similar to VAST, a functionally similar muscle, in this model and the standard model simulation. Finally, the BFSH muscle started earlier with a magnitude greater than the standard model BFSH prediction.

HAMS – 10 MUS

The HAMS – 10 MUS simulation exhibited a much longer BFSH excitation while GAST and PSOA timings were shorter compared to the standard model (Figure 7.6). GAST excitation time is so much shorter than that of the standard model it ended up contributing very little work or metabolic cost to this simulation (Table 7.1, Figure 7.3). Only SOLE and TIBA predicted greater activation amplitudes over the standard model. All other amplitudes were similar or lower than the standard model (Figure 7.7). Replacing HAMS resulted in a longer activation time for the BFSH to compensate for the missing HAMS as a knee flexor, but did not use the HAMS – knee to help compensate and there was no compensation by HAMS – hip to aid in hip extension. This minimal change in muscle activation pattern contributed to the smallest difference in metabolic cost of a 10 MUS model compared to the standard model.

GAST – 10 MUS

GAST – 10 MUS resulted in longer GAST – knee and GAST – ankle excitations relative to the muscles of the standard model BFSH and SOLE, functionally similar muscles, respectively (Figure 7.6). GMAX, PSOA, HAMS and BFSH all predicted shorter excitation times than the standard model. TIBA excitation is similar to the other two 10 MUS models, which means it begins its excitation later in the pedal cycle and continues into the downstroke. This timing for all 10 MUS simulations lead to negative work produced by TIBA (Table 7.2), but the GAST – 10 MUS model produced the largest amount of TIBA negative work. All muscle activation amplitudes were greater for GAST – 10 MUS. GAST – 10 MUS was the only model to increase the excitation times of both of the two new uniarticular muscles over the standard model's similarly functional muscles; however, this was balanced by much shorter times in several other muscles compared to the standard model excitation times, including BFSH, a similarly functional muscle to GAST – knee. This combination

contributed to the result of GAST – 10 MUS predicting only a moderately greater metabolic energy consumption over the standard model.

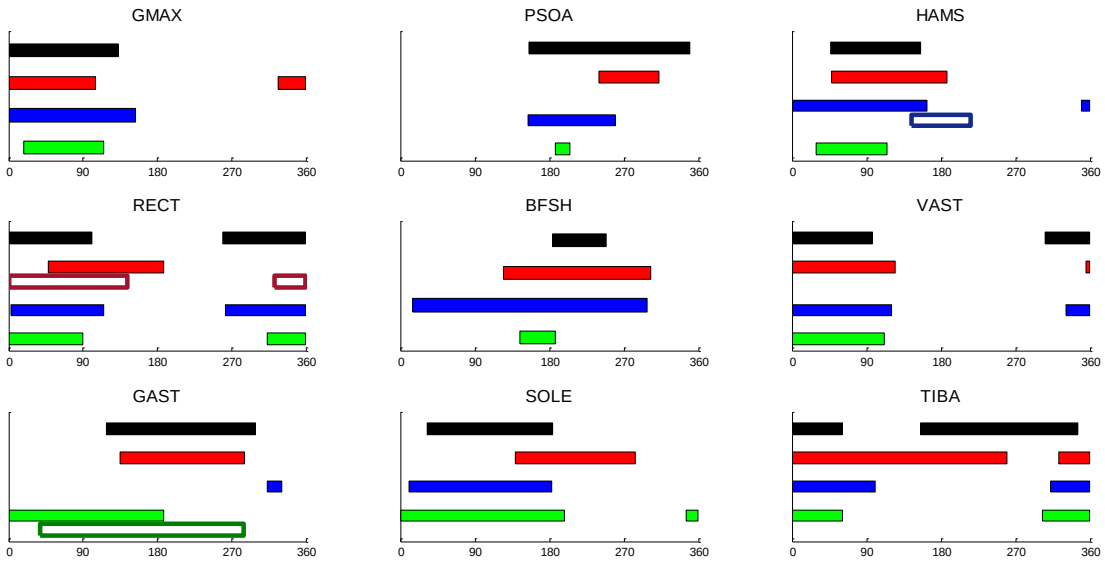

Figure 7.6: Muscle excitation timing across the pedal cycle (0° to 360°) of each model (SM9: black, RECT – 10 MUS: red, HAMS – 10 MUS: blue, GAST – 10 MUS: green). For each model, the two new muscles are represented in the figure of the muscle they replaced. The new proximal muscle retained the original color, while the new distal muscle is represented by the open bars, outlined in a darker shade of the original color. For example: the red bar in RECT – hip for MM10 – RECT is the original red, while the dark red, open bar is the RECT – knee.

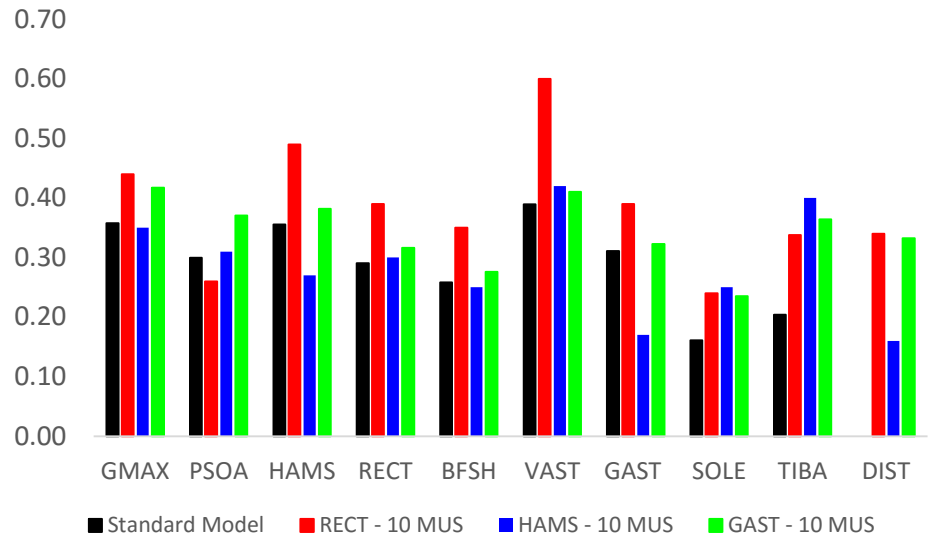

Figure 7.7: Muscle activation magnitude for each model. A value of 1 would represent maximal activation. The right-most group of bars represent the new distal muscle in the pair of uniarticular muscles that replace a biarticular muscle (e.g., uniarticular RECT at the knee in red.)

Contractile Element Work

For each simulation, regardless of the model used, the summed, net contractile element mechanical work in a single limb over the pedal cycle was 75 J, as dictated by the power (200 W) and cadence (80 rpm, or 1.33 Hz) constraints. The total mechanical work (75 J) achieved by the 10 MUS models occurred via greater amounts of net positive and negative work compared to the standard model (Figure 7.8). HAMS – 10 MUS and GAST – 10 MUS generated about the same amount of negative work, 22.5 J and 21.3 J respectively, while RECT – 10 MUS generated slightly less negative work, 15.5 J. These net differences are due to the individual muscle contributions (Table 7.2). Because the alteration in design was the replacement of an individual biarticular muscle with two uniarticular muscles, the different patterns of work can largely be understood by comparing the work of the two new muscles to the original biarticular muscle of the standard model. The RECT – 10 MUS model predicted 7.2 J (82.2%) more work by the two new uniarticular RECT muscles over the standard model RECT muscle. The increase was due to a relatively large contribution of the new

proximal RECT – hip muscle, which predicted 5.7 J of CE work over the 3.9 J by the standard model. The HAMS – 10 MUS model predicted 2.2 J (22.3%) more work produced by the two new uniarticular muscles over the standard model HAMS muscle. This smaller increase was due to modest increases in work produced by both HAMS – hip and HAMS – knee. The GAST – 10 MUS model also predicted a greater amount of work from the two new uniarticular muscles which resulted in the greatest relative difference 3.1 J (464.2%) over the standard model. GAST in the standard model predicted very little net work (0.67 J), due to almost equal periods of concentric (1.90 J) and eccentric (-1.23 J) work performed by the contractile element during the pedal cycle. In GAST – 10 MUS, the predicted increase is completely due to GAST – knee, as GAST – ankle predicted negative work (Table 7.2). Another interesting result was that the remaining biarticular muscles in each 10 MUS model also predicted greater contractile element work relative to the standard model (Table 7.2).

Table 7.2: CE work (J) of each muscle for the four simulations. The last column (DIST) contains the contractile element work of the new distal muscle of the uniarticular model represented (e.g., uniarticular GAST at the ankle).

	GMAX	**PSOA**	**HAMS**	**RECT**	**BFSH**	**VAST**	**GAST**	**SOLE**	**TIBA**	**DIST**
Standard Model	18.42	5.42	9.90	3.93	0.55	28.32	0.67	5.23	2.51	
RECT – 10 MUS	16.71	0.45	20.18	5.71	1.20	30.63	0.89	-2.82	0.87	1.45
HAMS – 10 MUS	11.13	3.34	10.50	4.25	0.30	37.78	-1.21	15.05	-7.77	1.61
GAST – 10 MUS	16.96	1.25	12.45	5.08	0.17	33.01	4.00	10.55	-8.36	-0.22

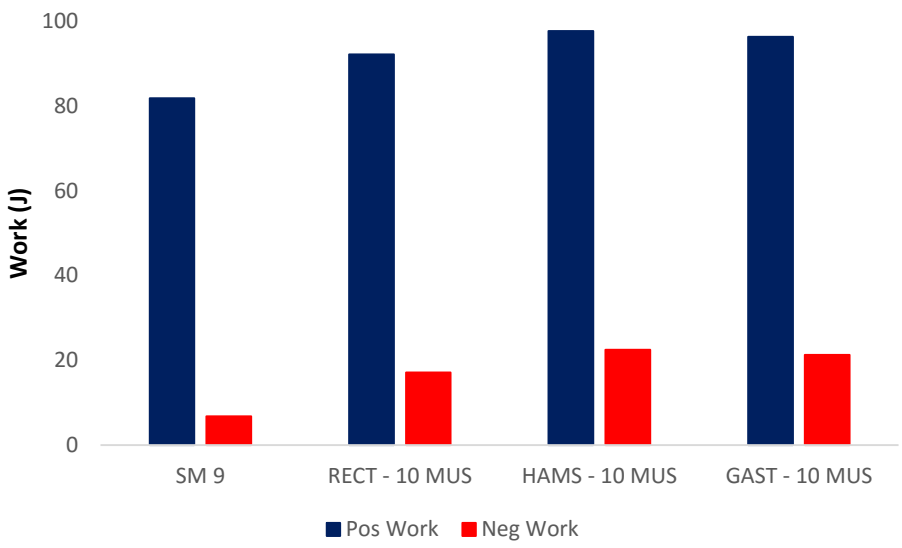

Figure 7.8: Total positive (blue) and negative (red) contractile element work (J) for each model. Positive and negative mechanical work were greater in all of the 10 MUS models than in the standard model. HAMS – 10 MUS predicted the greatest amount of positive and negative contractile element work. While RECT – 10 MUS predicted the least amount of positive and negative work.

Pedal Forces

The standard model index of effectiveness (IE) was 43.6%. The 10 MUS models all predicted lower IE values: RECT – 10 MUS 42.3%; HAMS – 10 MUS 34.8%; GAST – 10 MUS 38.6%. Approaching top dead center, RECT – 10 MUS predicted forces against the direction of travel of the crank, otherwise, the forces were very similar in direction to the standard model with slightly greater forces in some places (Figure 7.9). HAMS – 10 MUS predicted a small force transient after top dead center that was not seen in the standard model. During the second half of the downstroke, approaching the transition at bottom dead center, the forces for HAMS - 10 MUS were slightly more vertical than the standard model. GAST – 10 MUS predicted pedal forces that were most similar to the standard model, with the exception of some backward directed forces around top dead center. All

of the force discrepancies around top dead center are reflected in the patterns of ankle joint torque at or around the beginning of the pedal cycle for the three 10 MUS models (Figure 7.1).

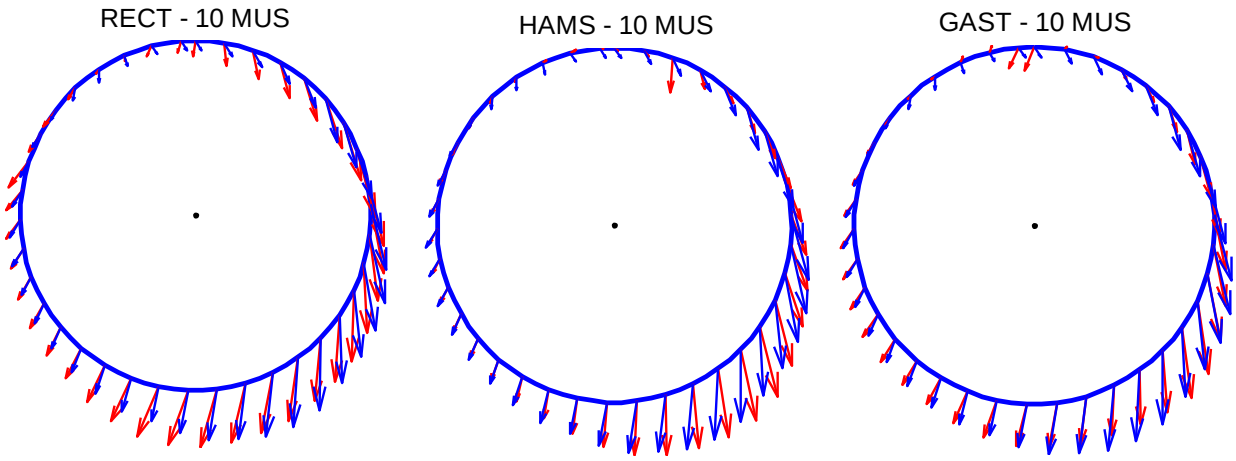

Figure 7.9: Pedal forces throughout the pedal cycle of each mono-articular model simulation (RED) compared to the standard model (BLUE). Except for a few deviations at or near top dead center all models matched the angle of force on the pedal relatively similarly to the standard model. Late in the downstroke, HAMS – 10 MUS had the most trouble matching the force application. Crank rotation is clock-wise.

Discussion

The purpose of this project was to assess whether the mechanical functions of biarticular muscles affect the metabolic cost of movement by independently replacing each of the three biarticular muscles of a standard model with 9 muscles with equivalent uniarticular muscles. While each of the three models with 10 muscles predicted greater metabolic cost than the standard model, none predicted a large difference. These results do support the prediction that the presence of the major biarticular muscles in the human lower limb reduces the cost of movement relative to alternative designs where there are two mechanically-equivalent uniarticular muscles in place of the biarticular muscles. However, no single proposed mechanism could simply or directly explain the differences. Rather, the explanation of the metabolic differences can be explained by the unique coordination pattern each altered musculoskeletal design adopted to meet the task demands of 200 W and 80 RPM.

Simulation results

The 10 MUS models were first used in a tracking solution to determine the capability of each model to pedal in a manner similar to the standard model. Statically, the three 10 MUS models matched the strength of the standard model and the tracking simulations of pedaling were used to assess the dynamic performance of the models (Appendix B). All 10 MUS models tracked experimental human data nearly as well as the standard model (Figure B-4, Table B-4). Thus, any differences in how the 10 MUS models pedaled in the predictive simulations relative to the standard model were primarily due to the unique characteristic of these models, rather than an inability to pedal like the standard model. The simulations used to address the question of whether biarticular muscles reduce the cost of pedaling were generated using a performance-based cost function that sought to minimize muscle activations (Ackermann & van den Bogert, 2010), thus allowing the

models to simulate pedaling without the use of experimental data. With the standard model, the simulated pedaling generally matched human pedaling data. Of all the variables analyzed, only pedal angle was more than two standard deviations from the mean of the experimental data for the standard model. Compared to the standard model, the crank torque of the 10 MUS models were similar (Figure 7.1). However, all of the 10 MUS models utilized a more pronounced toe down pedal angle and unique patterns of joint torques (Figure 7.1).

The differences in predicted metabolic cost for each of the 10 MUS model relative to the standard model can be partly understood by examining the hip, knee and ankle joint torques generated to accomplish the task. RECT – 10 MUS predicted the most dissimilar ankle torque to the standard model, but the hip and knee torques remained relatively similar in pattern to the standard model, with only slightly more hip extension torque throughout most of the pedal cycle (Figure 7.1). RECT – 10 MUS also predicted more co-contraction about the ankle than the other two altered designs (Figure 7.6). The greater co-contraction of SOLE, GAST and TIBA about the ankle contributed to the greater metabolic cost in RECT – 10 MUS. The greater co-contraction about the ankle resulted in the very different ankle torque and pedal (Figure 7.1) and ankle angle profiles (Figure 7.2) predicted by this model from the standard model and the other two altered models. HAMS – 10 MUS utilized more knee extension torque than the standard model. However, this increased knee extension torque was the result of the need to produce the correct amount of external torque for the task to compensate for the decreased hip extension torque (Figure 7.1). This knee extension torque was directly due to more VAST activity and less BFSH, GAST and HAMS – knee. GAST – 10 MUS predicted greater knee flexion torque during the upstroke. This is partially due to reduced hip flexion torque during the upstroke (Figure 7.1); PSOA is active for a very short time (Figure 7.6), minimally reducing the hip extension torque produced by GMAX and HAMS. Thus, knee flexion was necessary during the upstroke to flex the limb. Therefore, the metabolic cost can be explained by addressing the muscle activation differences and the effect on the joint torques.

Simultaneous Net Joint Torques

When biarticular muscles produce force they contribute to two joint torques simultaneously. For example, the RECT produces hip flexor and knee extension torques concurrently. If this net joint torque combination were necessary for task completion, then activating one biarticular muscle, rather than two uniarticular muscles, to produce the torques may be more cost effective (Herzog & Binding, 1994). This adaptation could mean that a musculoskeletal design with biarticular muscles may expend less metabolic energy than a model without biarticular muscles for an activity where a biarticular muscle can meet the necessary net joint torque demands. However, we found that in pedaling there are only very short periods in the pedal cycle where simultaneous net joint torques are produced that match those from each of the three biarticular muscles RECT, HAMS and GAST (Figure 7.5). For each muscle, these short periods occur around the transition phases at either top dead center (RECT) or bottom dead center (HAMS and GAST). In each case, the muscles contributed noticeably to the two net joint torques that matched their torque productions; however, this possible energy saving mechanism only exists for a relatively short period of the pedal cycle for all three muscles. In addition, the muscles were active for substantially more of the pedal cycle than when the net torques are in the same directions as the torques produced by the biarticular muscles.

The simulated results of joint torques and muscle activation timings from this study may differ slightly from experimental torque and EMG data (eg. van Ingen Schenau, et al., 1995; Neptune, Kautz, & Hull, 1997). However, small differences would not change the overall conclusions: the time during the pedal cycle which the simultaneous net joint torques occur is short, and while the biarticular muscles actively contribute to these torques, they contribute to the pedaling task in other ways for much longer periods of time during the pedal cycle. Thus, this possible mechanism does not appear to be an especially relevant factor influencing the metabolic cost of pedaling or explaining why the cost was greater in the 10 MUS models relative to the standard model.

During most of the pedal cycle, the hip and knee are moving in the same direction; hip and knee extension during the down stroke or hip and knee flexion during the upstroke. Herzog and Binding (1994) concluded that when two joints are moving in the same direction, like hip extension and knee extension, a model with only uniarticular muscles would be more mechanically effective at producing the necessary torques because a model with biarticular muscles predicted co-contraction of the two opposing biarticular muscles. This current study predicted co-contraction of the two biarticular muscles, HAMS and RECT, during the down stroke of the standard model pedaling simulation when the hip and knee were both extending. According to the generalized results of Herzog and Binding, the co-contraction predicted with the standard model would make the model less mechanically effective. However, after replacing the biarticular HAMS and RECT muscles, HAMS – 10 MUS resulted in a lower metabolic cost of the four muscles across these two joints than the model with the biarticular HAMS muscle while RECT – 10 MUS predicted a very similar metabolic cost across these two joints with the four muscles compared to the standard model (Figure 7.3). The difference in these results is most likely due to the fact that this pedaling model was dynamic, while Herzog and Binding examined force generation in static poses. Indeed, they warned against extrapolating their static solution to dynamic movements because the dynamics of two joints will affect biarticular muscles more than uniarticular muscles. Also, the models in the current study represented muscles as having contractile and series elastic elements, allowing for dynamic interactions of these elements to affect the kinematics and kinetics of the joints involved. Therefore, this study simulating a pedaling motion shows that the co-contraction predicted in the HAMS and RECT is not detrimental to the mechanical effectiveness or metabolic cost as was previously suggested.

Contractile Element Work

Muscle-tendon unit velocities are dependent on joint kinematics. Uniarticular muscle kinematics are simply dependent on the single joint the muscle crosses. Biarticular muscle kinematics are more complicated as they depend on the two joints the muscle crosses. For example, the RECT crosses the hip and the knee and the kinematics of the two joints dictate how the muscle changes length. Complicating the issue further, muscle-tendon unit kinematics do not define force production or the metabolic cost of that force. The contractile element produces force and dictates the metabolic cost. The velocity of the contractile element is a determinant of force production, however, contractile element velocity will also determine the contractile element work performed. If the contractile element produces force concentrically, it produces positive work; eccentrically, it produces negative work; isometrically, it produces zero work. How a muscle produces work also affects the metabolic cost. For example, generating work concentrically requires more metabolic energy than isometric work and even more than eccentric work (Abbott, Bigland, & Ritchie, 1952; Beltman, van der Vliet, Sargeant, & de Haan, 2004). Therefore, if the joint kinematics of two joints a biarticular muscle crosses are such that the biarticular muscle is shortening at one end and lengthening at another, biarticular force production may cost less than two uniarticular muscles, as it could be producing less work than two uniarticular muscles while contributing to the same two joint torques, thus resulting in metabolic savings. Since contracile element velocity by itself does not directly affect muscle metabolic cost (e.g., a high shortening velocity can have a low cost if activation is low) this mechanism was evaluated by comparing the mechanical work done by the biarticular muscles and the equivalent uniarticular muscles.

The results of the standard model show that the biarticular muscles produced net positive contractile element work, but by different amounts: HAMS produced 9.9 J of contractile element work, RECT 3.9 J of work and GAST 0.67 J of work (Table 7.2). As would be expected from the amount of muscular work, HAMS used the most metabolic energy (43.2 J), with RECT (17.3 J) and

GAST (14.5 J) contributing considerably less. In fact, HAMS was the third most expensive muscle in the standard model behind VAST (97.1 J) and GMAX (61.8 J). The only biarticular muscle that acts nearly isometrically while producing force was GAST. The small net contractile element work was because of small, but almost equal periods of concentric and eccentric force production rather than purely isometric force production. While the GAST performed little net work it incurred a metabolic cost similar to that of RECT, which performed more net work. Therefore, the general suggestion that biarticular muscles may act isometrically or nearly isometrically due to the joint kinematics of the two joints a muscle crosses and that this would contribute to the metabolic savings of biarticular muscles was not supported in this simulation. Thus, any explanation of metabolic savings via biarticular muscles in the context of contractile element work would have to come from investiaging whether the joint kinematics caused the biarticular muscles to produce less work than two uniarticular muscles in their place.

The advantage of this study is that the mechanical and metabolic effects of not having the biarticular muscles in the system can be quantified. If the biarticular muscles were more cost effective by producing less work at slower shortening velocities, the result would be seen in greater metabolic cost in the muscles of the 10 MUS models surrounding the affected joints. For example, RECT – 10 MUS would have an increased metabolic cost in the hip flexor and knee extensor muscles. The standard model PSOA, RECT and VAST produced 37.7 J of contractile element work at a cost of 144.2 J of metabolic energy. The four muscles in RECT – 10 MUS, PSOA, RECT – hip, RECT – knee, and VAST, produced 38.2 J of net contractile element work, at a cost of 129.1 J of metabolic energy. Thus, the net work of the hip flexors and knee extensors were similar between the two models, with a lower metabolic cost (15.1 J) in the four muscles of RECT – 10 MUS compared to the standard. The differences in the simulated results between the standard model and RECT – 10 MUS came from the less net work about the ankle: standard model had net 8.4 J of work about the ankle compared to -1.1 J in RECT – 10 MUS. However, this difference resulted the same amount of

metabolic energy (60 J) used by the three muscles surrounding the ankle (GAST, SOLE and TIBA). Thus the majority of the metabolic difference between the standard model and RECT – 10 MUS is due to a nearly 2 fold increase in work done by the HAMS to accomplish the task, leading to a greater metabolic cost of 26.9 J over the standard model by that muscle alone (Table 7.2). Replacing the biarticular RECT muscle did not have a large effect on the metabolic cost from muscles which work together with the replaced biarticular muscle (PSOA, RECT – hip, RECT – knee, and VAST), rather the compensating HAMS activity accounted for the majority of the difference in the metabolic cost of RECT – 10 MUS. Thus, the results for metablic cost were due to the fundamently different stargety that was used to meet the task demands, rather than being localized to the muscles with similar functions to the biatiuclar muscle that was replaced with uniartiucalr muscles.

HAMS – 10 MUS, which had the least different metabolic cost from the standard model of the three 10 MUS models, utilized less metabolic energy in the four muscles crossing the hip as extensors and the knee as flexors than the three muscles of the standard model: HAMS – 10 MUS 93.4 J and the standard model 108.4 J. This is the result of less net contractile element work in these muscles (Table 7.2). Since HAMS – 10 MUS did use more metabolic energy than the standard model, other muscles in the model were used to produce more work and thus used more energy. The two muscles that contributed the greatest difference in positive contractile element work were VAST and SOLE (Table 7.2). The increase VAST work corresponds to the reliance of this simulation on more knee extension torque over the standard model (Figure 7.1). SOLE work was countered by a relatively large amount of negative contractile element work by TIBA. The corresponding SOLE and TIBA co-activity resulted in a greater toe down pedal angle without creating a large plantar flexion torque (Figure 7.1). Thus, the reliance on knee extension and the co-contraction about the ankle caused the greater metabolic cost of this model over the standard model despite the decreased contribution from the four muscles affected by the replaced biarticular muscle. Once again, the two

new uniarticular muscles which replaced the biarticular HAMS did not directly account for the difference in metabolic cost.

The metabolic cost of GAST – 10 MUS was affected most by the new musculoskeletal design containing the two new uniarticular muscles that replaced the GAST biarticular muscle. GAST produced the least amount of positive work (0.67 J) by any of the three biarticular muscles in the standard model simulation. As was mentioned earlier, this small net work was due to almost equal parts positive and negative work. After replacing this biarticular muscle with the uniarticular GAST – knee and GAST – ankle muscles, the four new muscles in GAST – 10 MUS produced more than twice as much contractile element work as the three similar muscles in the standard model (standard model: 6.5 J and GAST – 10 MUS model: 14.5 J). This contractile element work difference resulted in more metabolic cost from the knee flexors and ankle plantar flexors in the GAST – 10 MUS simulation (Figure 7.3). There is relatively little difference in the work and metabolic cost from the other muscles crossing the hip and the knee (Figure 7.3, Table 7.2). Replacing the GAST created the need for more knee flexion to be produced (see ENERGY TRANSFER). This need was resolved as 4 J of positive knee flexion work produced by the new GAST – knee muscle. This work, plus the work of the new GAST – ankle muscle, only resulted in a 4.8 J net metabolic energy increase over the biarticular GAST from the standard model. Thus, the greater metabolic cost of this model must come from the increased use of HAMS for knee flexion (an increase of 22 J of metabolic energy over the standard model) and a similar co-contraction of the SOLE and TIBA seen in the other models. This co-contraction resulted in 25.0 J greater metabolic cost of SOLE and TIBA over the combination of the same muscles in the standard model. GAST – 10 MUS was the only model in which the two uniarticular muscles that replaced the biarticular muscle in the model directly affected the metabolic cost, and there was very little difference seen in most of the muscles about the other joints in other directions, such as knee extension. However, the cost difference between the standard model and

GAST – 10 MUS in the muscles about the ankle and knee was still so minor that it can be concluded that replacing the GAST had only a small overall effect on the metabolic cost of pedaling.

Energy Transfer

A biarticular muscle may transfer energy from one joint to another if the joints it crosses are moving in the same direction (e.g., both joints extending) (Cleland, 1867; Elftman, 1966; Bobbert, Huijing, & van Ingen Schenau, 1986; Jacobs, Bobbert, van Ingen Schenau, 1996). These joint kinematics would result in the muscle lengthening at one end and shortening at the other; thus, the lengthening end would be absorbing energy from the shortening end. This type of joint coordination causes the muscle to lengthen at one joint (power absorption) and shorten at another (power generation). This type of joint behavior occurs through most of the pedal cycle with the hip and knee joints: hip and knee extension during the downstroke and hip and knee flexion during the upstroke. Thus, there is the potential for biarticular muscles to transfer energy between the hip and the knee. There is less opportunity for transfer between the knee and the ankle as there is minimal ankle movement throughout the pedal cycle compared to the knee movement. Aiding in power generation at one joint in this manner could decrease the active muscle volume necessary to produce the required joint power. Decreasing active muscle volume would decrease the metabolic cost. From the standard model results, the biarticular muscles RECT, HAMS and GAST were determined to transfer energy at different times and by different amounts across the pedal cycle (Figure 7.4). HAMS transferred the greatest amount of energy from the knee to the hip during the downstroke aiding in hip extension. RECT transferred energy from the hip to the knee during the downstroke aiding in knee extension and a small amount from the knee to the hip during the upstroke aiding in hip flexion. GAST transferred very little energy during the upstroke from the ankle to the knee aiding in knee flexion.

If biarticular muscle energy transfer were an important mechanism of metabolic energy savings in pedaling then the result would be seen as increased metabolic cost in the 10 MUS models

from the muscles that cross the joints between which the energy was transferred. In the standard model, the HAMS had the greatest amount of biarticular muscle energy transfer while GAST had the least. If the transfer of energy via biarticular muscles was important in determining the metabolic cost of pedaling, then the HAMS – 10 MUS model should exhibit the greatest increase in metabolic cost, but it actually had the smallest increase. The HAMS – 10 MUS model was able to adapt the coordination pattern to meet the task demands with only a slightly elevated cost. In addition, GAST transferred very little energy in the standard model, but GAST – 10 MUS had a greater metabolic cost increase over the standard model than HAMS – 10 MUS. In addition, RECT transfers only a moderate amount of energy from the hip to the knee during the down stroke, but RECT – 10 MUS predicted the greatest metabolic cost. Therefore, energy transfer from biarticular muscles does not play a major role in metabolic savings in pedaling.

External Forces

Biarticular muscles may play a role in controlling the direction of forces exerted on the environment; such as on the pedal during pedaling (van Ingen Schenau, 1989; van Ingen Schenau, Pratt, & Macpherson, 1994; van Ingen Schenau, et al., 1995). If biarticular muscles are the main contributors to directing external forces, then removing them could cause the uniarticular muscles to produce excessive amounts of negative work to accomplish the task of directing force on the pedal (van Ingen Schenau, et al., 1995). This negative work would be overcome with more positive work to produce the necessary amount of external work to complete the task, thereby increasing co-contraction and the metabolic cost.

The index of force effectiveness (IE) determines the ratio of the tangential force applied to the crank relative to the total force applied to the pedal (Coyle, et al. 1991). For the standard model, IE was 43.6%, a value very similar to experimental data: 40% at 200 W and 80 rpm (Patterson & Moreno, 1990). The 10 MUS models predicted slightly lower IE values: RECT – 10 MUS 42.3%,

HAMS – 10 MUS 34.8% and GAST – 10 MUS 38.6%. In all three cases, the patterns of force application for the 10 MUS models were generally similar to the standard model, differing only in specific aspects that were unique to each 10 MUS model (Figure 7.9). Of particular interest to this study, the IE trend also does not follow the differences in metabolic cost. RECT – 10 MUS predicted the highest metabolic cost, but had the most similar IE to the standard model. Also of note, is that the very different ankle angle and torque profiles simulated by RECT – 10 MUS resulted in an IE most similar to the standard model. GAST – 10 MUS had the next highest metabolic cost, and it predicted the next closest IE to the standard model. HAMS – 10 MUS was the closest in metabolic cost to the standard model, thus the lowest metabolic cost of the three models with the altered design, and it predicted the lowest IE. Thus, while the predicted metabolic cost was higher and the effectiveness of force application on the pedal was lower in the 10 MUS models, IE did not predict the relative differences in metabolic cost among the 10 MUS models.

If biarticular muscles were not included in the musculoskeletal model, it was proposed that more negative muscular work would have to be performed to direct forces on the pedal effectively. This would increase the positive muscular work performed so as to accomplish the power requirement of the task, thus increasing metabolic cost. The three 10 MUS models did produce more net negative work, and thus more net positive work than the standard model (Figure 7.8). However, the overall increase in negative work does not follow the overall increase in metabolic cost. In fact, the order is exactly the opposite: HAMS – 10 MUS had the greatest net negative work, but had the smallest increase in metabolic cost over the standard model. Whereas, RECT – 10 MUS had the least net negative work, but exhibited the greatest increase in metabolic cost over the standard model. For all three 10 MUS models, TIBA predicted nearly zero or negative net contractile element work. The negative work of TIBA was countered by an increase in positive work by the SOLE in two models: HAMS – 10 MUS and GAST – 10 MUS. This compensation explains some of the greater metabolic cost in these two models, along with the redistribution of CE work among the remaining muscles not

crossing the ankle. RECT – 10 MUS predicted net negative SOLE CE work, which resulted in a very different ankle torque profile than the other two models. The net negative CE work of SOLE was not overcome by greater positive CE work of the GAST and TIBA in RECT – 10 MUS the way the net negative work of the TIBA was overcome by greater positive SOLE CE work in the other two altered models. So while there was negative work performed by SOLE, there was not a counter balance by the TIBA or GAST that could explain the increase in metabolic cost. The increase came primarily from HAMS, as other muscles predicted lower CE work as compared to the standard model. Therefore, the negative CE work predicted by the simulations of the three altered models did not follow the predicted outcome: more negative work would lead to greater metabolic cost over the standard model. Thus, this proposed mechanism does not explain the differences in metabolic cost.

Neuromuscular Adaptations

The increased metabolic cost predicted by the three altered musculoskeletal designs (RECT – 10 MUS, HAMS – 10 MUS and GAST – 10 MUS) over a standard model during this pedaling task was due to the different muscle activation patterns by each model to accomplish the task rather than any singular proposed characteristic of biarticular muscles. The altering of muscle activation patterns seen in this project is similar to the neuromuscular adaptation responses to altering the task seen in several studies. Namely, that if the task is altered, the muscular activations adapt to accomplish the task. For example, Hasson, et al (2008) found that a novel, single leg pedaling task, learned within one practice session, resulted in a different muscle activity patterns, in both timing and magnitude, from the oft practiced double leg pedaling task. Also similar to the current study, Hasson et. al (2008) found that both monoarticular and biarticular muscle activation patterns changed to accomplish the task. In another study, Neptune and Herzog (1999) found that the introduction of an elliptical chainring altered the magnitude of muscle activations, especially in the rectus femoris and tibialis anterior muscles, between the different task conditions. While their findings were not so universal as

the current study or Hasson, et al., both a biarticular muscle and a uniarticular muscle changed to contribute significantly to the altered pedaling task. Finally, Li and Caldwell, (1998) compared the muscle activity during uphill seated, uphill standing and level seated pedaling, and determined that both biarticular and uniarticular muscles presented alternative muscle activity patterns to accomplish the task. In these studies, the musculoskeletal design remained constant while the pedaling task was altered, they all showed that both biarticular and uniarticular muscle activity was altered to accomplish the new task. In the current study, a complimentary finding was presented, that if the musculoskeletal design is altered, and the task held constant, a similar neuromuscular adaption occurs, where both biarticular and uniarticular muscle activities change to accomplish the pedaling task.

Model Design Considerations

One of the limitations of this project was that a model with only uniarticular muscles was not used. While this altered model would have been ideal, no model could be designed under the constraints of this project. The main constraints were that the muscle characteristics, volumes and strength had to be the same as the standard model. A model with only uniarticular muscles could not be made within these constraints as large changes in volume, either through increases in contractile element length or maximal force production, would be necessary to match the joint torque angle curves of the standard model. Maintaining similar muscle volume was necessary so that any differences in metabolic cost could be singularly attributed to musculoskeletal design.

Another consideration was that pedaling was used as the mode of movement. Pedaling was chosen because it accentuates biarticular muscle activity with its large joint range of motions. However, pedaling is not as common to human movement as walking and running, and it could be argued that the human body was not designed to pedal, but rather to walk and run. In addition, the proposed mechanisms of how biarticular muscles may affect the metabolic cost of movement may

have greater roles during these activities than the minimal roles shown here in pedaling. Therefore, to complete the investigation of the effect of biarticular muscles on human movement, walking and running should be simulated using these models to further test of generality of the results.

A final consideration is that we assumed that minimizing muscle activations would result in realistic pedaling kinematics, kinetics and muscle activations for the 10 MUS models. This assumption is reasonable because of the effectiveness of this performance-based criterion in simulating submaximal pedaling using the standard model (STUDY ONE) and walking and running by other researchers (Ackermann & van den Bogert, 2010; Miller, Umberger, Hamill, & Caldwell, 2012). However, it is not conclusive whether this is the most appropriate criterion for simulating movement using a new musculoskeletal design.

Conclusion

The 10 MUS models with two mechanically-equivalent uniarticular muscles in place of the biarticular muscles resulted in a greater metabolic cost over the standard model. The metabolic effect was different for each biarticular muscle. No single proposed mechanism for metabolic energy savings by biarticular muscles from the literature could simply or directly explain the metabolic increase associated with replacing biarticular muscles with equivalent uniarticular muscles. Rather, each of the altered musculoskeletal designs adopted a unique coordination pattern to meet the task demands of pedaling. Identifying the causes of the increased cost required a detailed assessment of the activation patterns and mechanics of each muscle, and there were few consistencies across the three 10 MUS models. In conclusion, the presence of biarticular muscles in the human lower limb does appear to reduce the cost of human movement, at least for pedaling; however, there was no simple or consistent mechanism found that could explain the basis for the lower cost.

APPENDIX A - MUSCULOSKELETAL MODEL

A.1 Skeletal Model

The human skeletal model referred to in this project as *the standard model* represents a rider-bicycle system, including both lower limbs and the crank (Figure A.1). This two-dimensional, sagittal plane, seven-segment model contains nine frictionless hinge joints representing: the hip, knee, and ankle for each leg; two foot-pedal interactions; and the crank center. Each leg forms a closed loop with the crank segment, reducing the number of degrees of freedom to three. These degrees of freedom are represented by three generalized coordinates, which are the two pedal angles and the crank angle. The hip joints and crank center are fixed in space, representing a frame angle of 73°, and a pelvis segment fixed at 55° relative to the right horizontal. The parameter values for the segments, including the crank, are provided in Table A-1. Limb segment lengths (Delp, et al., 1990) and inertial values (de Leva, 1996) represent a human with a mass of 75.0 kg and height of 1.8m. The segments are modeled as rigid bodies, and the equations of motion were generated using Autolev software (OnLine Dynamics, Sunnyvale, CA).

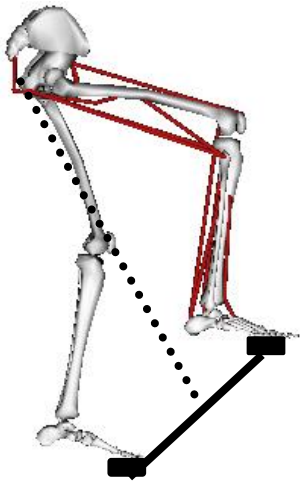

Figure A.1. A three-degrees of freedom, seven segment, two-dimensional human rider-bicycle model. Only muscles of the right leg are shown for clarity. The bicycle frame (shown as a dashed line) is not a segment of the model. (Image generated using OpenSim, SimTK®)

Table A-1: Skeletal parameters. Center of mass (CM) location is from the proximal joint.

Segment	Length (m)	Mass (kg)	CM location (m)	Moment of inertia ($kg \cdot m^2$)
Thigh	0.410	10.62	0.170	0.190
Shank	0.430	3.25	0.190	0.040
Foot	0.197	1.03	0.090	0.010

Additionally, exponential functions model the passive angular constraints imposed by ligamentous structures, capsular tissue, muscle parallel elasticity, and bone-on-bone contact forces (Reiner & Edrich, 1999). The resultant passive moments approximate the effects of all joint angles on the passive structures for a specific joint (φ represents joint angle):

$$M_{ankle} = exp(2.1016 - 0.0843\varphi_{ankle} - 0.0176\varphi_{knee}) - exp(-7.9763 + 0.1949\varphi_{ankle} + 0.0008\varphi_{knee}) - 1.792 \quad \text{(A-1)}$$

$$M_{knee} = exp(1.800 - 0.0460\varphi_{ankle} - 0.0352\varphi_{knee} + 0.0217\varphi_{hip}) - exp(-3.971 - 0.0004\varphi_{ankle} + 0.0495\varphi_{knee} - 0.0128\varphi_{hip}) - 4.280 + \exp(2.220 - 0.150\varphi_{knee}) \quad \text{(A-2)}$$

$$M_{hip} = exp(1.4655 - 0.0034\varphi_{knee} - 0.0750\varphi_{hip}) - exp(1.3403 - 0.226\varphi_{knee} + 0.0305\varphi_{hip}) + 8.072 \quad \text{(A-3)}$$

A.2 Muscle Model

A two-element, Hill-type muscle model represents each muscle in the model (van Soest & Bobbert, 1993) (Figure A.2). The two elements are the contractile elements of the muscle (CE) and the elastic structures in series (SEE) with the contractile elements. The muscle model contains mathematical representations of the SEE force-length relationship (Figure A.2), the CE force-length and force-velocity relationships (Figure A.2), and activation dynamics (Figure A.3). Nonlinear, first-order, ordinary differential equations describe the dynamic behavior of the muscle model: activation-relaxation and contractile element dynamics.

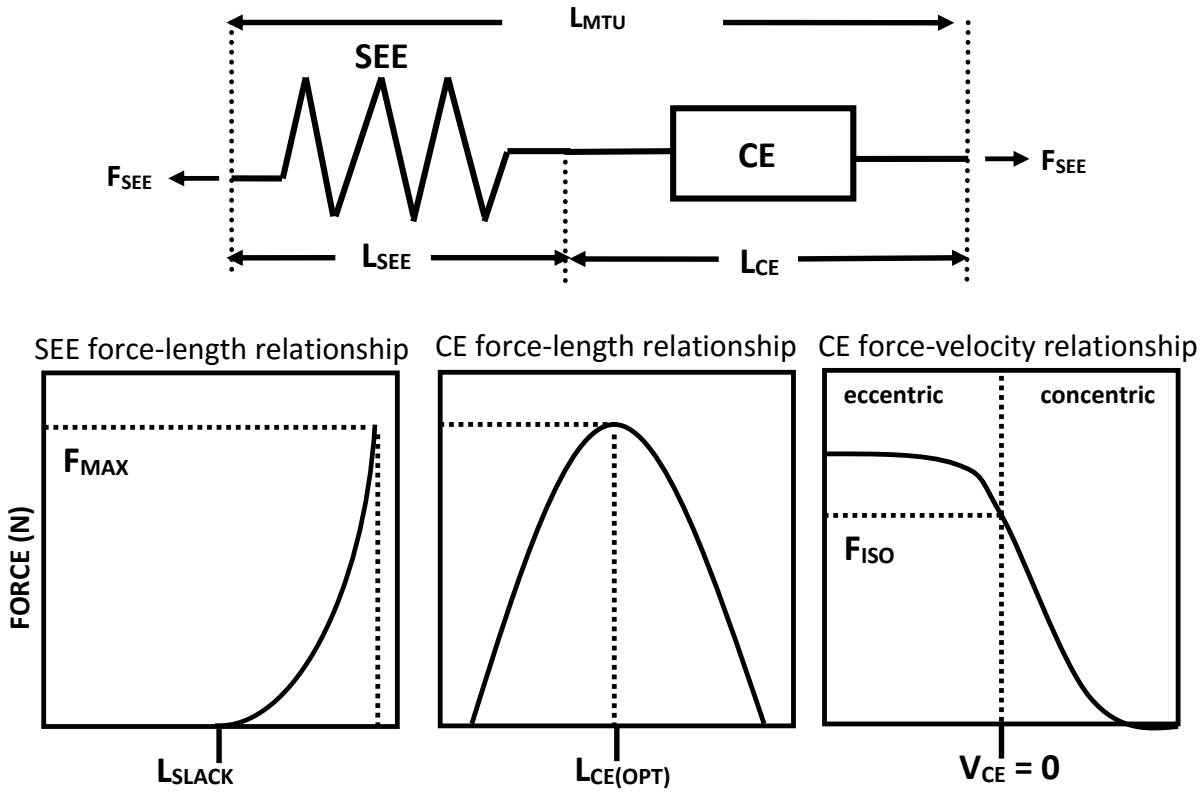

Figure A.2: The two-component Hill-type model consisting of a contractile element (CE) and a series elastic element (SEE), where L_{MTU} is the total muscle tendon unit length, L_{SEE} is the series elastic length, and L_{CE} is the contractile element length. Because the SEE is in series with the CE, the force output of the SEE (F_{SEE}) is equal to the F_{MTU}. Also shown are representatives of the SEE force-length, CE force-length, and CE force-velocity relationships.

A.3 Muscle Activation and Contraction Dynamics

The equations describing muscular dynamics, specifically muscle activation and contraction dynamics are linked to the skeletal model using custom written FORTRAN routines, which together form the representative musculoskeletal model. Neural input and the mechanical activation for each time step are represented by the first-order nonlinear differential equation (He, Levine, & Loeb, 1991):

$$\dot{act} = (exc - act) * (Q_1 * exc + Q_2)$$

(A-4)

In this equation, exc represents the neural input (0 to 1 where 0 = off) and act represents the nonlinear relationship between activation and excitation, which is graphically represented in Figure A.3. The constants Q_1 and Q_2 are determined from the activation (τ_{act}) and deactivation (τ_{deact}) constants defined for each muscle:

$$Q_1 = \left(\frac{1}{\tau_{act}} - Q_2\right) \text{ and } Q_2 = \left(\frac{1}{\tau_{deact}}\right). \quad \text{(A-5 \& A-6)}$$

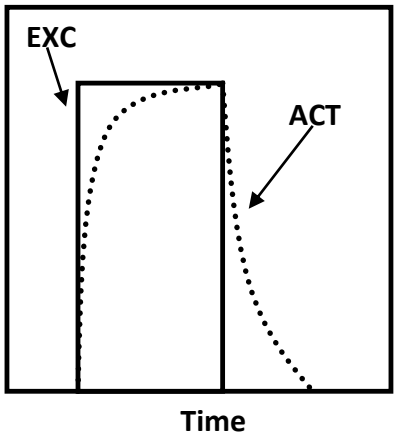

Figure A.3: The delay in activation and deactivation between muscle excitation (EXC) and the active state of the muscle (ACT).

Muscle contraction dynamics are represented mathematically by a series of equations adapted from van Soest & Bobbert (1993) and Nagano & Gerritsen (2001). At each time step, the length of SEE extension is found by subtracting the SEE slack length (L_{SLACK}) from the current length in L_{SEE}. L_{SEE} is found by subtracting the length of L_{CE} from the length of the muscle tendon unit (L_{MTU}). L_{MTU} is a function of joint angles, and is explained in a later section. The force in the SEE (F_{SEE}) is then determined first by applying the stiffness constant (k_{SEE}):

$$F_{SEE} = k_{SEE} \cdot (L_{SEE} - L_{SLACK})^2 \quad \text{(A-7)}$$

Because the CE and SEE are in series and there is no pennation angle, F_{SEE} equals F_{CE}. Thus, the force determined in the SEE is represented in further equations as F_{CE}. This force is then normalized to the CE force-length (f_{ISO}), and used to find v_{ce}.

If concentric, then:

$$v_{ce} = -1 * f_{act} * L_{CEOPT} * \left(\frac{(f_{ISO} + A_{REL}) * B_{REL}}{F_{CE}/(F_{MAX} * act) + A_{REL}} - B_{REL}\right) \quad \text{(A-8)}$$

where $f_{act} = min(1, 3.33 * act)$. The term, f_{act}, makes the velocity of CE dependent on the activation level (van Soest & Bobbert, 1993), which more closely replicates the force-velocity relationship found at different activation levels experimentally (Petrofsky & Phillips, 1980). (A_{REL} and B_{REL} are explained in detail later).

If eccentric, then the following equation represents the hyperbolic function:

$$v_{CE} = -1 * L_{CEOPT} * \left(\frac{C_1}{F_{CE}/(F_{MAX} * act) + C_2} + C_3\right) \quad \text{(A-9)}$$

and the linear asymptote is defined as:

$$vce = L_{CEOPT} * S_{lin} * \frac{F_{CE}}{(F_{MAX} * act) + \sqrt{(C_1/S_{lin}) + C_2} + L_{CEOPT} * (\sqrt{(C_1 * S_{lin})} - C_3)} \quad \text{(A-10)}$$

where S_{lin} is a constant (200) assuring a mathematical solution for the linear, eccentric portion (i.e., at high lengthening velocities) of the force-velocity curve (Figure A-2).

The constants C_1, C_2, and C_3 are determined by the following equations:

$$C_1 = (B_{REL} * {f_{ISO}}^2 * (1 - f_{maxecc})^2) / (S_{fac} * (f_{ISO} + A_{REL})) \quad \text{(A-11)}$$

$$C_2 = -1 * fiso * fmaxecc \quad \text{(A-12)}$$

$$C_3 = -1 * ((B_{REL} * f_{ISO} * (1 - f_{maxecc})) / (S_{fac} * (f_{ISO} + A_{REL}))) \quad \text{(A-13)}$$

where $fmaxecc$, the maximum eccentric force at infinitely high lengthening velocity, and S_{fac}, the slope for the lower lengthening velocities, are 1.5 and 2.0, respectively, for every muscle.

While the force-velocity curve is continuous (Figure A-2), the slopes about $v_{CE} = 0$ are not equal. This value means that the slope on the eccentric side is twice as steep as the concentric (van Soest & Bobbert, 1993).

A.4 Muscle Parameters

The musculoskeletal model contains 18 Hill-type muscle models, 9 for each leg. This standard model will be altered as part of this study, as biarticular muscles will be replaced by uniarticular muscles. A musculoskeletal design that represents only major muscle groups (e.g. the group of uniarticular hip flexors is represented by one muscle model) will simplify this aspect of the project while still adequately representing the major features of the human musculoskeletal system (Winters & Stark, 1985). The names of these muscles represent the type of muscle modeled. Muscular parameters scale the generic muscle model described above to represent specific muscle architectures and designs (Table A-2). The muscle parameters maximal isometric force (F_{MAX}) were adapted from Umberger, et al. (2006). For the purposes of developing this model with 9 muscles per leg, muscles duplicating actions in the Umberger 12 muscle model were combined (eg. iliacus and psoas major). Each muscle's series elastic element slack length ($Lslack$) and optimal contractile element length (L_{CEopt}) was determined via optimization, which is explained in more detail later.

Other muscle parameters are universal for all muscles. The width of the normalized force-length curve ($WIDTH$) was set to 0.56 for each muscle (Walker & Schrodt, 1973). Pennation angle is not included in the muscles of the standard model to permit the two designs in this project to be more comparable. Muscles in the human body have individualized pennation angles that fit form and function; however, this architectural characteristic will be unknown for the uniarticular muscles that will replace the biarticular muscles in the uniarticular-only design. Muscle mass was determined by finding the volume of each muscle (physiological cross-sectional

area multiplied by optimal fiber length) and multiplying that by the density of muscle (1.06 g/mL) (Mendez & Keys, 1960).

Table A-2 Muscle model parameter values

Muscle	mass (kg)	PCSA (cm^2)	$L_{CE(OPT)}$ (m)	F_{MAX} (N)	L_{SLACK} (m)
glutei	1.738	93.4	0.1756	2335	0.1130
iliapsoas	0.759	60.6	0.1182	1515	0.1306
biceps femoris(long)	1.46	80.4	0.1710	2009	0.3144
rectus femoris	0.478	44.7	0.1009	1118	0.3330
biceps femoris(short)	0.212	10.7	0.1870	267	0.0610
vasti	2.496	237.0	0.0994	5925	0.1355
gastrocnemius	0.417	55.4	0.0710	1384	0.3553
soleus	1.450	220.6	0.0620	5516	0.2312
tibialis anterior	0.553	58.6	0.0890	1466	0.2060

A.5 Determining L_{SLACK} and L_{CEopt}

The SEE slack length (L_{SLACK}) is impossible to determine *in vivo* because it is representative of elastic elements in series with the contractile elements and not a specific anatomical structure that can be measured. Because the force produced by the muscle-tendon unit is highly sensitive to this parameter (Out, Vrijkotte, van Soest, & Bobbert, 1996), L_{SLACK} must be carefully determined. Force produced by the muscle-tendon unit is also sensitive to the optimal LCE length (L_{CEopt}). This parameter could be estimated from experimental data (e.g. Martin, et. al, 2001; Ward, et al., 2009); however, because none of this model came from a single data set, optimizing both parameters insures that at given joint angles appropriate torque values can be produced by the muscles about that joint. In this study, L_{SLACK} and L_{CEopt} was determined by minimizing the difference between experimental joint torques (Anderson, Madigan, & Nussbaum, 2007) and those generated by the model at three different joint positions (e.g. Gerritsen & van den

Bogert, 1995; Umberger, 2003). The experimental and simulated joint torques were normalized to each data set's maximum joint torque before the difference between the torque values were minimized. Normalized values were used because the subjects from the experimental data and the musculoskeletal model are not of equal strength (Figure A.4).

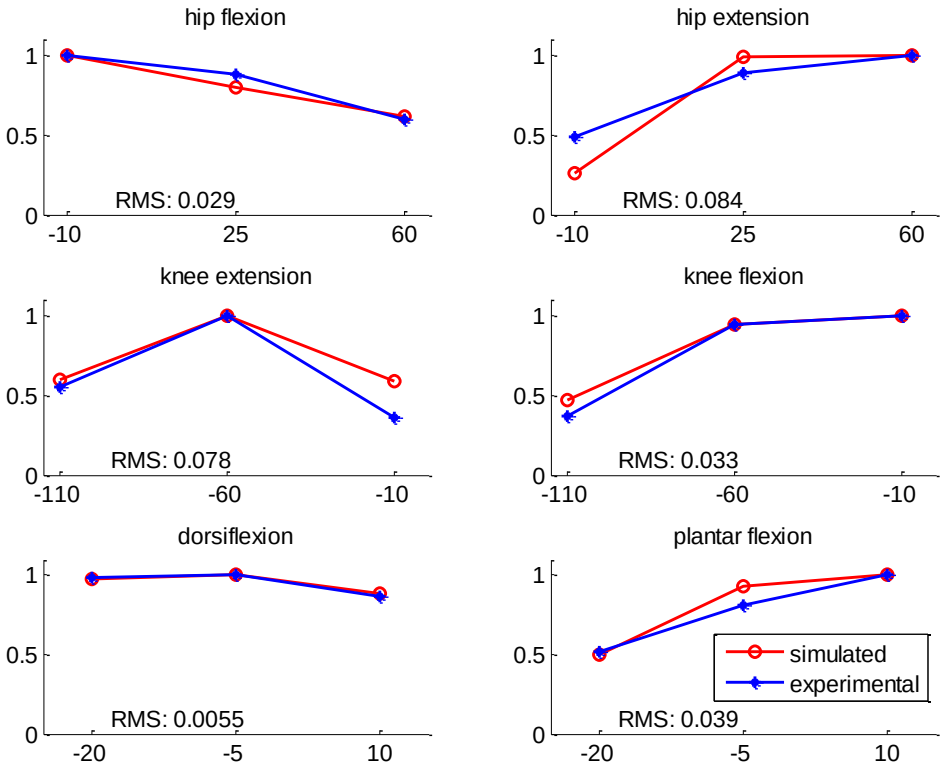

Figure A.4: A comparison of each optimized joint torque (black, open circles) to the Anderson, et al. (2007) experimental torques (blue, closed circles). The vertical scale represents the torque normalized to the maximum torque value. What do the horizontal scales represent? Root-mean-squared (RMS) values represent the differences in the normalized curves.

A.6 Fiber Type

Fiber-type distribution has been shown to affect the energetics of cycling (Coyle et al., 1992), and the inclusion of this muscle characteristic individualized for each muscle in a musculoskeletal model has proven to be an important factor in predicting the energetics of pedaling (Umberger, et al., 2006). While the fiber-types for muscles in the human leg can be

estimated from experimental data for musculoskeletal models (Umberger, et al, 2003; Umberger, et al., 2006), the muscle fiber-type distribution is unknown for a uniarticular-only model, which will be designed as part of this study. Thus, in the standard model, the 18 muscles will have the same muscle fiber type distribution, which is represented mathematically as 50% fast and slow twitch. This generalized fiber type will possibly affect the energetics of the system (see the section Energy Expenditure Model). For example, if this simplification overestimates the percent of fast twitch muscle fibers in the human leg, the result could overestimate the energetics for submaximal pedaling. However, given that both musculoskeletal models in this project will have the same fiber type, the energetic results will be attributable to the musculoskeletal design and not to any differences in fiber type composition. Fiber-type composition is represented in this model by the normalized "Hill constants" ($A_{REL}\ and\ B_{REL}$) which define the force-velocity curve shape and maximal shortening velocity. Additionally, fiber type distribution defines the activation and deactivation time constants (τ_{ACT} and τ_{DEACT}) which represent the temporal aspects of muscle activation and relaxation (Figure A-3). By designating the fiber-type distributions for all muscles as 50% fast, 50% slow twitch fibers, every contractile element will have the same force-velocity curve shape, maximal shortening velocity, and activation-deactivation relationships. The force-velocity parameter values A_{REL} =0.3 and B_{REL} = 3.6 were mathematically derived using the following equations (Winters & Stark, 1988):

$$A_{REL} = 0.1 + 0.4 \cdot (\%\,FT/100) \tag{A-14}$$

$$B_{REL} = A_{REL} \cdot \tilde{V}_{CE(MAX)} \tag{A-15}$$

where %FT is the percent of fast-twitch muscle fibers in a given muscle and $\tilde{V}_{CE(MAX)}$ is the maximal contractile element shortening velocity (12 $L_{CE(OPT)} \cdot s^{-1}$) (de Ruiter et al., 2000), expressed in multiples of $L_{CE(OPT)}$. The time constants for activation (τ_{ACT}) and deactivation (τ_{DEACT}) and were derived from the following relationship:

$$\tau = A_1 - A_2 \cdot \%FT$$

(A-16)

where A_1 and A_2 differ for activation and deactivation (τ_{ACT}: A_1=80 ms and A_2=0.50 ms, τ_{DEACT}: A_1=95 ms and A_2=0.60 ms) (Umberger, Gerritsen, and Martin, 2006). Therefore, for all muscles τ_{ACT} = 55.0, and τ_{DEACT} = 65.0.

A.7 Musculoskeletal Geometry

The human skeletal system is represented by six segments: thigh, shank and foot for each leg. These elements were explained in detail earlier. Each muscle length (L_{MTU}) is dependent on the joint configurations of the joints they cross. The effect of this dependence was modeled for each muscle by using a fourth-order polynomial with separate terms for all three joints (hip, knee and ankle) using the muscle-tendon unit length, joint angle relationships from Umberger, et al. (2003). The symbolic notation of this equation is:

$$L_{MTU} = A_0 + A_1\theta_H + A_2\theta_H^2 + A_3\theta_H^3 + A_4\theta_H^4 + A_5\theta_K + A_6\theta_K^2 + A_7\theta_K^3 + A_8\theta_K^4 + A_9\theta_A + A_{10}\theta_A^2 + A_{11}\theta_A^3 + A_{12}\theta_A^4 \quad \text{(A-17)}$$

The joint angles are in radians. The coefficients (A_0 – A_{12}) are listed in table A-4 for each represented muscle. The coefficients for the joint angles about which a given muscle does not cross were set to zero. All joint angles are zero at full extension. Partial derivatives of the muscle-tendon unit polynomial result in third-order polynomials representing the moment arm(s) of each muscle (Table A-4).

A.8 Energy Expenditure Model

Muscle metabolic energy expenditure was modeled using three heat rate terms and mechanical work rate of the contractile element ($\dot{w}_{CE}$) and represents the total energy utilized during muscular activity.

$$\dot{E} = \dot{h}_A + \dot{h}_M + \dot{h}_{SL} + \dot{w}_{CE} \quad \text{(A-18)}$$

The three heat rate terms are the activation heat rate ($\dot{h}_A$), the maintenance heat rate ($\dot{h}_M$), and the heat rate of shortening or lengthening ($\dot{h}_{SL}$). This model was validated and explained in greater detail by Umberger, et al., 2003, 2006, and Umberger, 2010.

Activation heat rate represents the energy spent moving calcium ions into and out of the sarcoplasmic reticulum against concentration gradients (Homsher, Mommaerts, Ricchiuti, & Wallner, 1972). Energy is also necessary for maintaining tension. The activation and maintenance heat can be considered together based on experimental results of heat production at full activation (Hatze & Buys, 1977; Bolstad & Ersland, 1978). This heat rate ($\dot{h}_{AM}$) is linearly related to the fiber-type composition:

$$\dot{h}_{AM} = 1.28 \cdot \%FT + 25 \qquad \text{(A-19)}$$

The heat rate of shortening or lengthening also is dependent on the fiber-type distribution within a muscle, and differs from each other. When the muscle is shortening, the heat is determined by:

$$\dot{h}_{SL} = -\alpha_{S(ST)} \cdot \tilde{V}_{CE} \cdot (1 - \%FT/100) - \alpha_{S(FT)} \cdot \tilde{V}_{CE} \cdot (\%FT/100) \qquad \text{(A-20)}$$

where

$$\propto_{S(ST)} = \frac{4 \cdot 25}{\tilde{V}_{CE(MAX-ST)}} \; and \; \propto_{S(FT)} = \frac{1 \cdot 153}{\tilde{V}_{CE(MAX-FT)}} \qquad \text{(A-21 \& A-22)}$$

When the muscle is lengthening, the heat is determined by:

$$\dot{h}_{SL} = \alpha_L \cdot \tilde{V}_{CE}\,, \qquad \text{(A-23)}$$

where $\propto_L = 0.3 \cdot \propto_{S(ST)}$

Finally, the mechanical work rate of the contractile element, $\dot{w}_{CE}$, is defined as:

$$\dot{w}_{CE} = -\frac{F_{CE} \cdot V_{CE}}{m} \quad \text{(A-24)}$$

with m as the mass of the particular muscle. The $\dot{w}_{CE}$ is the mechanical work rate of the contractile element, which differs from the work rate of the whole muscle tendon unit. If the work rate of the whole unit were used, the work done by or on the series elastic element would be included. These structures do not require metabolic energy, thus it is not included when determining metabolic cost.

Table A-3 The muscle-tendon unit (MTU) fourth-order and moment arm (MA) third-order polynomial coefficients for the nine represented muscles in a single leg.

	MTU length	HIP				KNEE				ANKLE			
MUSCLE	A0	A1	A2	A3	A4	A5	A6	A7	A8	A9	A10	A11	A12
glutei	0.211	0.062	-0.002	-0.005	0.001	-	-	-	-	-	-	-	-
iliapsoas	0.217	-0.030	0.002	-0.007	0.003	-	-	-	-	-	-	-	-
vasti	0.188	-	-	-	-	0.040	0.017	-0.018	0.004	-	-	-	-
biceps femoris(short)	0.238	-	-	-	-	0.022	-0.001	-0.010	0.004	-	-	-	-
tibialis anterior	0.306	-	-	-	-	-	-	-	-	-0.043	-0.005	0.004	0.002
soleus	0.322	-	-	-	-	-	-	-	-	0.035	-0.007	-0.005	0.001
bisceps femoris(long)	0.411	0.046	0.020	-0.011	0.001	0.029	-0.011	0.000	0.002	-	-	-	-
rectus femoris	0.416	-0.034	-0.017	0.005	0.001	0.041	0.023	-0.020	0.004	-	-	-	-
gastrocnemius	0.461	-	-	-	-	0.021	0.001	-0.006	0.002	0.043	-0.004	-0.007	0.001

	MA length	HIP			KNEE			ANKLE		
MUSCLE	A0	A1	A2	A3	A4	A5	A6	A7	A8	A9
glutei	-0.062	0.004	0.015	-0.002	-	-	-	-	-	-
iliapsoas	0.030	-0.003	0.022	-0.011	-	-	-	-	-	-
vasti	-0.040	-	-	-	-0.033	0.053	-0.016	-	-	-
biceps femoris(short)	0.022	-	-	-	0.003	0.030	-0.017	-	-	-
tibialis anterior	0.043	-	-	-	-	-	-	0.009	-0.013	-0.006
soleus	-0.035	-	-	-	-	-	-	0.014	0.015	-0.003
bisceps femoris(long)	-0.046	-0.040	0.034	-0.004	0.021	0.000	-0.008	-	-	-
rectus femoris	0.034	0.035	-0.015	-0.004	-0.045	0.061	-0.017	-	-	-
gastrocnemius	-0.043	-	-	-	-0.002	0.018	-0.009	0.008	0.020	-0.003

A.9 Model Validity

After developing the model as explained above, it was validated by tracking experimental data. The variables that were tracked are: x- and y-pedal forces, hip, knee and ankle moments, crank torque and pedal angle (Neptune & Hull, 1998). This section provides all kinematic (pedal, and hip, knee and ankle angles; Figure A.5) and kinetic (crank torque, x- and y-pedal forces, and hip, knee and ankle joint torques; Figure A.6) variables. There is no experimental joint angle data, but the data is provided here to show that the joint angles were within reasonable ranges of motion.

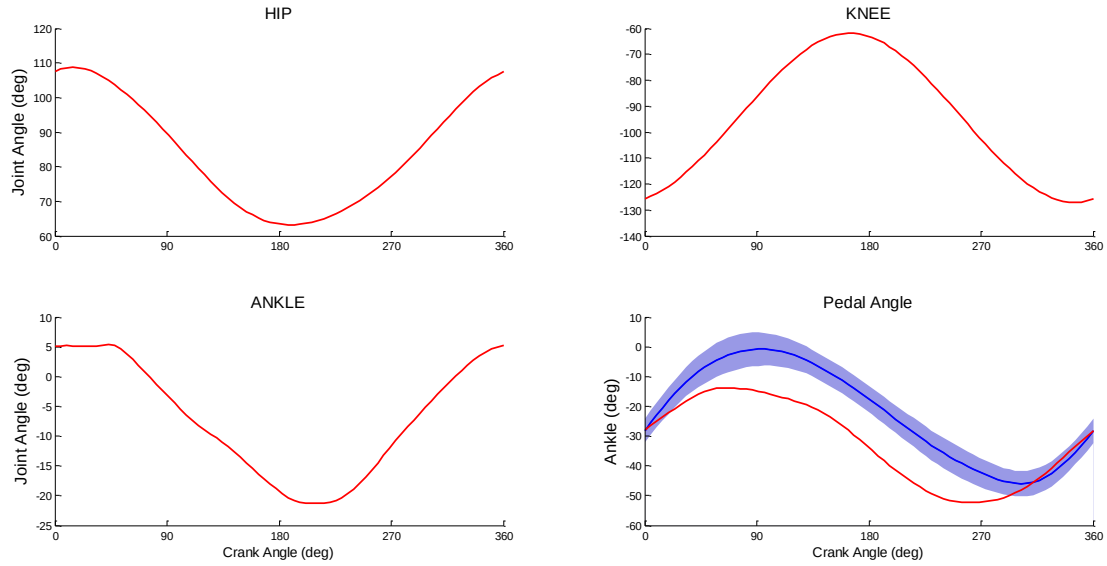

Figure A.5 Hip, knee, ankle and pedal angles of the simulated data from the standard model. The pedal angle is shown with experimental data from Marsh, Martin and Sanderson (2000) (RMSD = 2.5).

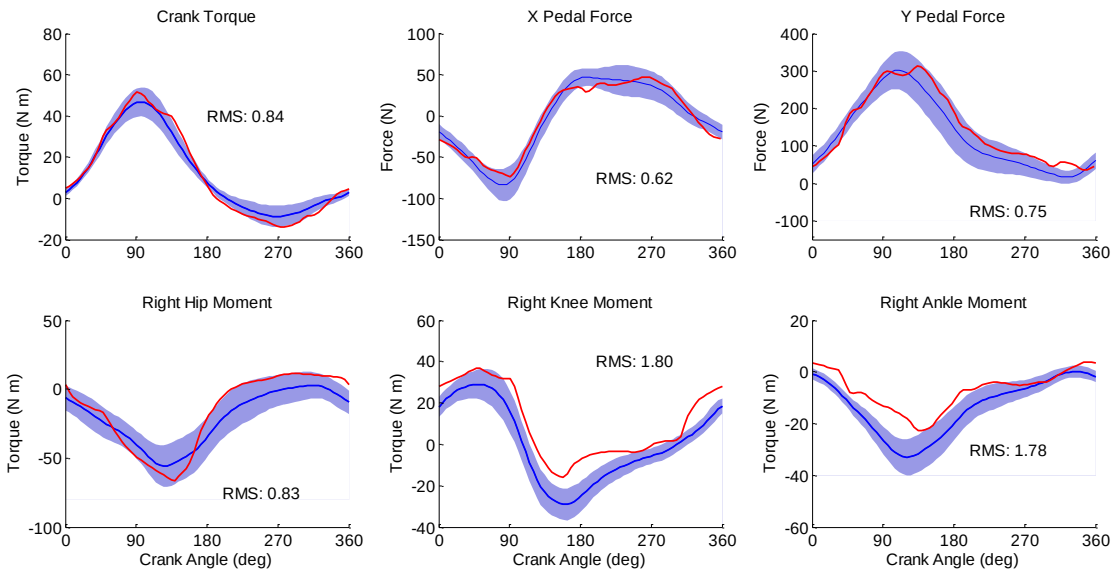

Figure A.6 Kinematic variables of crank torque, x- and y-pedal forces, and hip, knee and ankle joint moments comparing the experimental data (BLUE) with one standard deviation represented from Marsh, Martin and Sanderson (2000) with the simulated data from the standard model (RED). RMSD values reported on the figure.

APPENDIX B – 10 MUSCLE MUSCULOSKELETAL MODELS

B.1 Skeletal Model, Muscle Model and Activation Dynamics

The skeletal model, muscle model and activation dynamics of each of the three musculoskeletal models of this project is identical to that used in the standard model (Appendix A.1, A.2, and A.3).

B.2 Muscle Parameters

Three musculoskeletal models were designed by replacing each biarticular muscle separately with two uniarticular muscles crossing the same joints. For each model, the parameters FMAX, LCEopt and LSLACK of two new uniarticular muscles and the original uniarticular muscles of the same joints as the biarticular muscle were optimized to replicate the torque-angle curves of the standard model. For the new uniarticular muscles, the muscle-tendon unit length was also optimized. All other muscle parameters were unchanged from the standard model. For each new musculoskeletal design, the total muscle volume change was less than 2%.

B.2.1 Rectus Femoris

The biarticular rectus femoris was replaced by two uniarticular muscles (RECT H, RECT K). During the optimization process the muscle parameters of psoas (PSOA) and vastus (VAST) were also altered (Table B-1). The total volume change was +1.60%. Knee flexion torque angle values of the uniarticular musculoskeletal design followed the same pattern as the standard model with a fairly even magnitude difference (RMS = 10.85 Nm) (Figure B-1). The hip flexion torque angle values of the uniarticular musculoskeletal design and the standard model were virtually (RMS = 0.54 Nm); however, the uniarticular design resulted in a different torque-angle profile (Figure B-1).

Table B-1 Altered parameters of the new musculoskeletal model replacing the rectus femoris.

MM10 RECT				**MTU Length**
	Fmax	**LCEopt**	**Lslack**	**Ao**
PSOA	965.7	0.103	0.1581	0.2600
RECT H	1555.7	0.1467	0.1158	0.2934
RECT K	201.4	0.1800	0.0575	0.2748
VAST	5900.0	0.0900	0.1402	0.1880

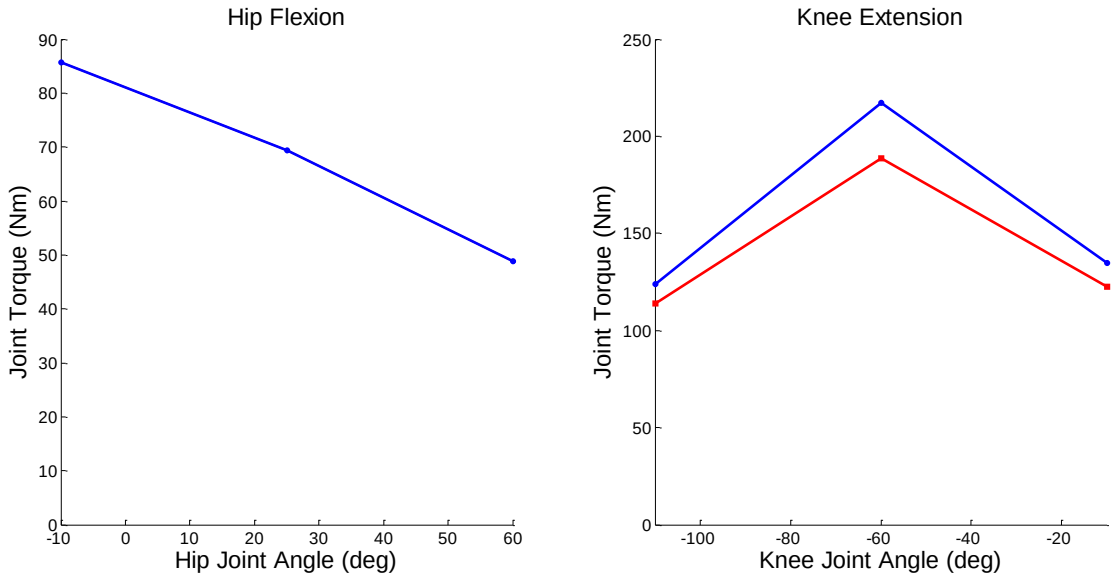

Figure B.1 The hip flexion (RMS = 0.54 Nm) and knee extension (RMS = 10.85 Nm) torque-angle relationships for the new musculoskeletal model (MM: RED line) replacing the rectus femoris. (SM: BLUE line) stands for the standard model.

B.2.2 Hamstrings

The biarticular hamstring muscle was replaced by two uniarticular muscles (HAMS H, HAMS K). During the optimization process the muscle parameters of gluteus maximus (GMAX) and

biceps femoris short head (BFSH) were also altered (Table B-2). The total volume change was +1.61%. Knee flexion torque angle relationship (RMS = 4.40 Nm) of the uniarticular musculoskeletal model maintained the same profile of the standard model, with slightly lower values across all three angles (Figure B-2). This results in fairly weak knee flexion at the most extreme angle (110°). Again, this angle and motion at that angle are not relevant to pedaling, thus this model was deemed acceptable. The hip extension torque angle relationship (RMS = 9.16 Nm) of the uniarticular musculoskeletal model produced a similar profile to the standard model, with the most extreme difference at the largest hip angle (60°) (Figure B-2). The hip extension torques are high, thus the difference at this angle does not represent a weak model at these greater joint angles, so this model was deemed acceptable for pedaling.

Table B-2 Altered parameters of the new musculoskeletal model replacing the hamstrings.

MM10 HAMS				**MTU Length**
	Fmax	**LCEopt**	**Lslack**	**Ao**
GMAX	1507.53	0.1750	0.1045	0.2130
HAMS H	2355.26	0.1486	0.1172	0.2070
HAMS K	1948.39	0.1030	0.0915	0.2202
BFSH	307.07	0.1688	0.0719	0.2580

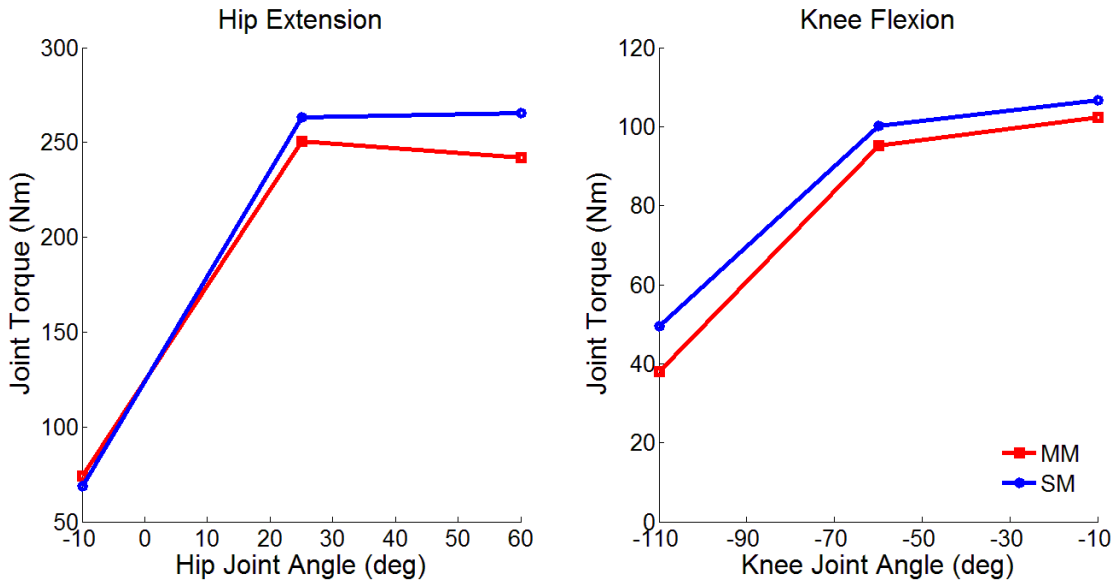

Figure B.2 The hip extension (RMS = 9.16 Nm) and knee flexion (RMS = 4.40 Nm) torque-angle relationships for the new musculoskeletal (MM: RED line) replacing the hamstrings. SM (BLUE line) stands for the standard model.

B.2.3 Gastrocnemius

The gastrocnemius was replaced by two uniarticular muscles (GAST K, GAST A). During the optimization process the muscle parameters of soleus (SOLE) and biceps femoris short head (BFSH) were also altered (Table B-3). The total volume change was +0.00%. The knee flexion torque angle relationship (RMS = 4.36 Nm) deviated from the standard model torques only at the most extended angle (-10°) (Figure B-3). Again this angle does not occur in pedaling, thus this model was deemed suitable. The ankle plantar angle torque values of the uniarticular model was virtually identical to the standard model (RMS = 3.56) (Figure B-3).

Table B-3 Altered parameters of the new musculoskeletal model replacing the gastrocnemius.

MM10 GAST				**MTU Length**
	Fmax	**LCEopt**	**Lslack**	**Ao**
BFSH	192.77	0.1282	0.0915	0.258
GAST K	1157.41	0.0644	0.1695	0.2591
GAST A	1077.64	0.0512	0.1929	0.2442
SOLE	5527.55	0.0608	0.2273	0.2918

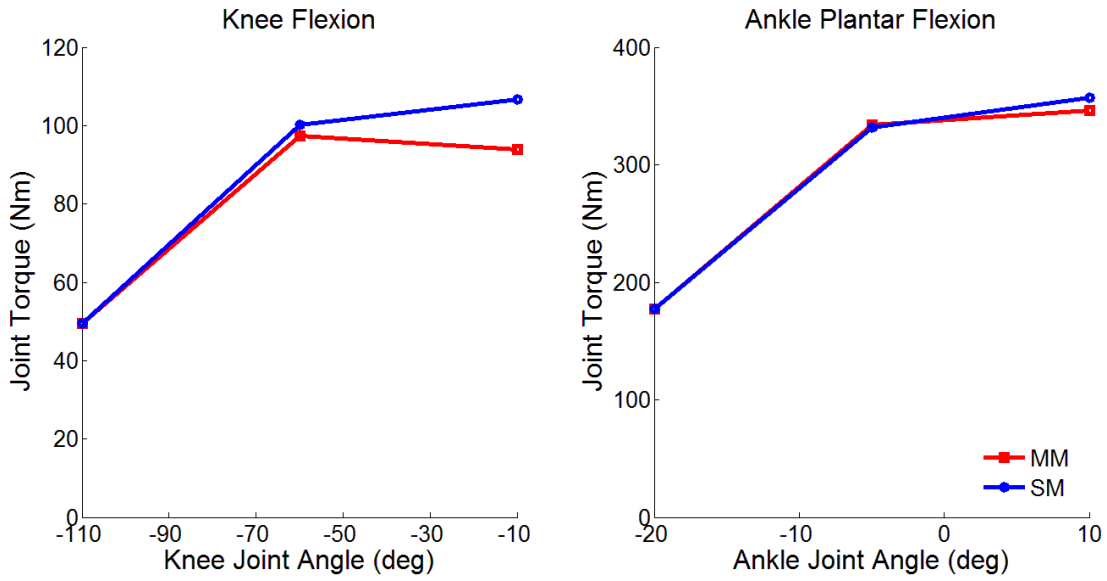

Figure B.3 The knee flexion (RMS = 4.36) and ankle plantar flexion (RMS = 3.56) torque-angle relationships for the new musculoskeletal model (MM: RED line) replacing the gastrocnemius. SM (BLUE line) stands for the standard model.

Model Evaluation - Tracking

Tracking simulations were generated to test whether the 10 MUS models, which have essentially the same static torque-angle profiles as the standard model, could also generate similar results in the dynamic task of pedaling. Deviations from the tracking data were expressed as root mean square errors (RMSE) in multiples of the standard deviations (SD) of the mean experimental

data. All 10 MUS models could track experimental human data reasonably well, though not quite as well as the standard model (Figure B-4, Table B-4). The variable with the highest RMSE for the 10 MUS models was pedal angle, with values between 1.47 RMSE (HAMS – 10 MUS) and 2.61 RMSE (RECT – 10 MUS). All other variables for the 10 MUS models had RMSE values below 1.0, with the exception of the knee moments for the uniarticular GAST – 10 MUS model (1.82 RMSE) and RECT – 10 MUS model (1.35 RMSE). The uniarticular RECT – 10 MUS model also replicated the ankle moment worse than the other models with an RMSE value of about 2 RMSE. It is not surprising that the standard model had the lowest RMSE values, as the experimental data were obtained from subjects who possess similar biarticular muscle design. Nevertheless, the 10 MUS models were all capable of generating simulated pedaling in a manner that is qualitatively similar to normal human pedaling.

Table B-4: The results of tracking experimental pedaling data (STUDY ONE). Root mean squared errors (RMSE), reported in standard deviations, between the mean experimental data and the simulations from the standard model (SM9) and the three musculoskeletal models with two uniarticular muscles in place of one of the biarticular muscles.

	Pedal Angle	**Crank Torque**	**Hip Moment**	**Knee Moment**	**Ankle Moment**
Standard Model	0.74	0.37	0.71	0.84	0.52
RECT – 10 MUS	2.61	0.55	0.99	1.35	2.07
HAMS – 10 MUS	1.47	0.69	0.86	0.97	0.94
GAST – 10 MUS	2.02	0.80	0.61	1.82	0.67

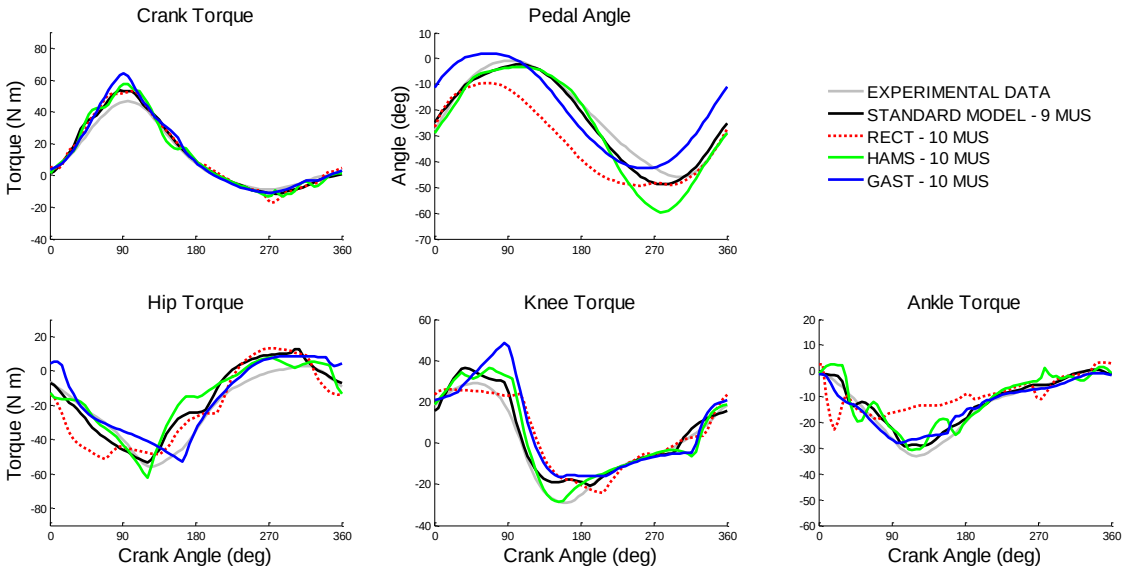

Figure B.4 Tracking simulation results for the standard model and the three musculoskeletal models with two uniarticular muscles in place of a singular biarticular muscle.

BIBLIOGRAPHY

Abbott, B.C., Bigland, B. & Ritchie, J.M. (1952). The physiological cost of negative work. *Journal of Physiology*, *117*, 380-390.

Abrantes, C., Sampaio, J., Reis, V.M., Sousa, N., & Duarte, J.A. (2012). Physiological Responses to Treadmill and Cycle Exercise. *International Journal of Sports Medicine, 33*, 26 – 30.

Ackermann, M. & van den Bogert, A. (2010). Optimality principles for model-based prediction of human gait. *Journal of Biomechanics, 43*, 1055-1060.

Anderson, D., Madigan, M., & Nussbaum, M. (2007). Maximum voluntary joint torque as a function of joint angle and angular velocity: Model development and application to the lower limb. *Journal of Biomechanics, 40*, 3105-3113.

Anderson, F. & Pandy, M. (2001). Dynamic Optimization of Human Walking. *Journal of Biomechanical Engineering, 123*, 381-390.

Andrews, J. (1987). The functional roles of the hamstrings and quadriceps during cycling: Lombard's Paradox revisited. *Journal of Biomechanics, 20*, 565-575.

Belli, A. & Hintzy, F. (2002) Influence of pedaling rate on the energy cost of cycling in humans. *European Journal of Applied Physiology, 88*, 158-162.

Beltman, J., van der Vliet, M., Sargeant, A., & de Haan, A. (2004). Metabolic cost of lengthening, isometric and shortening contractions in maximally stimulated rat skeletal muscle. *Acta Physiologica Scandinavia* (182), 179-187.

Bigland-Ritchie, B. & Woods, J.J. (1976). Integrated electromyogram and oxygen uptake during positive and negative work. *Journal of Physiology*, 260, 267-277.

Bobbert, M. & van Ingen Schenau, G. (1988). Coordination of vertical jumping. *Journal of Biomechanics, 21*, 241-262.

Bobbert, M., Huijing, P., & van Ingen Schenau, G. (1986). An estimation of power output and work by the human triceps surae muscle-tendon complex in jumping. *Journal of Biomechanics, 19* (11), 899-906.

Bolstad, G., & Ersland, A. (1978). Energy metabolism in different human skeletal muscles during voluntary isometric contraction. *European Journal of Applied Physiology, 38*, 171-179.

Böning, D., Gönen, Y., & Maassen, N. (1984). Relationship between work load, pedal frequency, and physical fitness. *International Journal of Sports Medicine, 5*(2), 92-97.

Braune, W. & Fischer, O. (1899). Über den den Schwerpunkt des menschlichen Körpers, mit Rücksickt auf die Aüstrustung des deutschen Inganteristen. *Abh. sächs Gesellschaft Wissenschaften, 26*, 561-672.

Broker, J.P. & Gregor, R.J. (1994) Mechanical energy management in cycling: source relations and energy expenditure. *Medicine and Science in Sports and Exercise, 26* (1), 64-74.

Caldwell, G.E. & Forrester, L.W. (1992). Estimates of mechanical work and energy transfers: demonstratoin of a rigid body power model of the recovery leg in gait. *Medicine and Science in Sports and Exercise, 24*(12), 1396-1412.

Cavagna, G.A. & Margaria, R. (1966). Mechanics of walking. *Journal of Applied Physiology, 21*(1), 271-278.

Cavagna, G.A., Thys, G., & Zamboni, A. (1976). The sources of external work in level walking and running. *Journal of Physiology, 262*, 639-657.

Cavanagh, P.R. and Kram, R. (1985). The efficiency of human movement- a statement of the problem. *Medicine and Science in Sports and Exercise, 17*(3): 304-308.

Cleland, J. (1867). On the actions of muscles passing over more than one joint. *Journal of Anatomy and Physiology, 1*, 85-93.

Chavarren, J. & Calbet, J.A.L.(1999). Cycling efficiency and pedalling frequency in road cyclists. *European Journal of Applied Physiology, 80*, 555-563.

Cleland, J. (1867). On the Actions of Muscles passing over more than One Joint. *Jornal of Anatomy and Physiology, 1*(1), 85-93.

Coast, J.R. & Welch, H.G. (1985). Linear increase in optimal pedal rate with increased power output in cycle ergometry. *European Journal of Applied Physiology and Occupational Physiology, 53*, 339-342.

Coyle, E.F., Feltner, M.E., Kautz, S.A., Hamilton, M.T., Montain, S.J., Baylor, A.M., Abraham, L.D., & Petrek, G.W. (1991). Physiological and biomechanical factors associated with elite endurance cycling performance. *Medicine and Science in Sports and Exercise, 23*, 93-107.

Crowninshield, R. & Brand, R. (1981). A physiological based criterion of muscle force prediction in locomotion. *Journal of Biomechanics, 14* (11), 793-808.

Davy, D. & Audu, M. (1987). A dynamic optimization technique for predicting muscle forces in the swing phase of gait. *Journal of Biomechanics, 20* (2), 187-201.

Delp, S., Loan, J., Hoy, M., Zajac, F., Topp, E., & Rosen, J. (1990). An interactive graphics-based model of the lower extremity to study orthopaedic surgical procedures. *IEEE Transactions on Biomechanical Engineering, 37*, 757-767.

Duchenne, G. (1885). Physiologie und Bewegungen. *Th. Fischer, Cassel und Berlin (cited in Kuo, 2001).*

Dul, J., Johnson, G., Shiavi, R., & Townsend, M. (1984). Muscular synergism - II. A minimum-fatigue criterion for load sharing between synergistic muscles. *Journal of Biomechanics, 17* (9), 675-684.

Elftman, H. (1939a). Forces and energy changes in the leg during walking. *American Journal of Physiology, 125*, 339-356.

Elftman, H. (1939b). The function of muscles in locomotion. *American Journal of Physiology, 125*, 357-366.

Elftman, H. (1940). The work done by muscles in running. *American Journal of Physiology, 129*, 672-684.

Elftman, H. (1966). Biomechanics of Muscle: with particular application to studies of gait. *The Journal of Bone and Joint Surgery, 48*, 363-377.

Fenn. W.O. (1923). A quantitative comparison between the energy liberated and the work performed by the isolated sartorius muscle of the frog. *Journal of Physiology, 58*(2-3), 175-203.

Fenn, W.O. (1924). The relation between the work performed and the energy liberated in muscular contraction. *Journal of Physiology*, *58*(6), 373-395.

Fenn, W. O.(1930). Frictional and kinetic factors in the work of spring running. *American Journal of Physiology, 92*, 583-611.

Fischer, E. (1931). The oxygen consumption of isolated muscle for isotonic andisometric twitches. *American Journal of Physiology, 96*, 78-88.

Flash, T. & Hogan, N. (1985). The coordination of arm movements: an experimentally confirmed mathematical model. *Journal of Neuroscience, 5* (7), 1688-1703.

Foss, O. & Hallen, J. (2004). The most economical cadence increases with increasing workload. European Journal of Applied Physiology, 92, 443 - 451.

Fregly, B.J. & Zajac, F.E. (1996) A state-space analysis of mechanical energy generation, absorption, and transfer during pedaling. *Journal of Biomechnics, 29*, 81-90.

Gaesser, G.A. & Brooks, G.A. (1975). Muscular efficiency during steady-rate exercise: effects of speed and work rate. *Journal of Applied Physiology, 38*(6), 1132-1139.

Gerritsen, K. & van den Bogert, A. (1995). Force-length parameters of lower extremity muscles derived from maximal isometric strength tests. *Proceedings of the XIXth Annual Meeting of the American Society of Biomechanics.*, (pp. 125-126). Standford, USA.

Goffe, W., Ferrier, G., & Rogers, J. (1994). Global Optimization of Statistical Functions with Simulated Annealing. *Journal of Econometrics, 60* (1/2), 65-99.

Gregoire, L., Veeger, H., Huijing, P., & van Ingen Schenau, G. (1984). Role of Mono- and Biarticular Muscles in Explosive Movements. *International Journal of Sports Medicine, 5*, 301-305.

Gregor, R., Cavanagh, P., & LaFortune, M. (1985). Knee flexor moments during propulsion in cycling- a creative solution to Lombard's Paradox. *Journal of Biomechanics, 18*, 307-316.

Hasson, C., Caldwell, G., & van Emmerik, R. (2008). Changes in muscle and joint coordination in learning to direct forces. *Human Movement Science, 27* (4), 590-609.

Hatze, H., & Buys, J. (1977). Energy-optimal controls in the mammalian neuromuscular system. *Biological Cybernetics, 27*, 9-20.

He, J., Levine, W., & Loeb, G. (1991). Feedback gains for correcting small perturbations to standing posture. *IEEE Transactions on Automatic Control, 36*, 322-332.

Hering, H. (1897). Uber die Wirkung zweigelenkiger Muskeln auf drei Gelenke und uber die pseudo-antagonistiche Synergie. *Archiv fur die gesammte Physiologie, 65*, 627-637. *(cited in Kuo, 2001).*

Herr, H. & Kornbluh, R. (2004). New horizons for orthotic and prosthetic technology: artificial muscle for ambulation. MIT Media Laboratory, Cambridge.

Herzog, W. & Binding, P. (1994). Effects of replacing 2-joint muscles with energetically equivalent 1-joint muscles on cost-function values of non-linear optimization approaches. *Human Movement Science, 13*, 569-586.

Herzog, W. & Leonard, T. (1991). Validation of optimization models that estimate the forces exerted by synergistic muscles. *Journal of Biomechanics, 24* (1), 31-39.

Higginson, J. S., Neptune, R.R., & Anderson, F.C. (2005). Simulated parallel annealing within a neighborhood for opitmization of biomechanical systems. Journal of Biomechanics, 38, 1938-1942.

Hill, A.V. (1938). The heat of shortening and the dynamic constants of muscle. *Proceedings of the Royal Society of London B, 126*(843), 220-228.

Hill, A.V. (1949). Work and Heat in a Muscle Twitch. *Proceedings of the Royal Society of London B, 136*(883), 220-228.

Homsher, E., Mommaerts, W., Ricchiuti, N., & Wallner, A. (1972). Activation heat, activation metabolism and tension-related heat in frog semitendinosus muscles. *Journal of Physiology, 220*, 601-625.

Huxley, A. F. (1957). Muscle structure and theories of contraction. Progress in biophysics and biophysical chemistry, 7, 257-318.

Jacobs, R., Bobbert, M., & van Ingen Schenau, G. (1996). Mechanical output from individual muscles during explosive leg extensions: the role of biarticular muscles. *Journal of Biomechanics, 29* (4), 513-523.

Johnson, T., Moore, S., Quinn, L., & Smith, B. (2004). Energy cost of walking in children with cerebral palsy: relation to the Gross Motor Function Classification System. *Developmental Medicine and Child Neurology, 46*, 34-38.

Jorge, M. & Hull, M.L.(1986) Analysis of EMG measurements during bicycle pedalling. *Journal of Biomechanics, 19*(9), 683-694.

Katz, B. (1939). The relation between force and speed in muscular contraction. *Journal of Physiology, 96*, 45-64.

Kautz, S. & Neptune, R. (2002). Biomechanical determinants of pedaling energetics: internal and external work are not independent. *Exercise and Sports Science Reviews, 30* (4), 159-165.

Koeslag, P.D. & Koeslag J.H. (1993). The mechanics of biarticular muscles. *South African Journal of Science, 89*, 73-76.

Kautz, S.A., Neptune, R.R., & Zajac, F.E. (2000) General Coordination Principles Elucidated by Forward Dynamics: Minimum Fatigue Does Not Explain Muscle Excitation in Dynamic Tasks. *Motor Control, 4*, 75 - 80.

Kuo, A. (2001). The Action of Two-Joint Muscles: The Legacy of W.P. Lombard. In M. Latash, & V. Zatsiorsky, *Classics in Movement Science* (pp. 289-315). Champaign, Illinois: Human Kinetics.

Lehman, S. & Stark, L. (1982). Three algorithms for interpreting models consisting of ordinary differential equations: sensitivity coefficients, sensitivity functions, global optimization. *Mathematical Biosciences, 62*, 107-122.

de Leva, P. (1996). Adjustments to Zatsiorsky-Seluyanov's segment inertia parameters. *Journal of Biomechanics, 29*, 1223-1230.

Li, L. & Caldwell, G. (1998). Muscle coordination in cycling: effect of surface incline and posture. Journal of Applied Physiology, 85(3):927-934.

Lichtwark, G., & Wilson, A. (2005). A modified Hill muscle model that predicts muscle power output and efficiency during sinusoidal length changes. *Journal of Experimental Biology, 208*, 2831-2843.

Lieber, R. (1990). Hypothesis: biarticular muscles transfer moments between joints. *Developmental medicine and child neurology, 32* (5), 456-458.

Lombard, W. (1903). The action of two-joint muscles. *American Journal of Physical Education Review, 9*, 141-145.

Marsh, A.P., Martin, P.E.. & Foley, K.O. (2000). Effect of cadence, cycling experience, and aerobic power on delta efficiency during cycling. *Medicine and Science in Sports and Exercise, 32* (9), 1630 - 1634.

Marsh, A.P., Martin, P.E., & Sanderson, D. (2000). Is a joint moment-based cost function associated with preferred cycling cadence? *Journal of Biomechanics, 33*, 173-180.

Martin, D.C., Medri, M.K., Chow, R.S., Oxoron, V., Leekam, R.N., Agur, A.M., and McKee, N.H. (2001) Comparing human skeletal muscle architectural parameters of cadavers with in vivo ultrasonographic measurements. *Journal of Anatomy, 199*(4), 429 - 434.

MacLennan, D.H. & Holland, P.C. (1975). Calcium transport in sarcoplasmic reticulum. *Annual Review of Biophysics and Bioengineering, 4*, 377-404.

McDaniel, J., Durstine, J.L., Hand, G.A., & Martin, J.C. (2002). Determinants of metabolic cost during submaximal cycling. *Journal of Applied Physiology, 93*(3), 823-828.

Mendez, J. & Keys, A. (1960). Density and composition of mammalian muscle. *Metabolism, 9,* 184-188.

Metaxiotis, D. & Doederline, L. (2004). In C. Panteliadis, & H.-M. Strassburg, *Cerebral Palsy: principles and management* (pp. 219-233). Thessaloniki, Greece: Giapoulis publications.

Miller, R.H., Umberger, B.R., Hamill, J., & Caldwell, G.E. (2012). Evaluation of the minimum energy hypothesis and other potential optimality criteria for human running. *Proceedings of the Royal Society B, 279* (1733), 1498 - 1505.

Morin, J.B., Samozino, P., Bonnefoy, R., Edouard, P., & Belli, A. (2010). Direct measurement of power during one single sprint on treadmill. *Journal of Biomechanics, 43,* 1970-1975.

Nagano, A. & Gerritsen, K. (2001). Effects of neuromuscular strength training on vertical jumping performance – A computer simulation study. *Journal of Applied Biomechanics, 17,* 113-128.

Neptune, R.R. & Herzog, W. (2000). Adaption of muscle coordination to altered task mechanics during steady-state cycling. *Journal of Biomechanics, 33,* 165 - 172.

Neptune, R. & Hull, M. (1998). Evaluation of performance criteria for simulation of submaximal steady-state cycling using a forward dynamic model. *Journal of Biomechanical Engineering, 120,* 334-341.

Neptune, R. & Kautz, S. (2001). Muscle Activation and Deactivation Dynamics: The Governing Properties in Fast Cyclical Human Movement Performance? *Exercise and Sports Science Reviews, 29* (2), 76-81.

Neptune, R., Kautz, S., & Zajac, F. (2000). Muscle contributions to specific biomechanical functions do not change in forward versus backward pedaling. *Journal of Biomechanics, 33,* 155-164.

Norman, R., Sharratt, M., Pezzack, J., & Noble, E. (1976). Re-examination of the mechanical efficiency of horizontal treadmill running.In P. Komi, (Ed.), *Biomechanics V-B. International Series on Biomechanics*. (pp.87-93). Baltimore: University Press.

Out, L., Vrijkotte, T., van Soest, A., & Bobbert, M. (1996). Influence of the parameters of a human triceps surae muscle model on the isometric torque-angle relationship. *Journal of Biomechanical Engineering, 118* (1), 17-25.

Patterson R.P. & MOreno, M.I. (1990). Bicycle pedalling forces as a function of pedalling rate and power output. Medicine and Science in Sports and Exercise, 22(4), 512 - 516.

Pandy, M. (2001). Computer Modeling and Simulation of Human Movement. *Annual Review of Biomedical Engineering, 3,* 345-373.

Pandy, M., Garner, B., & Anderson, F. (1995). Optimal Control of Non-Ballistic Muscular Movements: A Constraint-Based Performance Criterion for Rising From a Chair. *Journal of Biomedical Engineering, 117,* 15-26.

Petrofsky, J.S. & Phillips, C.A. (1980). The influence of recruitment order and fibre composition on the force.velocity relationship and fatiguability of skeletal muscles in the cat. Medical and Biological Engineering and Computing, 18(4), 381-390.

Pierrynowski, M.R., Winter, D.A., & Norman, R.W. (1980). Transfers of mechanical energy within the total body and mechanical efficiency during treadmill walking. *Ergonomics, 23*(2), 147-156.

Pope, M. (1976). Giovanni Alfonso Borelli--the father of biomechanics. *Spine, 30* (20), 2350-2355.

Prilutzky, B. & Gregor, R. (2000). Analysis of Muscle Coordination Strategies in Cycling. *IEEE Transactions on Rehabilitation Engineering, 8* (3), 362-370

Prilutsky, B.L., Petrova, L.N. & Raitsin, L.M. (1996). Comparison of mechanical energy expenditure of joint moments and muscle forces during human locomotion. *Journal of Biomechanics*, 29(4), 405-415.

Prilutsky, B.I., Herzog, W., & Leonard, T. (1996). Transfer of mechanical energy between ankle and knee joints by gastrocnemius and plantaris muscles during cat locomotion. *Journal of Biomechanics, 29*(4), 391-403.

Prilutsky, B.I. & Zatsiorsky, V.M. (1994). Tendon action of two-joint muscles: Transfer of mechanical energy between joints during jumping, landing, and running. *Journal of Biomechanic*s, 27(1), 25-34.

Prilutsky, B. & Zatsiorsky, V. (2002). Optimization-Based Models of Muscle Coordination. *Exercise and Sports Science Reviews, 30* (1), 32-45.

Quanbury, A.O., Winter, D.A., & Reimer, G.D. (1975). Instantaneous power flow in body segments during walking. *Journal of Human Movement Studies, 1*, 59-67.

Raasch, C. & Zajac, F. (1999). Locomotor strategy for pedaling: muscle groups and biomechanical functions. *Journal of Neurophysiology, 82*, 515-525.

Raasch, C., Zajac, F., Ma, B., & Levine, W. (1997). Muscle coordination of maximal-speed pedaling. *Journal of Biomechanics, 30*, 595-602.

Ralston, H. (1976). *Energetics of human walking.* (R. Herman, S. Grillner, P. Stein, & D. Stuart, Eds.) New York: Plenum Press.

Rasmussen, J., Damsgaard, M., & Voigt, M. (2001). Muscle recruitment by the min/max criterion - a comparative numerical study. *Journal of Biomechanics, 34*(3), 409 - 415.

Ratel, S., Williams, C.A., Oliver, J., & Armstrong, N. (2004). Effects of age and mode of exercise on power output profiles during repeated sprints. *European Journal of Applied Physiology, 92*, 204-210.

Riener, R. & Edrich, T. (1999). Identification of passive elastic joint moments in the lower extremities. *Journal of Biomechanics, 32*, 539-544.

Robertson, D.G. & Winter, D.A. (1980). Mechanical energy generation, absorption and transfer amongst segments during walking. *Journal of Biomechanics, 13*(10), 845-854.

Rohrer, B., Fasoli, S., Krebs, H., Volpe, B., Frontera, W., et al. (2002). Movement Smoothness Changes during Stroke Recovery. *The Journal of Neuroscience, 22* (18), 8297-8304.

de Ruiter, C.J., Didden, W.J.M., Jones, D.A., & de Haan, A. (2000). The force-velocity relationship of human adductor pollicis muscle during stretch and the effects of fatigue. *Journal of Physiology, 526*, 671-681.

Sasaki, K., Neptune, R.R., & Kautz, S.A. (2009). The relationships between muscle, external, internal and joint mechanical work during normal walking. *Journal of Experimental Biology 212*(5),738-744.

Seireg, A. & Arvikar, R. (1975). The prediction of muscular load sharing and joint forces in the lower extremities during walking. *Journal of Biomechanics, 8* (2), 89-102.

Sidossis, L.S. Horowitz, J.F., & Coyle, E.F. (1992). Load and Velocity of Contraction Influence Gross and Delta Mechanical Efficiency. *International Journal of Sports Medicine*, 13(5), 407-411

Sparrow, W. & Newell, K. (1998). Metabolic energy expenditure and the regulation of movement economy. *Psychonomic Bulletin and Review, 5*, 173-196.

Taylor, R.C & Heglund, N.C. (1982). Energetics and mechanics of terrestrial locomotion. *Annual Review of Physiology, 44*, 97-107.

Takaishi, T., Yamanoto, T., Ono, T, Ito, T., & Moritani, T. (1998). Neuromuscular, metabolic, and kinetic adaptations for skilled pedaling performance in cyclists. *Medicine and Science in Sports and Exercise, 30* (3), 442 - 449.

Umberger, B. (2003, August). Effects of cycle rate on the mechanics and energetics of human locomotion. *Dissertation*. Arizona: Arizona State University.

Umberger, B. (2010). Stance and swing phase costs in human walking. *Journal of the Royal Society Interface, 7*, 1329-1340.

Umberger, B., Gerritsen, K., & Martin, P. (2003). A Model of Human Energy Expediture. *Computer Methods in Biomechanics and Biomedical Engineering, 6* (2), 99-111.

Umberger, B., Gerritsen, K., & Martin, P. (2006a). Muscle fiber type effects on energetically optimal cadences in cycling. *Journal of Biomechanics, 39*, 1472-1479.

Umberger, B., Gerritsen, K., & Martin, P. (2006b). Muscle fiber type effects on energetically optimal cadences in cycling. *Journal of Biomechanics, 39*, 1472-1479.

van Ingen Schenau, G. (1989). From rotation to translation: constraints on multi-joint movements and the unique action of biarticular muscles. *Human Movement Science, 8*, 301-337.

van Ingen Scheau, G. (1990). On the action of biarticular muscles, a review. *Netherlands Journal of Zoology, 40*, 521-540.

van Ingen Schenau, G.J., Boots, P.J.M., deGroot, G., Snackers, R.J., & van Woensel,W.W.L.M. (1992). The constrained control of force and position in multi-joint movements. *Neurosciences, 46*(1), 197-207.

van Ingen Schenau, G., Dorssers, W., Welter, T., Beelen, A., deGroot, G., & Jacobs, R. (1995). The control of mono-articular muscles in multijoint leg extensions in man. *Journal of Physiology, 484*, 247-254.

van Ingen Schenau, G.J., Pratt, C.A., & Macpherson, J.M. (1994). Differential use and control of mono- and biarticular muscles. *Human Movement Science, 13*(3-4), 495-517.

Vanrenterghem, J., Bobbert, M., Casius, L., & Clercq, D. (2008). Is energy expenditure taken into account in human sub-maximal jumping? - A simulation study. *Journal of Electromyography and Kinesiology, 18*, 108-115.

van Soest, A. & Bobbert, M. (1993). The contribution of muscle properties in the control of explosive movements. *Biological Cybernetics, 69*, 195-204.

Walker, S. & Schrodt, G. (1973). I-segment Lengths and Thin Filament Periods in Skeletal Muscle Fibers of the Rhesus Monkey and the Human. *The Anatomical Record, 178* (1), 63-81.

Ward, S.R., Eng, C.M., Smallwood, L.H. & Lieber, R.L. (2009). Are current measurements of lower extremity muscle architecture accurate? *Clinical Orthopaedics and Related Research, 467*(4), 1074 - 1082.

Waters, R. & Mulroy, S. (1999). The energy expenditure of normal and pathologic gait. *Gait and Posture, 9* (3), 207-231

Wells, R. (1988). Mechanical energy costs of human movement: An approach to evaluating the transfer possibilities of two-joint muscles. *Journal of Biomechanics, 21* (11), 955-964.

Winter, D.A. (1979). A new definition of mechanical work done in human movement. *Journal of Applied Physiology, 46*, 79-83.

Winters, J.M. & Stark, L. (1985) Analysis of Fundamental Human Movement Patterns Through the Use of In-Depth Antagonistic Muscle Models. *IEEE Transactions on Biomedical Engineering, 32* (10), 826-839.

Zajac, F., Neptune, R., & Kautz, S. (2002). Biomechanics and muscle coordination of human walking: Part I. Introduction to concepts, power transfer, dynamics and simulations. *Gait and Posture, 16* (3), 215-232.